

Dynamic Interaction Between Event Deck Structures and a Jumping Crowd

The influence of human-structure interaction on impact force peaks and
internal stresses



Stef Appelman

Delft University of Technology

in partial fulfillment of the requirements for the degree of
Master of Science

12 October, 2022

Dynamic Interaction Between Event Deck Structures and a Jumping Crowd

The influence of human-structure interaction on impact force peaks and
internal stresses

By
Stef Appelman

in partial fulfillment of the requirements for the degree of
Master of Science
in Civil Engineering

at the Delft University of Technology,
to be defended on 20 October, 2022, at 09:30 AM.



Faculty of Civil Engineering and Geosciences
Masters: Civil Engineering
Track: Structural Engineering
Specialisation: Structural Mechanics

In collaboration with:



Student Number:	5185289	
Project Duration	Jan. 03, 2022 - Oct. 20, 2022	
Thesis Committee:	Dr. ir. H.R Schipper	TU Delft, Chair
	Dr. ir. K.N. van Dalen	TU Delft, Supervisor
	Ir. P.A. de Vries	TU Delft, Supervisor
	Avni Jain	TU Delft, Daily supervisor
	Ing. J. van Wijk	Tentech, Daily supervisor
	Ir. R. Houtman	Tentech, Supervisor

An electronic version of this thesis is available at <http://repository.tudelft.nl/>

Abstract

Human-induced rhythmic loading is an increasingly critical aspect in the design process of civil engineering structures such as sports stadiums and floors accommodating gym and aerobic classes. There are two main reasons for this trend. First, structures are becoming more slender with improvements in materials and construction techniques and modern trends in architectural designs. And second, crowds are getting livelier than previously was the case, their activities can become better synchronized due to the presence of various auditory and visual stimuli at above mentioned events.

In recent years there is also a growing discussion on the strength and stability of event structures. A very common type of structure is an event deck structure. Visitors gather on top of these decks during festivals and in some cases festival organizers place bars underneath them to efficiently use the structure. Personnel working in these bars experience the movement of the structure due to a dancing crowd and tend to feel uncomfortable. Engineers at Titech are aware of this phenomenon through contacts with clients.

Nowadays, in the Netherlands, event deck structures are designed to withstand a vertical static load of 5 kN/m^2 , prescribed by Dutch design codes. The amplitude of this static load is based on a dense static crowd. But according to existing literature, a synchronically jumping crowd can cause a vertical load which far exceeds the design load prescribed by design codes. This provides a reason to further investigate the extreme load case of a synchronically jumping crowd on an event deck structure.

A missing element in the standard design of structures subjected to a synchronically jumping crowd is the consideration of dynamic interaction between human and structure. In this research the focus is on how human-structure interaction (HSI) can influence the human-induced loading and the internal stresses caused by that loading in the structure. This is done by building a 3D finite element model in Abaqus.

A 3D finite element model is used to easily vary in the position of a jumper on the structure. Modelling group effects such as the coordination factor is also easier when using a 3D model. And in the case of an event deck structure a 3D model will result in more detailed results compared to 2D models because mechanical properties of an event deck can vary over the third dimension.

A mass-spring system is suggested to represent a jumping person. To simulate a synchronically jumping crowd, multiple mass-spring systems are used. By assigning an initial velocity to the mass in the mass-spring system, it is possible to simulate a similar mechanism as a jumping person colliding with a structure. By analysing the force in the spring over time it is possible to draw conclusions on the influence of human-structure interaction on the impact peak force. And by comparing the impact forces with the reaction forces which are measured at the base of the structure, the effects of structural vibrations on the internal stresses are determined.

It is found that taking HSI into account does influence the impact peak force and the internal stresses of the structure. But for an event deck structure with a natural frequency of 20 Hz or higher, this only accounts for an individually jumping person. It is found that the more people jump on a structure, the less significant the effect of HSI will be, even when a crowd tries to jump synchronically. This is caused by the natural time lag between each jumping person.

Acknowledgement

I would like to acknowledge and express my gratitude to the people who have helped me over the last months during my thesis:

First, I would like to thank my graduation committee, Roel Schipper, Avni Jain, Karel van Dalen, Peter de Vries, Jasper van Wijk and Rogier Houtman. I am grateful for your feedback and critical questions during our meetings, that steered me in the right directions. Thanks to you I have gained valuable knowledge about the dynamic interaction between humans and structures which will certainly be useful in my career.

I would like to thank my parents for always encouraging me to achieve my goals, and helping me in every possible way. I owe this to you.

Thanks to my friends at TU Delft who have made this past three years such an unforgettable experience.

Stef Appelman
Westwoud, October 2021

Contents

1	Problem introduction	1
1.1	Current norm values	1
1.2	Norm validation	3
2	Literature study	4
2.1	Accidents in the past	4
2.2	The extreme dynamical load case of a jumping crowd	4
2.2.1	Varieties in dynamic amplification factor	6
2.2.2	Varieties in the amount of people per square meter	7
2.2.3	Varieties in coordination factor	8
2.3	Human-structure interaction (HSI)	14
2.3.1	The magnitude of the dynamic peak force	14
2.3.2	Modelling of human-structure interaction during jumping	18
2.4	The Royal HaskoningDHV report on the collapsed grandstand of the NEC stadium De Goffert	22
2.4.1	The Impact Factor	23
2.4.2	Lock-in effect	25
3	Main research question	26
3.1	Sub questions on the impact force peak error	26
3.2	Sub questions on the impact factor	26
4	Hypothesis	26
4.1	Hypothesis on the impact force peak error	26
4.2	Hypothesis on the impact factor	27
5	Model	28
5.1	Choice in model software	28
5.2	Modelling plan	29
5.3	Modeling the human part of the system	29
5.3.1	A non-linear spring	30
5.3.2	Determination of human system parameters	30
5.4	Modeling the structural part of the system	31
5.4.1	Structural elements, properties and dimensions	32
5.4.2	Model assumptions	34
5.5	FEM model	37
5.6	Modelling randomly timed group jumps	38
5.7	Soundness of the model - <i>IPF</i>	40
5.8	Soundness of the model - <i>IF</i>	46
6	Results	49
6.1	The impact force peak error	49
6.1.1	Simultaneous group jump	49
6.1.2	Randomly timed group jump	51
6.1.3	Double randomly timed group jump	54
6.2	The impact factors (IF)	55
6.2.1	Simultaneous group jump	55
6.2.2	Randomly timed group jump	59
6.2.3	Double randomly timed group jump	60
7	Discussion	61
8	Conclusions	62

8.1	The impact force peak error (<i>IFE</i>)	62
8.2	The impact factor (<i>IF</i>)	63
9	Recommendations	64
	References	66
A	Jumping simulation	68

1 Problem introduction

The last couple of years engineers at Tentech received complaints from staff working at festivals. At some festivals grandstand structures were placed around stages to provide a better view. Bars were placed underneath these grandstands to efficiently use the created space. But during the festival the crew members working in these bars felt unsafe and made complaints about the event deck structure under which they were working. As the crowd started to jump on the musical beat, the large deformations of the structure frightened the crew. When many people gathered and danced on these grandstands, they introduced severe dynamic forces on the structure. Tentech is one of the few engineering firms in The Netherlands working with demountable lightweight event structures which are used at festivals. The engineers started having doubts on the structural integrity of structures excited by crowd-induced forces. Especially when dynamical forces come into play. They see their designs being pushed more and more to the limits as more people gather on event deck structures. According to [31], crowds are getting livelier than before and, according to Tentech engineers, structural elements are being pushed to their limits to favour the needs of their clients. Which is why they reached out to the TU Delft to take a closer look on the dynamic forces on lightweight event structures.



Figure 1: Platform structure at a festival



Figure 2: Triple deck structure at a festival

1.1 Current norm values

The largest source of distrust by Tentech engineers is the lack of dynamical consideration in the Eurocode. Their engineering instinct tells them that a jumping crowd produces a greater vertical excitation

then a very dense static crowd. To find out if this is true, research has been done on the origin of the currently applied vertical design force for grandstand structures. NEN-EN 13782, the Dutch norm on temporary structures, tents and safety prescribes a characteristic vertical load of 5 kN/m^2 . To justify this value, they refer to the Eurocode. Grandstands at festivals with open access to visitors are C5 classified. This holds the structure is designed to withstand large and dense crowds of people. The characteristic value for this load case equals $q_k = 5 \text{ kN/m}^2$. After research it becomes clear how this value has come about. Back in 1989 TNO conducted a rapport considering the backgrounds on loads according to concept NEN 6702 [7]. They concluded that for extreme floor loads 5 kN/m^2 was valid. This was based on the following 2 studies:

- Sentler L. Live load surveys - A review with discussions Report 78, Division of Building Technology, Lund Institute of Technology, Lund, Sweden, 1976 [20]
- Paloheimo, E. and M. Ollila Researches in the live load of persons Ministry of Domestic Affairs, Finland, 1973 [9]

The most interesting conclusions these 2 studies made regarding extreme load cases for floors can be obtained in figure 3.

Naar de invloed van verschillende activiteiten is onderzoek gedaan door Sentler [17] en Paloheimo [18]. De resultaten zijn vermeld in tabel 3.11

Tabel 3.11 Vloerbelasting veroorzaakt door bewegingen van personen

Sentler [17] Activiteit	Factor dynamisch / statisch	Paloheimo [18] Activiteit	Maximaal waargenomen belasting
dansen	3,5	dansen	2,9 - 5,0
springen	4,0	springen	2,3 kN/m ²
langzaam ver- plaatsende menigte	1,1	stilstaande menigte	5,5 kN/m ²
lopen	1,5	party	4,0 kN/m ²
hardlopen	3,0	party in ruimte die gedeeltelijk met stoelen is gevuld	2,4 kN/m ²
plaats springen	5,0	opstaan uit stoelen	3,4 kN/m ²

Figure 3: Maximum observed loads for different types of activities [7]

From figure 3 it can be concluded that a dense static crowd introduces a higher (5.5 kN/m^2) vertical load than a jumping (2.3 kN/m^2) or dancing crowd ($2.9 - 5.0 \text{ kN/m}^2$). To verify their conclusions TNO compared their values with quantities from other norms. Figure 4 shows the most relevant characteristic design values used by standards in other countries.

Tabel 3.12 Extreme vloerbelasting voor zalen e.d. in kN/m²

bron	restaurant	concertzaal	danszaal	tribunes zit plaatsen	sta plaatsen
NEN 3850 [6]	4	4	4	4	5
NKB [7]	4	4	4	4	5
ISO [8]	2,5	4	4	4	5
DS 409 [9]	2,5	4	4	4	4
NBN [10]	3	4	5	4	4
ANSI [11]	4,9	2,8	4,9	4,9	4,9
TR 479 [13]	2-5	5	5	5	5
SIA 160 [22]	5-7	5	7	5	7
DIN [23]	5	5	5	5	7,5
NEN 6702	5	5	5	5	5

Figure 4: Value comparison with other norms [7]

1.2 Norm validation

Considering the conclusions made in the TNO rapport there are some serious doubts about the load magnitude of jumping people. According to [9] the maximum observed load by jumping people is $2,3 \text{ kN/m}^2$. To justify the doubts, a simple calculation is made using a basic formula (1) to determine the magnitude of a jumping person:

$$\text{Weight of a person} \cdot g \cdot \text{Dynamic amplification factor} = \text{Vertical dynamic load} \quad (1)$$

The average weight of a Dutch male in 2019 is approximately 85 kg [6] and according to [20] the dynamic amplification factor of a jumping person is 4,0. Assuming 1 person per square meter would come down to a value of:

$$85 \cdot 9.81 \cdot 4.0 = 3335 \text{ N/m}^2 = 3.3 \text{ kN/m}^2$$

It is remarkable that 1 jumping person per square meter can produce a vertical peak force which is $1,0 \text{ kN/m}^2$ higher than is concluded in the study of [9]. Engineers at Tentech confirm the chance of multiple people jumping on a square meter during a festival is a very high. Assuming (1) is the right way to calculate the vertical excitation by a human there would only be $5.0/3.3 = 1.5$ people per square meter needed to reach the vertical characteristic load of grandstands prescribed by the Eurocode.

This finding has led to a more thorough literature study on this topic. One could argue that the load case of a crowd jumping on a structure has been happening for a long time now and is not something new which implies there is not much more research needed. This is a valid argument, but things are changing in the last decades according to [31] and [27]. The Vibration Engineering Section (VES) of the university of Exeter agrees on this as [31] introduced in the paper "DYNAMIC LOADS DUE TO SYNCHRONOUS RHYTHMIC ACTIVITIES OF GROUPS AND CROWDS" by stating "*Predicting vibration performance of civil engineering structures due to human-induced rhythmic loading is an increasingly critical aspect of the design process of structures such as sports stadia used for pop/rock concerts, floors accommodating gym and aerobic classes, and footbridges used as spectator galleries during regatta events. Two main reasons for this trend are (1) structures are becoming more slender with improvements in materials and construction techniques and modern trends in architectural design, and (2) groups/crowds are in general becoming livelier than previously was the case, i.e. their activities can become better synchronised due to the presence of various auditory and visual stimuli at above mentioned events*".

2 Literature study

2.1 Accidents in the past

A lot of research has already been done on the topic of determining crowd-induced loads. The combination of dynamic crowd-induced loads and lightweight structures is no exception. The reason for this is the fact that many accidents already happened due to this combination. [33] states that “Ninety three cases of collapse were found between the years 1889 and 2008, in which more than 85 people died and 6350 were injured.” “An analysis of the causes showed that unexpected or excessive loads were the major contributing cause, followed by problems with supports, connections, and bracing.”. This has led to the acknowledgement of the risks by research groups. Many studies have been conducted on this topic over the past 20 years because of these accidents. Figure 5 shows statistical data on the cases of collapse according to the type of event and what caused the collapse. From the charts can be concluded that most accidents happen in sport events and shows. This is an observation which is expected as in these types of events crowds are expected to be the liveliest. Another interesting conclusion that can be drawn from cart b is that excessive loading is the biggest reason for failure.

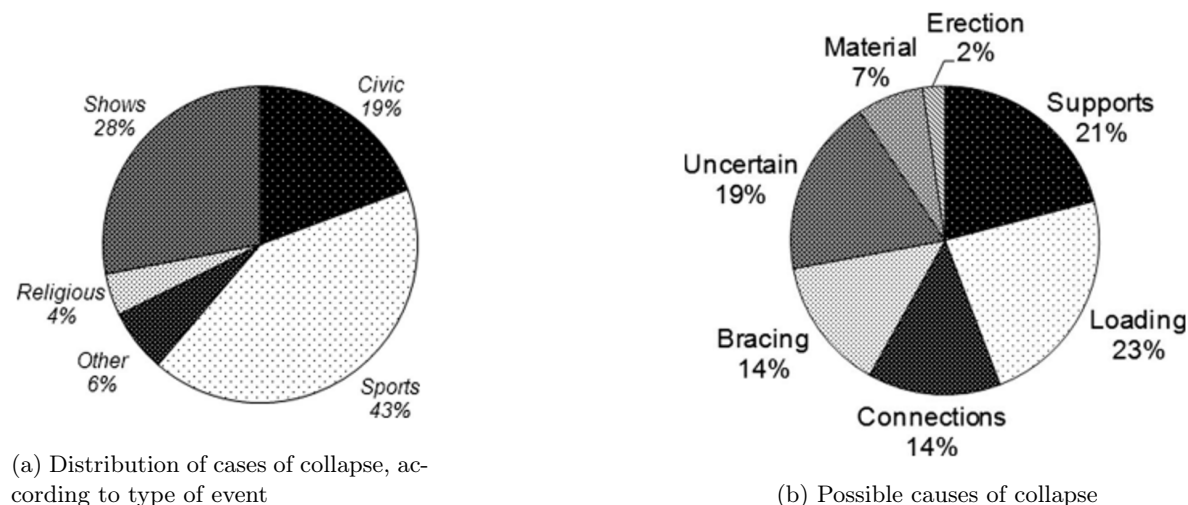


Figure 5: Pie charts statistics of accidents using demountable event structures [33]

2.2 The extreme dynamical load case of a jumping crowd

Because the extreme load case of a dynamical crowd is not something new it is to be expected that this load case is determined very well. But as can be obtained from the literature there is a high variance in design values. The Vibration Engineering Section (VES) of Sheffield University (transferred to Exeter in 2013) has done a lot of research on this topic. In 2010 they published [19]. In this paper they reviewed the most relevant studies considering human induced dynamic loads. Figure 6 shows the contradicting conclusions made in these studies.

Author	Average immobile person	Tuan and Saul [82]	Ebrahimipour et al. [67]	Moreland [29]	Tilden [64]
Action	Static	Rhythmic jumping	Periodic jumping	Jumping	'Jouncing'
Frequency	N/A	2.2 Hz	3 Hz	Unknown	N/A
Participants	1	1	1	90	1
Coordination	N/A	N/A	N/A	Unknown	N/A
Load observed	0.75 kN/person	4.50 kN/m ²	2.85 kN/person	1.13 kN/person	2.04 kN/person
Plan load (kN/m ²)	2.15	4.50	8.14	3.23	5.83
Author	Tilden [64]	Tuan [65]	Tuan [65]	Homan et al. [52]	Homan et al. [52]
Action	Sway (front-back)	Sway (side-side)	Sway (front-back)	Sway (front-back)	Sway (side-side)
Frequency	Unknown	2.2 Hz	2.2 Hz	Unknown	Unknown
Participants	1	1	1	Up to 9	Up to 9
Coordination	N/A	N/A	N/A	Unknown	Unknown
Load observed	0.36 kN/seat	0.34 kN/m of seating	0.44 kN/m of seating	0.13 kN/m of seating	0.35 kN/m of seating
Plan load (kN/m ²)	0.51	0.49	0.63	0.19	0.50

Figure 6: Observed equivalent static loads [19]

Figure 6 shows a great variety in plan loads (kN/m^2). The differences between these values can be explained by the setup of the study. Ebrahimpour et al. concludes there should be a vertical plan load of $8.14 kN/m^2$ considered, but Moreland suggests a plan load of $3.23 kN/m^2$. The fact that Ebrahimpour et al. suggests a plan load which is about 2.5 times larger than Moreland concludes, raises questions. After extensive research on the existing literature the reason for the differing values becomes clear. So, in what way is the vertical load of a jumping crowd determined? This question is answered by studies conducted by B.R. Ellis [12] [11] [13]. The conclusions drawn in these papers are accepted and referred to by prominent figures in the industry like the International Standardization Organization (ISO)[2] and Royal HaskoningDHV [3] as they refer to the work done by Ellis in their reports. The next formula (2) describes how to calculate the dynamical excitation by a crowd nowadays. An important detail in this formula and the papers by Ellis is that a rigid force plate is used by measuring the vertical force. This implies that human-structure interaction (HSI) is not considered. In this rapport the focus is on flexible structures so HSI will have an influence on the vertical force of a jumping crowd. This will be discussed later in the literature study.

$$N \cdot Q \cdot \frac{F(t)}{Q} \cdot C(N) = q(t) \quad (2)$$

In which:

- N = The amount of people per square meter
- Q = The static load of a person
- F(t) = The dynamic peak load of a jumping person
- C(N) = The coordination factor
- q = Vertical load per square meter

The differences in plan load between studies like Ebrahimpour et al. and Moreland are due to variations in the parameters of (2). Parameters like the average weight of a person do not differ much between studies. But a parameter like the amount of people per square meter has great influence on the outcome of a study. Many studies who aim to determine the load of a jumping crowd use crowd densities of 1 to 2 persons per square meter. According to Tentech engineers this density is easily reached at a festival with a lively crowd. In figure 7 ISO states that the maximum observed amount of people per square meter is 6, even for a lively crowd. On the other hand, is this density only expected in a most extreme situations and is very unlikely to occur on an event deck structure. Next to the amount of people per square meter there are two other uncertain parameters, the dynamic amplification factor ($\frac{F(t)}{Q}$) and the coordination factor. To say something about the possible ranges of these parameters they are considered in more detail in the following sections.

Table A.1 — Examples of design parameters for coordinated activities at stationary location

Activity	Common range of forcing frequency, f Hz	Crowd density		Numerical coefficient		
		Common value ^a	Maximum observed	α_1	α_2	α_3
Swaying (horizontal load) areas with seats	0.5 to 1.5	one person per seat		0,25	0,05	—
areas without seats	0.5 to 1.5		6 persons per m ²			
Vertical actions for seated audience	1.5 to 3.0	one person per seat		0,5	0,25	0,15
Coordinated jumping ^b (including jump dancing and rhythmic exercises) areas without seats	1.5 – 3.5	1,25 m ² per person	6 persons per m ²	2,1 – 0,15(f)	1,9 – 0,17(2, f)	1,25 – 0,11(3, f)
areas with seats	1.5 – 3.5	one person per seat				

^a Density of participants found in commonly encountered conditions. For special events, the density of participants can be greater and, in any case, should be verified.
^b As a first approximation, the values of α_1 , α_2 and α_3 can be taken as constant values of 1.7, 1.0 and 0.4, respectively.

Figure 7: Amount of people per square meter according to [2]

2.2.1 Varieties in dynamic amplification factor

In the 90's and 00's the researchers B.R. Ellis and T. Ji conducted multiple relevant studies. They did experiments and computed mathematical models to learn more about human-induced loads. They started off by determining dynamic amplification factors of a jumping individual, $\frac{F(t)}{Q}$, in which $F(t)$ is the measured vertical force and Q the static force of the individual. One can imagine that the dynamic amplification factor varies proportionately with the height of the jump. [12] concluded the dynamic amplification factor of a jumping individual varies between 2.3 and 4.7. They linked the amplification with a contact ratio (α). The contact ratio is a ratio between the contact duration (t_p) of the jumping person with the ground and the period of the jumping load:

$$\alpha = \frac{t_p}{T_p} \leq 1.0 \quad (3)$$

With:

- t_p = the contact duration
- T_p = the period of the jumping load

The contact period t_p can vary from 0 to T_p corresponding to different movements and activities. Therefore, different contact ratios characterize different rhythmic activities, these can be obtained in Table 1.

Table 1: Typical values of the contact ratio α for various activities [12]

Activity	α
Low impact aerobics	2/3
Rhythmic exercises, high impact aerobics	1/2
Normal jumping	1/3

Figure 8 shows a normalized load-time history for jumping with $\alpha = 1/3$ and $f_j = 1/T_p = 2.0$ Hz. The normalized load of 1.0 corresponds to the static weight of the person. The vertical axis shows the dynamic amplification factor $\frac{F(t)}{Q}$.

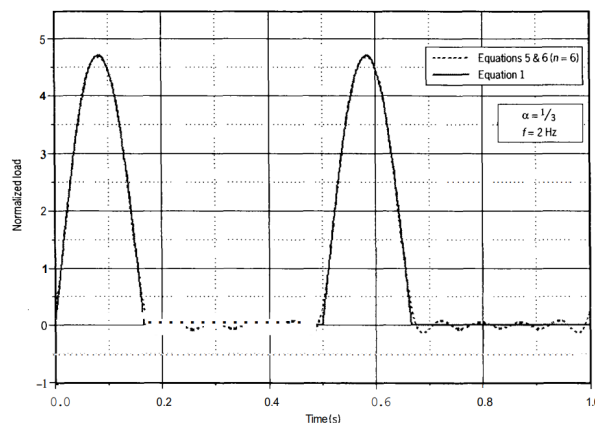
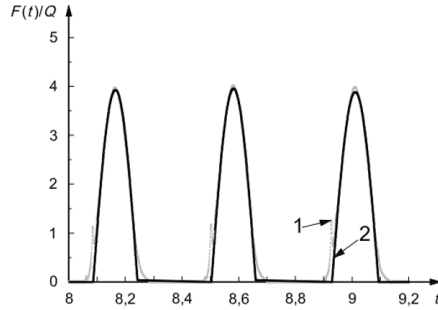


Figure 8: Load-time history for one person jumping [12]

These conclusions are considered to be valid by ISO 10137:2007. Figure 9 shows how ISO 10137:2007 considers the dynamic amplification of a jumping person with a contact ratio which is slightly higher than $\frac{1}{2}$. It can be obtained that the dynamic amplification is lower (4.0) than in figure 8 (4.7), which again proves the correlation between the dynamic amplification factor and the contact ratio.



Key
 t time, s
 $F(t)/Q$ normalized amplitude
 1 measured
 2 fitted half sine wave

Figure 9: Dynamic amplification factor of a jumping person by ISO 10137:2007

From these conclusions the wide variety in the considered load case can immediately be observed. It raises the question “what contact ratio needs to be considered for an extreme load case induced by a crowd?”. The amplitude of the dynamic amplification factor is in the end depending on the crowd, so a range of values can be considered. But because a high jump requires more energy it is assumed that high jumps are less likely to occur and for a shorter time span than low jumps.

2.2.2 Varieties in the amount of people per square meter

As is discussed earlier in the literature study, the amount of people per square meter is one of the most important parameters when determining the extreme vertical load. To gain a better understanding on the amount of people which can be present on a square meter, visual images are used.

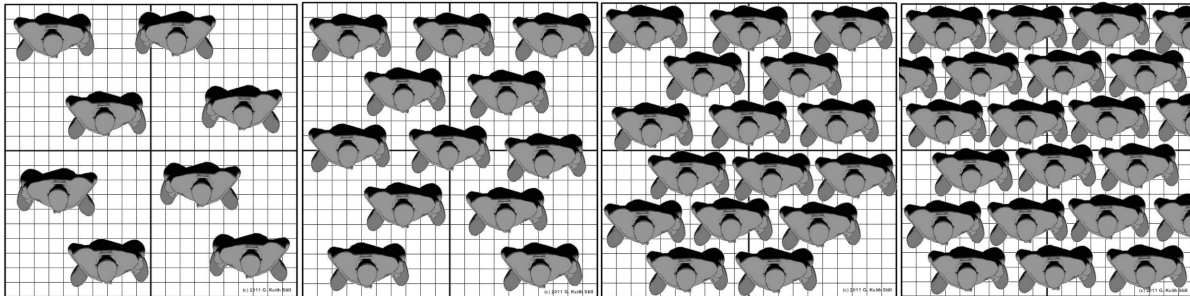
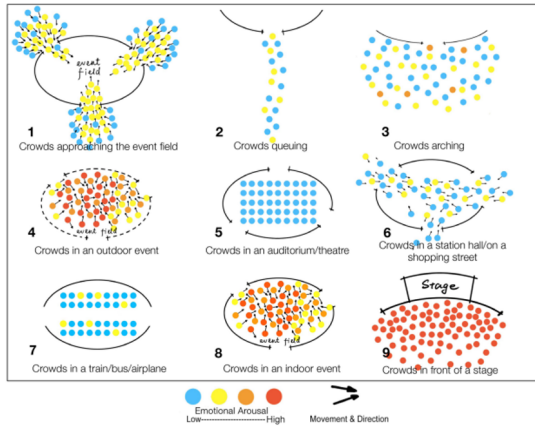


Figure 10: Visualisation of crowd densities of 2, 3, 4 and 5 persons per square meter from left to right respectively [29]

The amount of people per square meter strongly depends on the type of event and the position of a grandstand at a festival. [1] concludes that the position of a grandstand at a festival is an important parameter for the amount of people per square meter. The first rows in front of a stage are in most cases the densest. This also accounts for the front rows on a deck structure. In the industry this is named “the active viewing zone”. The crowd density in the active viewing zone is depending on multiple parameters as well.



(a) Crowd densities at different events [21]



(b) Differences in crowd densities around a stage [1]

Figure 11: Differences in crowd densities at events

In figure 7 ISO prescribes six people per square meter for a crowd which jumps in a coordinated manner. This is the maximum observed value. Considering figures 10 and 12 it can be concluded that 6 people per square meter is an extremely dense crowd. According to [29] at this density people start to panic so chances of this density occurring on a grandstand are very slim unless it is positioned in front of a stage.

Crowd density versus crowd flow rate

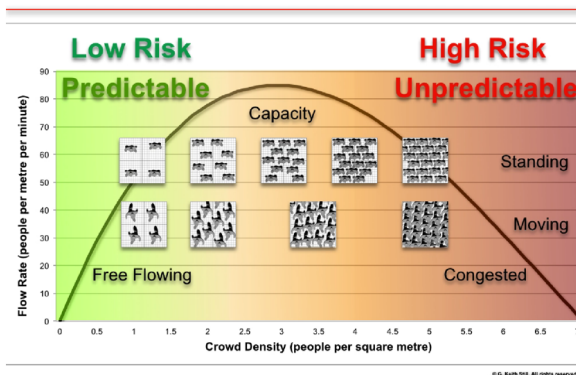


Figure 12: Crowd mobility over density according to [29]

A good indicator of how densely a jumping crowd can get is the crowd at the Goffert stadium at the moment its grandstand collapsed. Royal HaskoningDHV estimated that the static load of the crowd was $3,5 \text{ kN/m}^2$. This is based on the amount of people on the stand and the average weight of a Dutch male. Assuming the average weight of these spectators is 85 kg, this comes down to 4,2 individuals per square meter. They did not factor women in this calculation as there were none at the moment of collapse.

2.2.3 Varieties in coordination factor

The final crucial parameter of (2) is the coordination factor. This factor takes the effect into account of people not jumping exactly synchronised. If the coordination factor is not included, the assumption would be made that every excitation peak of every individual is exactly at the same moment in time. Studies show that this is not likely to occur. Figure 13 shows the vertical excitation by 2 jumping people. Both individual excitations have an amplitude of approximately 2250N, but when added together the maximum peak reaches only 3500N. If the 2 individuals would have jumped at exactly the same

moment in time a doubling of amplitude would be obtained which comes down to $2 \cdot 2250 = 4500\text{N}$. The coordination factor is determined to be $\frac{3500}{4500} = 0.78$. So the maximum value of the coordination factor is equal to 1.0.

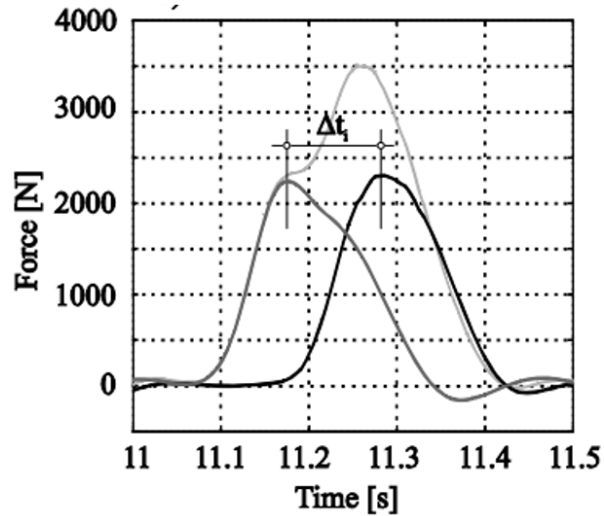


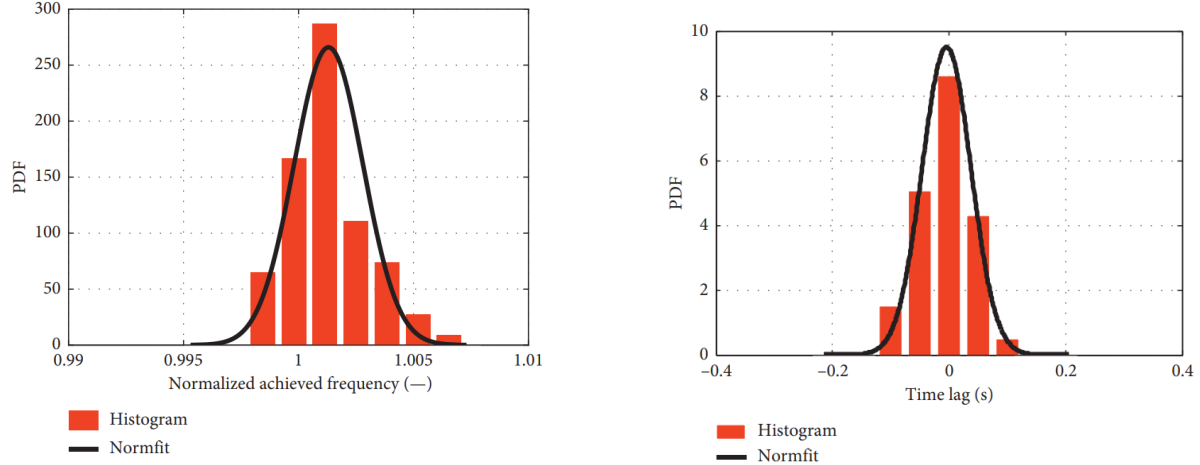
Figure 13: Time lag between jumping individuals [31]

The time lag between force peaks is a random process and can be estimated with a normal distribution. [17] wrote an extensive data-driven rapport on the synchronization of a bouncing crowd and is the most elaborate paper on crowd synchronization known by the author. Figure 14 gives an impression of the way the experiment was set up.



Figure 14: Experiment set up [17]

In [17] infrared cameras were used to track each of the forty-eight individuals. The group of participants were asked to bounce on the beat of a metronome. Figure 15a shows the estimated Probability Density Function (PDF) of the normalized achieved bouncing frequencies for all participants for the reference configuration at 1.8 Hz. Figure 15b shows the estimated PDF of the time lags identified for the reference configuration at 1.8 Hz.



(a) PDF of normalized achieved bouncing frequencies for all participants for the reference configuration at 1.8 Hz.[17]

(b) PDF of the time lags identified for the reference configuration at 1.8 Hz.[17]

Figure 15

In figure 15a it can be observed that the mean value of the normal distribution slightly shifted to the right. This implies that the metronome beat of 1.8 Hz is too slow to bounce on for the participants. Figure 16 shows that when the music frequency gets higher, it gets easier for the crowd to follow the beat.

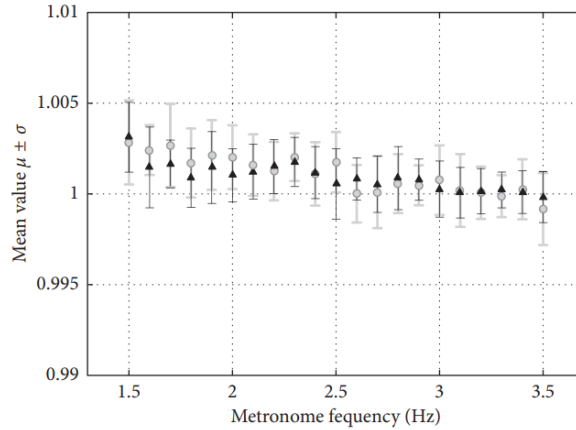


Figure 16: Distribution summary of normalized achieved frequencies in two tests for the reference configuration [17].

In [17] the coordination factor is calculated in the following way:

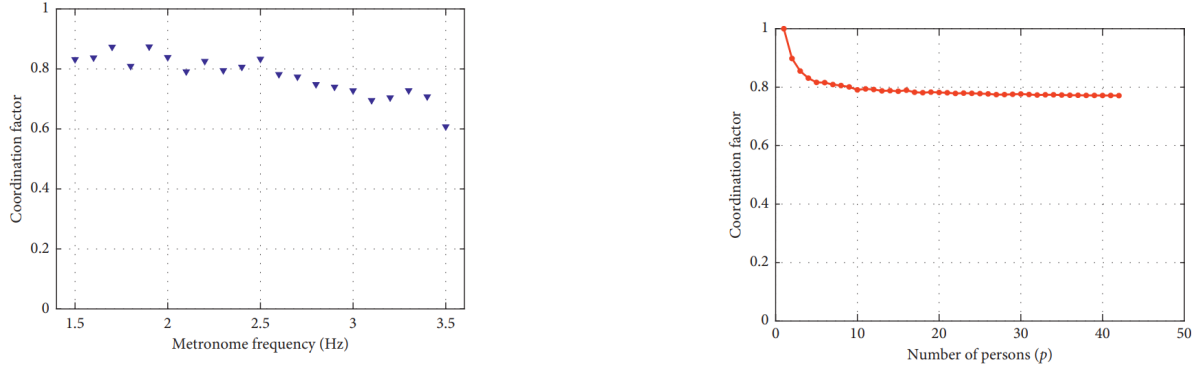
$$\rho = \frac{A_{crowd}(f_s)}{1/N \sum_{i=1}^N A_i(f_s)} \quad (4)$$

With:

- ρ = The coordination factor
- $A_{crowd}(f_s)$ = The peak Fourier amplitude of the overall crowd motion acceleration
- $A_i(f_s)$ = The peak Fourier amplitude of each individual clavicle acceleration
- N = The amount of participants

– f_s = The achieved bouncing frequency

The coordination factor ρ ranges from 0 to 1. Values of ρ close to 1 indicate a good synchronization of the crowd. On the contrary, ρ close to zero are a sign of poor synchronization. The results are shown in figure 17.



(a) Summary of coordination factors identified from the peak value of the Fourier spectrum of the overall crowd and individual motion for the reference configuration.[17]

(b) Mean value of coordination factors with different numbers of persons for the reference configuration at 1.8 Hz. [17]

Figure 17

The most important conclusion to be draw from these results is the fact that the coordination factor drops after a beat is going faster than 2.5 Hz and the fact that ρ approaches a slightly descending line after approximately 10 participants or more.

The coordination factor can be influenced by more parameters, such as the distance between people, visual and auditory guidance. These parameters are also considered in [17]. Figure 18 shows how the coordination factor relates to spatial differences between participants. Figure 18a differentiates in lateral distances and 18b in frontal distances.

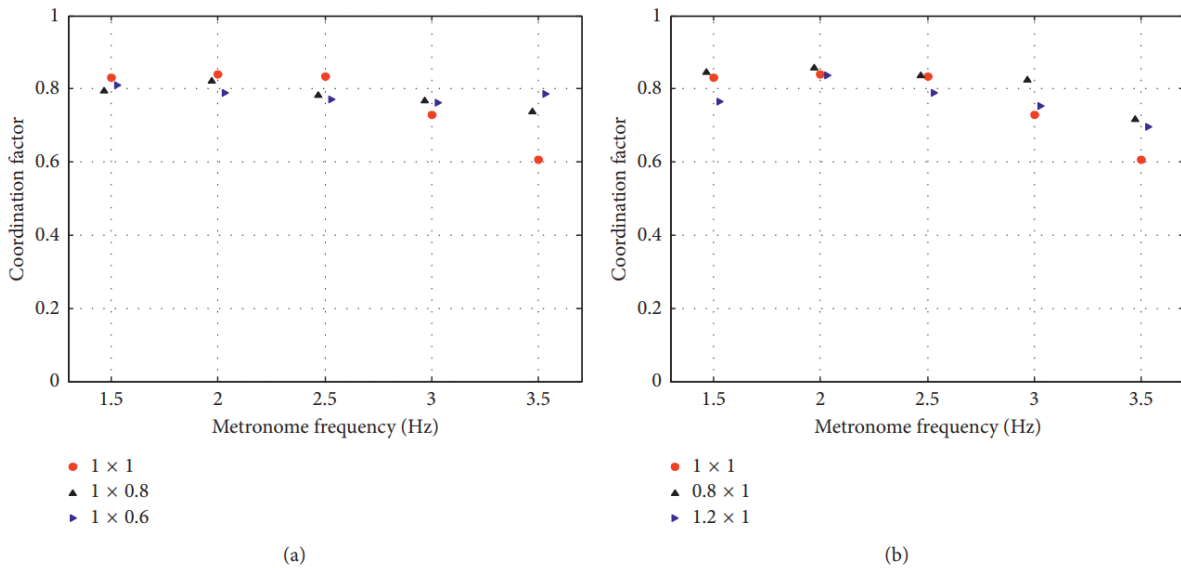


Figure 18: Comparison of coordination factors with three configurations in two groups. (a) Coordination factors in lateral differences; (b) coordination factors in frontal differences. [17].

Figure 18 shows us that spatial differences between participants hardly influences the coordination

factor in lateral and frontal perspective. It is a pity this study has only considered a minimal lateral and frontal distance of 0.6 and 0.8 respectively. In this study the focus lies on dense crowds. So data of a situation with 4 people per square meter would be preferred. But studies on coordination factors with a crowd density of 4 people per square meter are not known by the author. If the data is combined it could be concluded that the coordination factor is not affected when participants are positioned 0.6m x 0.8m apart, assuming lateral and frontal spatial differences do not influence each other.

The next parameter on the coordination factor which is studied is the influence of visual stimulation. Participants were asked to wear eye patches to determine the influence of visual stimuli to the coordination factor. The results are shown in figure 19.

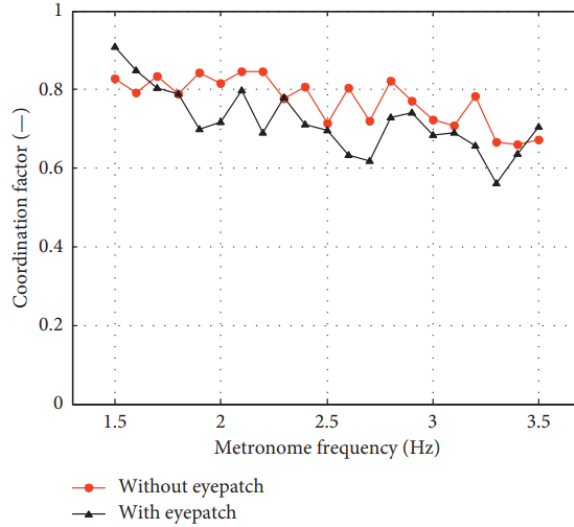


Figure 19: Comparison of the coordination factors for visual stimuli, with and without an eyepatch [17].

From figure 19 it can be concluded that the visual stimuli have indeed an influence on the coordination factor as absence of stimuli results into a lower value of ρ . In this study crowds at festivals and sport events are considered so a crowd without any visual disability is assumed.

The final parameter is a very relevant one in this study on crowd behaviour. It is the difference of auditory stimulation by a metronome or a song. This research on crowd behaviour considers a crowd stimulated by music as will be the case at festivals or sport events.

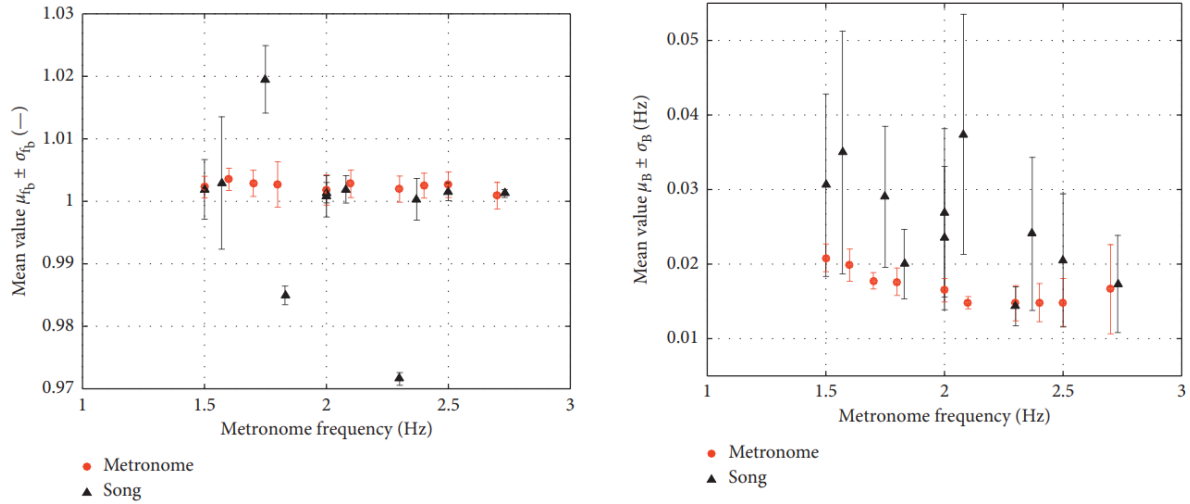


Figure 20: Comparison of the normalized achieved bouncing frequency (left) and equivalent bandwidth (right) for auditory stimuli.[17].

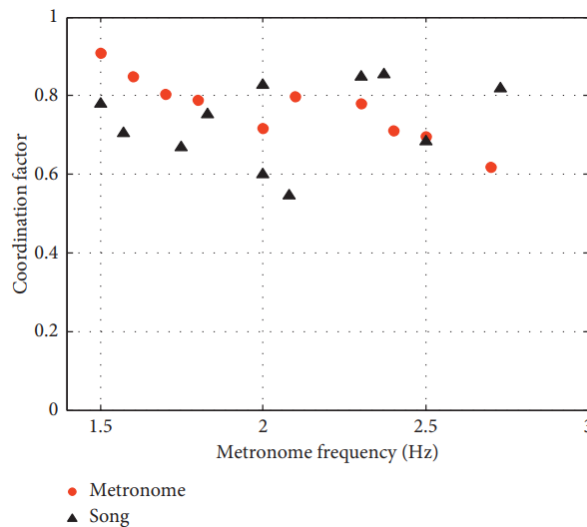


Figure 21: Comparison of the coordination factors for auditory stimuli — metronome and song. [17].

[17] concludes that "The results indicate that significantly higher levels of synchronization and a lower degree of the intrapersonal variability are attained with a metronome cue compared to the beat of songs."

Important to state with these results is that they dealt with a well organised form of synchronized bouncing. These results are relevant in the determination of what is possible in extreme situations. At festivals the expect coordination factor will be lower than 0.8, but since this research is trying to model an extreme dynamic crowd load, all possible outcomes need to be considered.

Another interesting parameter on the configuration of the coordination factor could be the influence of individuals interlocking their arms as this is often observed at festivals en sport events. The kinaesthetic sense could potentially have an influence just like the visually and auditory senses had on the coordination factor.

Furthermore the ethnicity of the participants could influence the results found in [17]. For example, Caucasian people are heavier and taller on average than the Asian participants in the study. A crowd of people with mixed ethnic backgrounds might give different results. But since the coordination factor

is determined by the ability of multiple people to jumping synchronically and not by the mechanical properties of the jump itself, it is expected that the influence of ethnic background will not result into substantially different results.

The last point of discussion is the consideration of human-structure interaction in this experiment. The experiment was conducted on a rigid floor. Hence, these conclusions are more suitable for rather stiff structures than slender structures sensitive to human-induced vibrations.

2.3 Human-structure interaction (HSI)

In the previous sections the focus was on the determination of the vertical excitation by a jumping crowd. All the information is based on experiments using rigid force plates to measure the vertical excitation by jumping people. Because of the rigidity of those force plates, there is no interaction between the jumping person and the structure. In this study the focus lies on flexible event deck structures. Because of the flexibility of event deck structures, there will be interaction between the jumping person and the structure. In existing literature this is called human-structure interaction or HSI. Because structures like event decks are so flexible, it might be preferred to take HSI into account in the determination of vertical excitation by a crowd. HSI could have an influence on the following parameters:

- The magnitude of the dynamic peak force
- The economy of the structure
- The jumping behaviour of the crowd

By taking HSI into account it is expected that a lower amplitude for the dynamic peak force will be found. It is expected that because of the flexibility of the structure, the human body will experience less g-forces which results into a lower dynamic peak force. Therefore, the structure can be designed using smaller elements which benefit the economy of the structure.

We also think that HSI can influence the jumping behaviour of the crowd. During the opening of the Millennium bridge in London in 2000 it was obtained that the vibrations of the bridge influenced the walking behaviour of the people who walked across. Because of the lateral forces excited by walking humans, the bridge started vibrating in the same direction. This caused people to correct their step which caused many people to walk in a synchronized manner. This synchronization, in turn, amplified the vibration of the bridge. The same phenomenon might occur in vertical direction on event deck structures as well.

2.3.1 The magnitude of the dynamic peak force

As is stated in the introduction of human-structure interaction, it is expected that the flexibility of a structure reduces the excitation force exerted by the human. In the paper of [26] an interesting study on HSI during short-distance free falls is described. In this study they considered a dummy child falling from 0.5 and 0.9 meter on different floor structures. They compared the peak contact force experienced by the child between a rigid structure and lightweight flexible floor structures. They found that ignoring the floor dynamics can result in an up to 35% overestimation of the contact force experience by a human.

So how does this peak reduction occur? To answer that question, it is useful to first obtain this phenomenon in a scheme. This scheme is shown in figure 22.

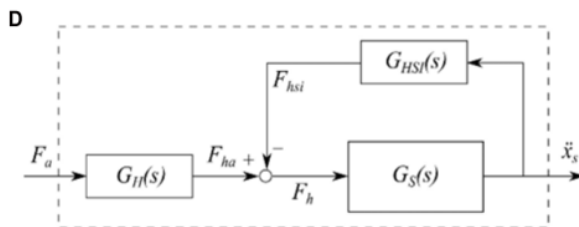


Figure 22: Schematization of the force reduction caused by HSI according to [8]

The left arrow in figure 22 is the human driving force. In [8] all forces are rewritten as Laplace transforms. So $G_H(s)$ is the Laplace transform of the human driving force, $G_S(s)$ is the Laplace transform of the forces in the structure and $G_{HSI}(s)$ represents the forces due to HSI. F_{ha} represents the force generated by humans without including the force transmitted to them due to the structural movement. Then it can be obtained that F_{hsi} is having a negative influence on F_{ha} which results into F_h . F_h represents the contact force between human and structure. Figure 22 also shows how the structural feedback influences F_{hsi} and how the forces in the system are affecting each other.

In [26] the reason for this peak reduction is explained by 3 physical mechanisms. Each mechanism has its own contribution.

The first mechanism is related to the exchange of momentum between the masses of the two impacting bodies. According to Newton's third law of motion and the principle of conservation of linear momentum, the momentum of the impacting bodies before (1) and after (2) and the collision are equal, assuming zero energy dissipation:

$$m_h \dot{x}_{h,1}(t) + m_s \dot{x}_{s,1}(t) = m_h \dot{x}_{h,2}(t) + m_s \dot{x}_{s,2}(t) \quad (5)$$

According to this principle, part of the momentum of the human body before impact is transferred to the structural mass during impact and therefore the momentum of human body decreases compared to impacting a solid object. Knowing that changes in the momentum of an object ($m \cdot \Delta v$) is equal to the impulse ($F \cdot \Delta t$) experienced by that object,

$$F \cdot \Delta t = m \cdot \Delta v \quad (6)$$

it can be concluded that the human body experiences lower magnitude of force when impacting structure compared to a solid object. In this analogy Δt is assumed to be the same for both scenarios.

The second mechanism is predominantly related to the stiffness of the impacting object. An event deck structure has less stiffness compared to a rigid object; it gives more time to the human body to decelerate during impact. This means that, for the same Δv in (9), Δt has larger magnitudes and therefore the peak impact force F is lower compared to the case of impacting a rigid object.

The third mechanism is related to the dissipation of energy by the damping of the floor structure. The energy transmitted to the floor structure during impact is dissipated by its damping while the floor structure oscillates.

In the paper of [26] they studied the peak reduction using a wide range of structural and human dynamic parameters. Before their results can be elaborated it is important to know how they described the quantity of peak reduction in their paper. The 'impact force peak error' or 'IPE' is calculated using the following formula:

$$IPE = \left[\frac{(F_{max,non,int} - F_{max,int})}{F_{max,non,int}} \right] \cdot 100 \quad (7)$$

In which:

- IPE = impact force peak error [%]
- $F_{max,non,int}$ = the peak impact force, neglecting dynamic interaction
- $F_{max,int}$ = the peak impact force, not neglecting dynamic interaction

To simulate a child falling on a force plate they used two SDOF models which are regulated by means of an agent-based model (ABM). The model is shown in figure 23.

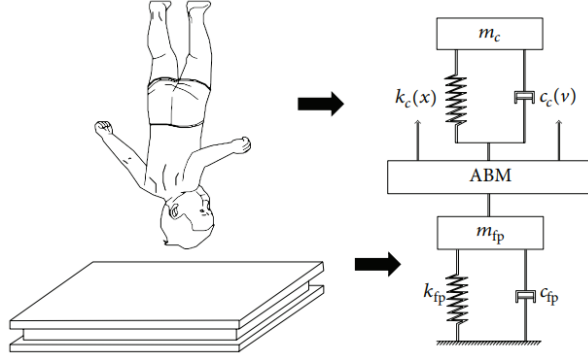


Figure 23: The schematic of the child-force plate model featuring agent-based model (ABM) at the interface between the body and the force plate [26]

Important to know in this paper is that *interaction* refers to the mutual dynamic effects of two of more independently moving DoF's in a mechanical system on one another. Based on this definition, the mere taking into account the stiffness and/or damping of the impacting surface (e.g., due to falling on a carpet) is not considered interaction here. Moreover, the focus of the proposed contact model in this study is more on the dynamics of the impact, rather than contact mechanics. The latter traditionally aims to solve problems of stress and displacement distributions in the contact surfaces during an impact, as well as the propagation of the impact wave through the impacting objects. Which is where the focus lies in this research. However, in [26], they are interested in peak impact forces acting on a falling body. To activate the system, they assigned an initial velocity to the child mass. A body falling freely through the air under the effect of gravity will experience an opposing force due to air resistance. However, this resisting force is shown to be insignificant for fall heights of less than 15 m [28] [5]. Assuming linear acceleration and neglecting air resistance, the vertical velocity “ v ” at the beginning of impact can be calculated using the following well-known formula:

$$v = \sqrt{2gh} \quad (8)$$

Where h is the initial height of the fall and g is the gravitational acceleration.

To simulate the interaction in the model they made use of an agent-based model (ABM). An ABM, sometimes called an individual-based model, is a class of computational micro scale models [16] for simulating the actions and interactions of autonomous “agents” to assess the overall system behavior. Agents are the smallest elements of the system that interact with other parts of the system. Conceptually, ABM defines the behavior of agents at the micro level, and the macro behavior of the system emerges from all the interactions between entities [23]. This architecture allows agents to perceive their “environment” and provides them with initiative, independence, and ability to interact with other agents [18].

In the paper of [26] they performed a parametric study using the model in figure 23. They varied in floor structures, so they varied in structural mass, damping coefficients and natural frequencies. And also in human properties like damping coefficients, mass and frequency. The results of this parametric study can be obtained in figure 24. Sub-figures 24a, 24c and 24e show the results regarding a typical building floor and sub-figures 24b, 24d and 24f show the results regarding a raised floor system. In sub-figures 24a and b they varied in the human damping coefficient (ζ_h), in sub-figures 24c and d they varied in effective structural mass (m_s) and in sub-figures 24e and f they varied in the natural frequency of the structure (f_s). All sub-figures show the impact peak error on the vertical axis in percentages. The higher the impact peak error, the more the peak force is reduced compared to a non-interactive floor. The horizontal axes in all sub-figures vary in human mass (m_h) and human natural frequency (f_h). The results of this study are mentioned and used in the hypothesis of this research in section 4.

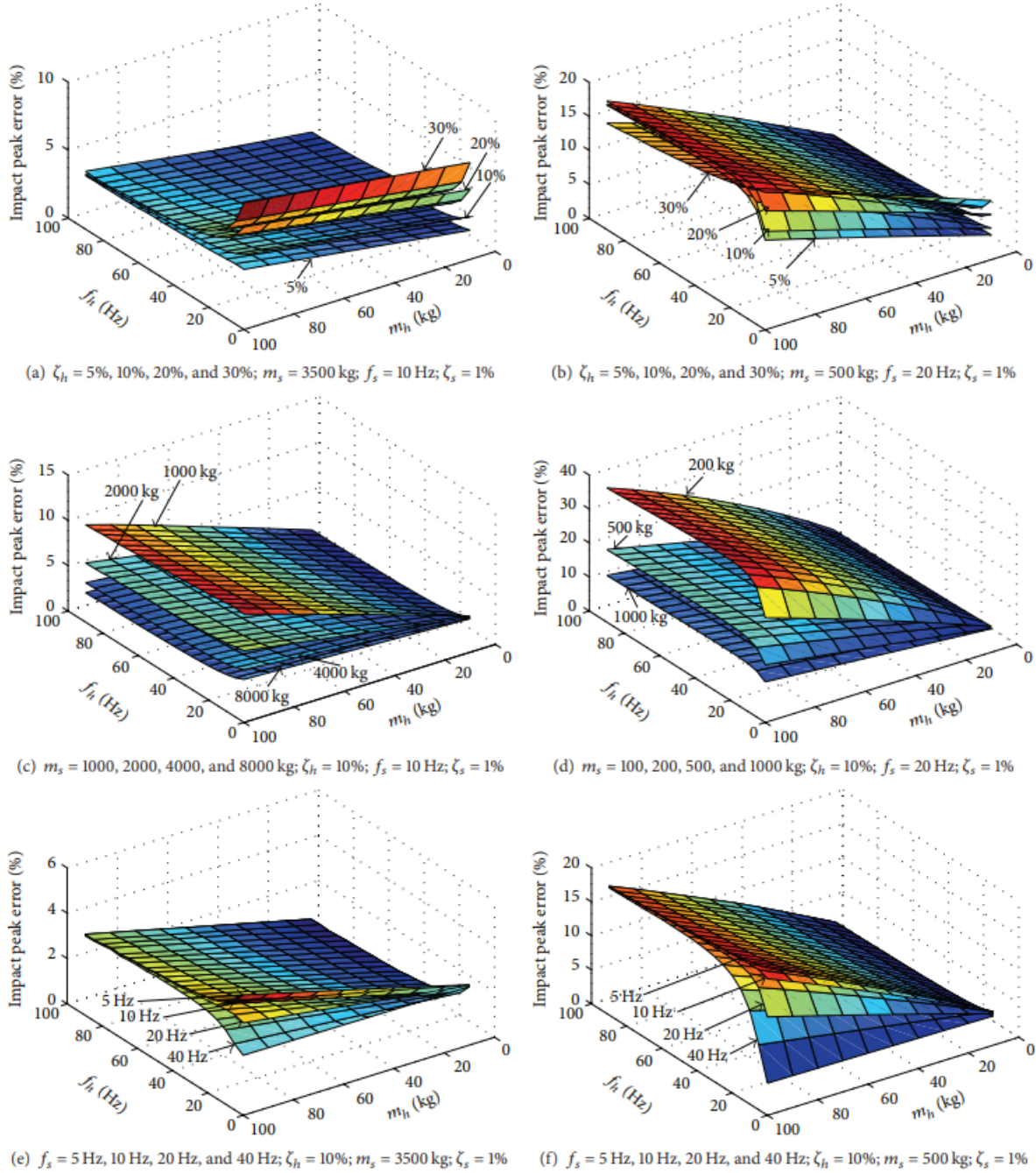


Figure 24: Effects of taking into account the floor dynamics on the peak impact force experienced by a human body: a typical building floor ((a), (c), and (e)) and a raised floor ((b), (d), and (f)) [26]

From figure 24 it can be concluded that under certain circumstances the peak force of a falling person can be reduced by 35% due to HSI. Nevertheless, in standard literature about jumping people HSI is not considered in most cases. This might have something to do with the difference between jumping and falling on a structure. But literature on HSI, especially regarding IPE, caused by a jumping crowd is very slim. This gives reason for more research on this topic.

2.3.2 Modelling of human-structure interaction during jumping

Just as the reduced peak force, the term HSI is also used to indicate that people are taken into account in the total dynamic system. So instead of seeing people on a structure solely as a load, the people participate in the total dynamic system. Because human mass for example, has influence on the natural frequency of a structure. Which means that different natural frequencies are found for empty structures than for occupied ones. In most literature like [10], HSI is all about the changing dynamical properties of a structure while occupied by a crowd. They found interesting results. The first vertical natural frequency of a grandstand can reduce from 16 Hz (empty structure) to 5 Hz (fully occupied). Especially for event structures, as they are light in weight and are high in frequency (about 30 Hz). Figure 25 shows Autospectra for vertical vibrations of a temporary grandstand: (a) with no crowd, (b) with full crowd.

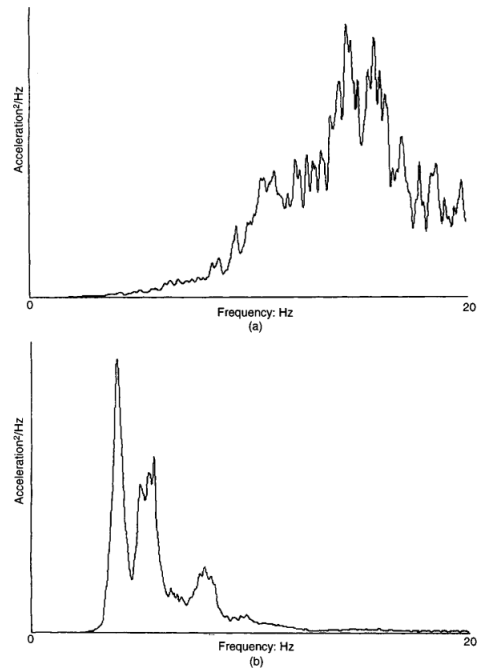


Figure 25: Autospectra for vertical vibrations of a temporary grandstand: (a) with no crowd, (b) with full crowd [10]

In [10] the authors analysed the dominant frequency of 136 different measurements. Figure 26 shows each dominant frequency per file. It clearly depicts the difference between an empty and full grandstand.

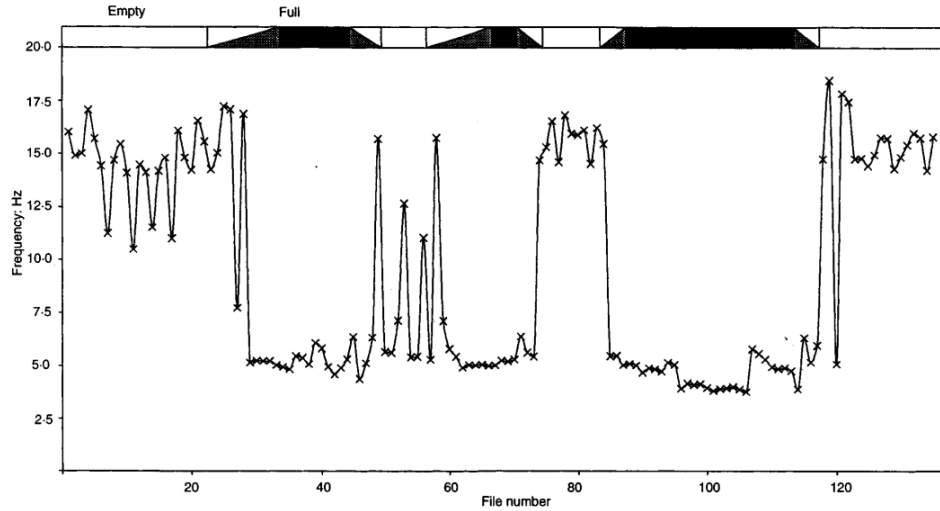


Figure 26

Important to know is that the crowd on these grandstands was not moving. So as the structure vibrated, the people vibrated with it. According to [10], "*Jumping and walking provided interesting results in that they did not affect the measured system characteristics, either frequency or (as far as can be resolved) damping, although the forced response could be seen clearly. The unchanged system characteristics would appear to be because the human body is not vibrating with the beam and hence for these situations it acts solely as a load.*"

In the last couple of years, the interest of modelling jumping people on flexible structures has intensified. In standard literature about the determination of jumping forces [11] [12] [13], HSI was often neglected. It was only of interest if it regarded the changes of dynamical properties of the system. In 2019 a research team published a paper in which they tried to simulate the time history of a jumping person on a flexible structure [15]. This is the most accurate paper on the simulation of a jumping person on a flexible structure known by the author. Figure 27 shows the results of a jumping person on a force plate which is placed on top of a vibrating structure. The left graph shows the difference between the body inertial force and the measurements from the force plate. The body inertial forces are of the same magnitude as expected from a person jumping on a rigid structure. This clearly shows the IPE in this system.

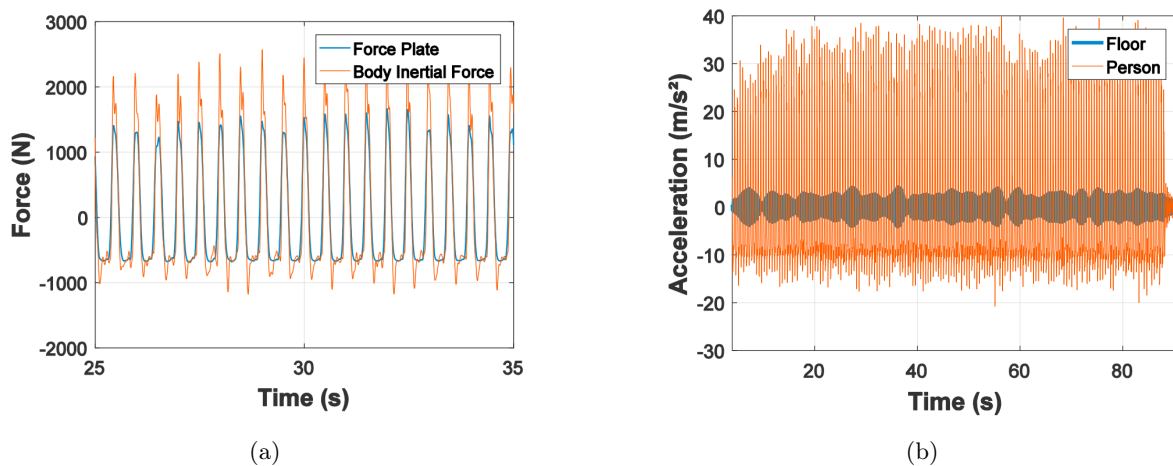


Figure 27: Time history results of a person jumping on a force plate which is attached to a vibrating structure [14]

In this paper they used a flexible structure with a fundamental frequency of 3.84 Hz. To learn which model estimates the time history of a jumping person on a flexible structure best, they considered 3 models. These 3 models are shown in figure 28. Model (a) prescribes a force-only model. Note a force $P'_{gnd}(t)$ is used. The apostrophe implies they included the IPE. Model (b) uses the same model but with an increased participating mass m_{os} . m_{es} represents the weight of an empty structure, m_{os} has included the participating mass of the crowd. In model (c) the crowd is modelled as a second degree of freedom with dynamical properties k_h and c_h .

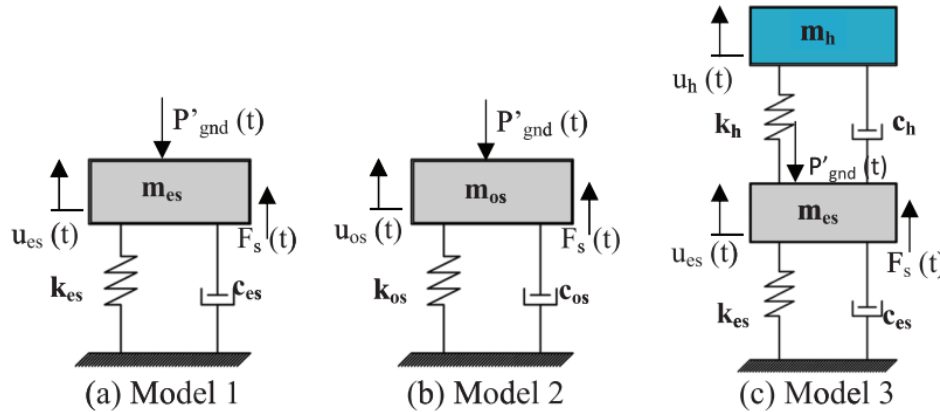


Figure 28: Models considered in [15]

Table 2 shows the results of the experimental structural response compared to model 1. The first important conclusion that can be made is that the results are depending on the jumping frequency of the person. It can be observed that the model does not predict the experimental motion very accurately, except when jumping with a 2.27 Hz frequency. But if the person jumps at a resonant frequency of 1.89 Hz ($2 \times 1.89 = 3.84$, so in second harmonic) the analytical results can differ 192% from the experiment.

Table 2: Experimental results against numerical results of model 1 [15]

Rhythmic activity frequency (Hz)	Human body response			Experimental structural response			Numerical structural response (model 1 - SDOF force-only)		
	Normalised force (P'_{gnd}/G)	Normalised acceleration (a/g)	Displacement (m)	a_p ($m s^{-2}$)	$a_{w,rms}$ ($m s^{-2}$)	VDV ($m s^{-1.75}$)	a_p ($m s^{-2}$)	$a_{w,rms}$ ($m s^{-2}$)	VDV ($m s^{-1.75}$)
1.89	3.10 ± 0.21	1.93 ± 0.29	0.021 ± 0.012	7.05	2.86	11.10	20.57 (192%)*	7.31 (156%)	31.63 (185%)
2.00	3.22 ± 0.22	4.46 ± 0.31	0.100 ± 0.008	4.24	1.88	6.60	6.57 (55%)	2.59 (38%)	9.71 (47%)
2.27	3.74 ± 0.23	5.23 ± 0.23	0.080 ± 0.012	2.62	0.86	3.13	2.52 (-4%)	0.91 (6%)	3.30 (5%)
2.86	3.64 ± 0.15	5.17 ± 0.15	0.054 ± 0.009	1.93	0.65	2.46	2.36 (23%)	0.80 (24%)	3.09 (26%)

*The values in brackets indicate the relative differences between the numerical and the experimental acceleration.

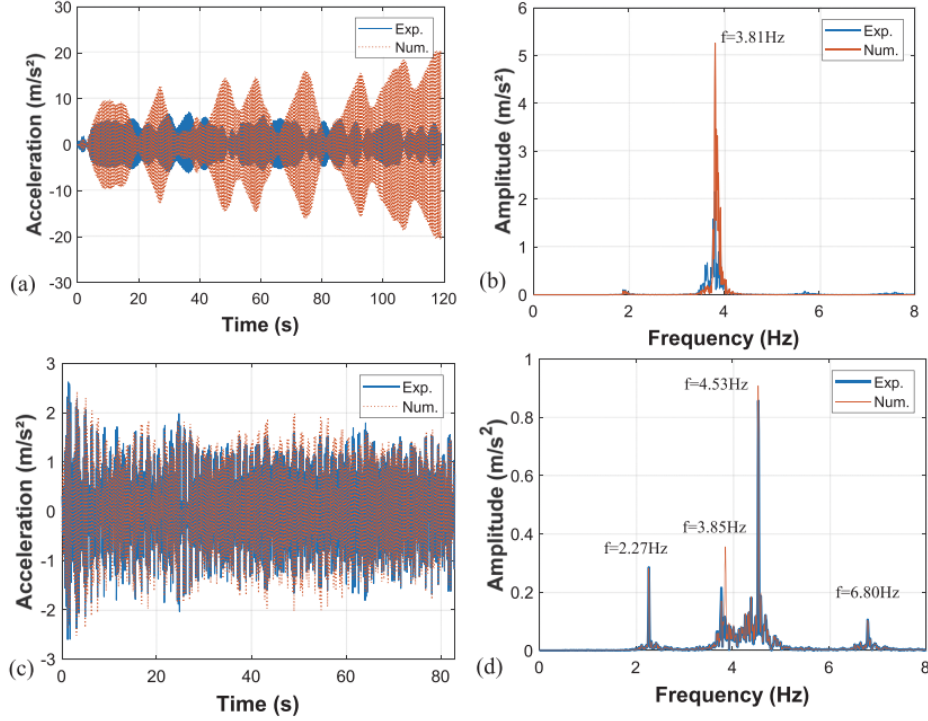


Figure 29: Results model 1 of 1.87 Hz. excitation (a and b) and 2.27 Hz. (c and d)

Because of the poor results using model 1 considering the resonance frequency, [15] considered models 2 and 3. Table 3 shows the used dynamic properties of both models. From table 4 the results relative to the experiment can be obtained and figure 30 depicts the results of the experiment and model 3 over time and in frequency domain.

Table 3: Optimized Dynamic body parameters model 2 and 3

Rhythmic activity frequency (Hz)	Occupied structure (model 2 - SDOF)					Occupied structure (model 3 - 2DOF)				
	m_{os} (kg)	c_{os} (N.s/m)	k_{os} (N/m)	f_{os} (Hz)	ξ_{os} (%)	m_h (kg)	c_h (N.s/m)	k_h (N/m)	f_h (Hz)	ξ_h (%)
1.89	1987.94	1287.87	1100000.10	3.744	1.38	66.45	1555.38	59696.33	4.77	39.05
2.00	1964.53	510.59	1119693.93	3.800	0.54	35.48	1336.05	43721.56	5.59	53.64
2.27	1961.71	710.93	1136427.75	3.831	0.75	26.77	596.62	8702.88	2.87	61.80
2.86	1949.18	677.30	1132759.83	3.837	0.72	26.16	466.65	6215.59	2.45	57.86

Table 4: Relative results model 2 and 3 to the experiment

Rhythmic activity frequency (Hz)	Occupied structure (model 2 - SDOF)			Occupied structure (model 3 - 2DOF)		
	a_p ($m s^{-2}$)	$a_{w,rms}$ ($m s^{-2}$)	VDV ($m s^{-1.75}$)	a_p ($m s^{-2}$)	$a_{w,rms}$ ($m s^{-2}$)	VDV ($m s^{-1.75}$)
1.89	6.05 (-14%)*	2.46 (-14%)	9.82 (-12%)	6.09 (-14%)	2.52 (-12%)	10.07 (-9%)
2.00	3.92 (-8%)	1.72 (-9%)	6.10 (-8%)	3.87 (-9%)	1.69 (-10%)	6.03 (-9%)
2.27	2.25 (-14%)	0.85 (-1%)	3.04 (-3%)	2.26 (-14%)	0.86 (0%)	3.06 (-2%)
2.86	1.82 (-5%)	0.63 (-3%)	2.37 (-3%)	1.83 (-5%)	0.63 (-3%)	2.38 (-3%)

*The values in brackets indicate the relative differences between the numerical and the experimental acceleration

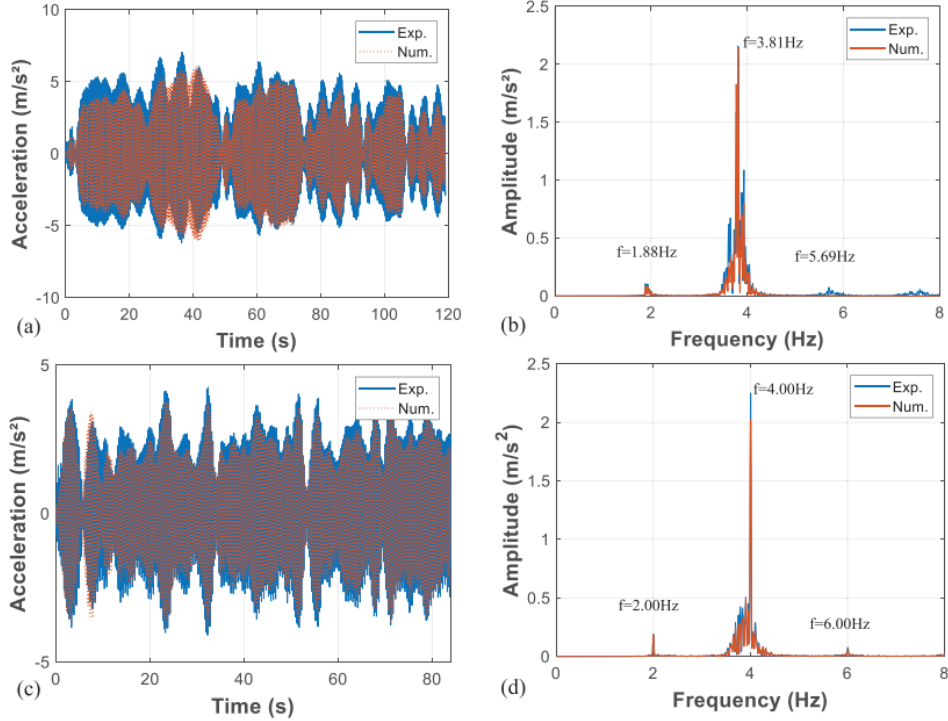


Figure 30: Dynamic response of the floor considering the experimental (blue lines) and the numerical accelerations (red lines – Model 3): In time domain during jumping at 1.89 Hz (a) and 2.00 Hz (c) and their corresponding amplitudes in frequency domain at 1.89 Hz (b) and 2.00 Hz (d)

Considering the results from [15], model 2 and 3 both simulate the experimental results well. From this paper it can be concluded that when simulating a jumping person on a flexible structure, the participating weight should at least be taken into account. Another important conclusion from this paper is that when simulating the dynamics of a structure which is excited by a jumping person, a load which takes the IPE into account needs to be considered.

2.4 The Royal HaskoningDHV report on the collapsed grandstand of the NEC stadium De Goffert

On Sunday the 17th of October 2021, a grandstand element of The Goffert stadium collapsed during a football match between NEC and Vitesse. At the moment of collapse, the grandstand was occupied by fans. Figure 31 shows a picture of the collapsed element after the game.



Figure 31: Collapsed grandstand element NEC stadium. Source: <https://www.vi.nl/nieuws/ingenieursbureau-doet-onderzoek-naar-ingestorte-tribune-goffertstadion>

The main reason for the collapse was an extremely high excitation caused by a dense crowd who were jumping to a musical beat. Although a grandstand structure like this does not share the same dynamical properties as an event deck, this event has a major overlap with the subjects which are discussed in this research. A very dense crowd jumped to a musical beat which caused a dynamic excitation of approximately 9 kN/m^2 [3]. This incident shows how large forces of a jumping crowd can get. The report written by Royal HaskoningDHV (RHDHV) is analysed to find out how prominent structural engineers analysed this incident. To determine the dynamic load of a jumping crowd they considered the following 4 factors:

- The dynamic amplification factor
- The coordination factor
- The resonance factor
- The impact factor

In this literature study the dynamic amplification factor and the coordination factor are already discussed. It is expected that the resonance factor will not have a substantial impact on the determination of the jumping load of a crowd because of the significant difference between jumping frequency (1.5 to 2.8 Hz) and the first vertical natural frequency of an event deck (about 30 Hz). So this factor will not be discussed in this literature study. The effect of the resonance factor will always be taken into consideration in this research if it turns out that the resonance factor does have an influence on the determination of crowd-induced loads on event deck structures.

2.4.1 The Impact Factor

So what is the impact factor (IF) exactly? According to the RHDHV rapport: "*The impact factor is a factor considering the response of the structure on a single jump, expressed as the ratio between the maximum internal force caused by a single jump and the dynamical force relating to the jump.*" Thus, the RHDHV rapport determined the impact factor by dividing the internal response peak force with the imposed peak force, extracted from their dynamic model. They claim the impact factor is equal to 1.0 for rigid structures. When the stiffness decreases the impact factor will increase, but for very flexible structures the value will decrease and reach values below 1.0. Analogous to a normalized seismic response spectrum like depicted in figure 32. Most structures which are excited by a jumping crowd will have an impact factor somewhere between 1.05 and 1.9 depending on the stiffness of the structure.

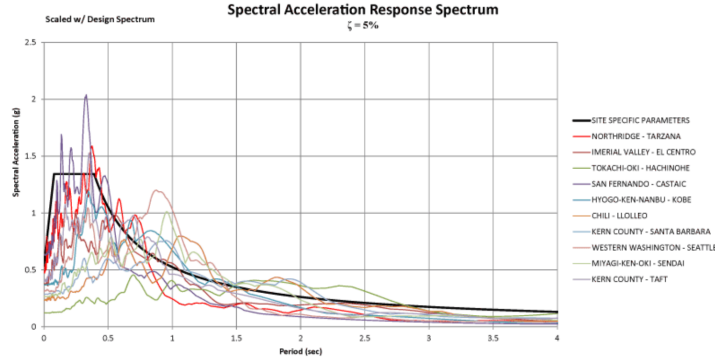


Figure 32: Seismic response spectrum

Just like a seismic response spectrum, the impact factor is influenced by the natural frequency of a structure and the shape of the excitation. In [3] it can be obtained how a square-like pulse excitation results in a higher impact factor compared to a sinusoidal shaped force. When they considered the NEC grandstand structure, which is a stiffer structure ($\omega_n = 10\text{-}12\text{ Hz}$) than the one considered in [14], they observed the impact factor being higher than 1.0.

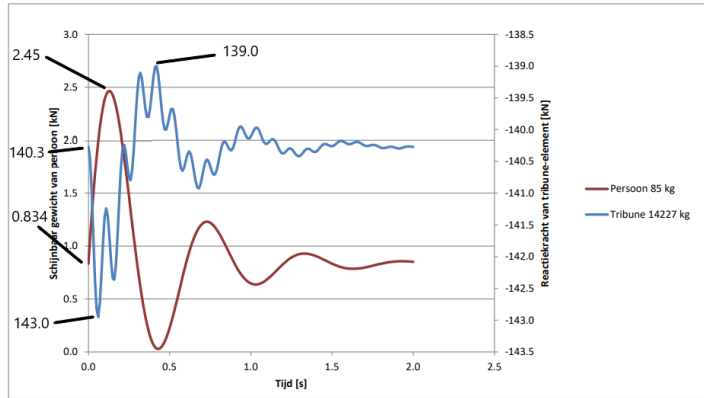


Figure 33: Indication of the interaction between a person with a mass of 85 kg who jumps on a grandstand with a structural mass of 14227 kg and an eigenfrequency of 10 Hz [3]

Figure 33 shows how the impact factor is determined. The blue line represents the reaction force of a grandstand structure. Be aware of the double vertical axis, the left axis relates to the imposed force, the right axis relates to the internal force. The red line shows the force-time diagram of a jumping person. The values of both lines at $t=0$ represent their static quantities. For the jumping person this is 0.843 kN, for the grandstand this is 140.3 kN. When the person jumps and reaches its peak value, the reaction force in the grandstand reaches its highest value at almost the same time. The difference between static and peak value of the jumping person is $2.45 - 0.834 = 1.616\text{ kN}$. The difference between static and peak value of the reaction for in the grandstand is $143.0 - 140.3 = 2.7\text{ kN}$. So the impact factor is determined to be $2.7 / 1.616 = 1.67$.

Figure 34 shows the dynamic response of the NEC grandstand. The left two figures show the result of a non-damaged structure with $f_n = 10\text{ Hz}$ and the figures on the right depict a damaged structure with f_n being 5 Hz. For the stiffer non-damaged structure it is observed that the impact factor approaches a value of 1.0. For the damaged structure it is obtained that the impact factor has increased as the difference between the internal peak and the imposed peak has amplified.

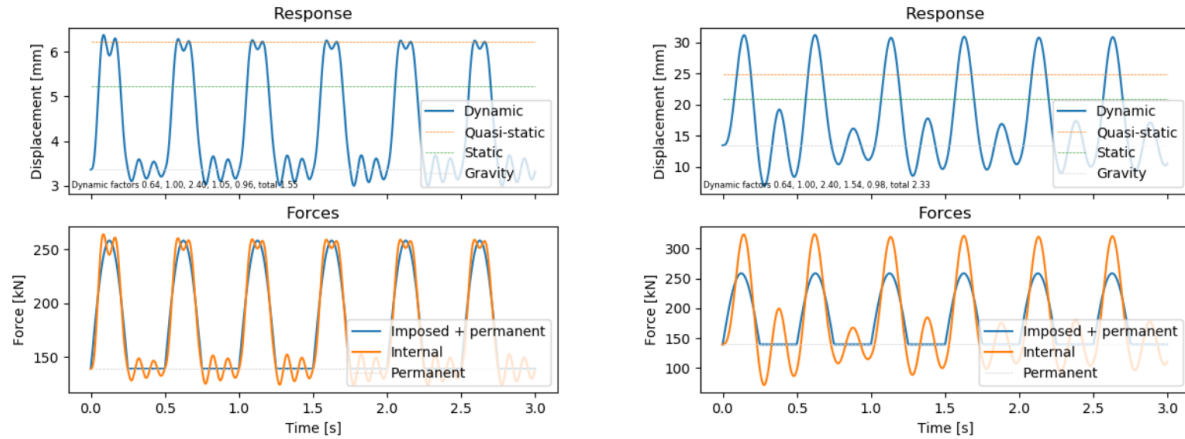


Figure 34: Results linear SDOF analysis, damaged (right two graphs) and undamaged (left two graphs) [3]

From these results it can be concluded that the impact factor can have large influences on the internal stresses of structures. Event decks are usually checked using static equivalent forces. Impact factors can only be obtained using dynamical models. So it can be assumed that during the design of event decks, the impact factor is not taken into account. Which could result into large design errors as an impact factor can reach values up till 1.9.

2.4.2 Lock-in effect

The lock-in effect represents the effect of exerting a force at the same time a structure is moving downwards. This results in a larger resonant factor. Figure 35 shows how the lock-in effect results in larger deformations considering the NEC grandstand structure.

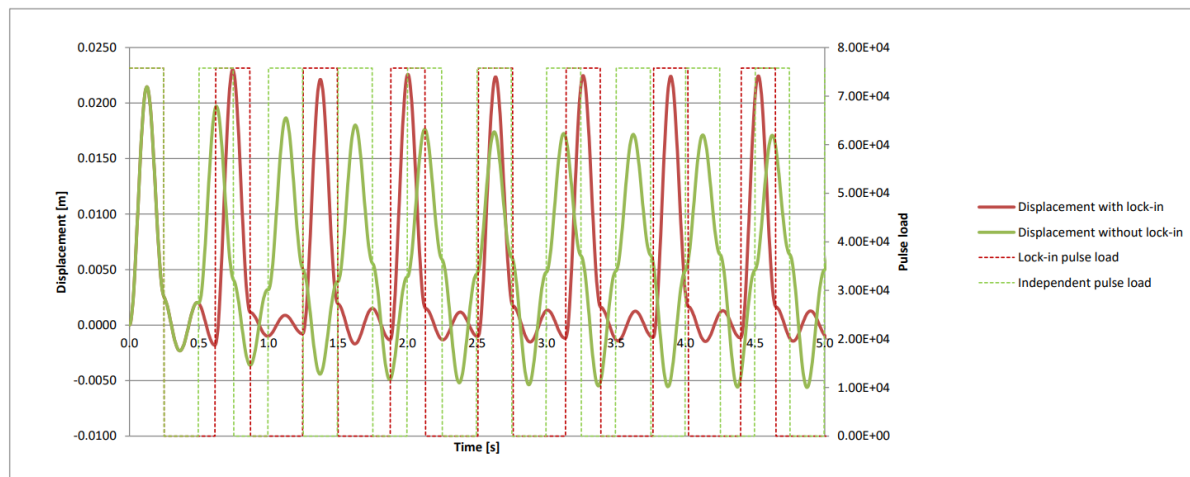


Figure 35: Lock-in effect considering the NEC grandstand in [3]

RHDHV only considers a lock-in effect using pulse excitations. To obtain the effect, the structure is set to have an eigenfrequency of 4 Hz and the excitation the be 2 Hz. This is the result shown by the green dashed line. The red dashed line is chosen in such a way that the pulse load is applied at the moment the displacement of the structure is at its highest point (peak negative value). This results in an excitation of 1.7 Hz. From figure 35 it can be obtained that the lock-in effect can cause a $0.022 / 0.016 = 1.375$ (peak displacements after 4.5 seconds of jumping) amplification of the resonance factor.

3 Main research question

From the literature study it can be concluded that during the design phase of event structures dynamic interaction is often neglected. Studies have shown that neglecting human-structure interaction can lead to errors up to 35% in the determination of impact loads. This error could potentially be used to reduce the load which is assumed for jumping humans on flexible structures. Reducing this load can lead to more economic structures.

Next to this reduction, factors like the impact factor can increase structural stresses up to 90% compared to stresses resulting from equivalent static forces. Nowadays event deck structures are designed assuming static loads. If the impact factor causes significantly higher stresses in the structural elements, this can lead to dangerous situations. These findings have led to the following research question:

What is the effect of dynamic interaction on an event deck structure when it is vertically excited by a jumping crowd?

In this question dynamic interaction is defined to regard the following 2 factors:

- The impact force peak error (*IFE*)
- The impact factor (*IF*)

In this paper the influence of these two factors on structures will be researched. The focus is on event deck structures which are light in weight and have a first natural frequency in vertical direction of approximately 30 Hz. Both factors will be overseen in the same manner which leads to the following sub questions:

3.1 Sub questions on the impact force peak error

- What parameters influence the impact force peak error?
- How do these parameters influence the impact force peak error?
- To what extent does the impact force peak error influence the imposed force on an event deck structure which is excited by a jumping crowd?
- Does the coordination factor of a jumping crowd affect the impact force peak error?
- Do structural vibrations influence the impact force peak error in event decks?

3.2 Sub questions on the impact factor

- What parameters influence the impact factor?
- How do these parameters influence the impact factor?
- To what extent does the impact factor influence the stresses in an event deck structure which is excited by a jumping crowd?
- Does the coordination factor of a jumping crowd affect the impact factor?
- Do structural vibrations influence the impact factor in event decks?

4 Hypothesis

4.1 Hypothesis on the impact force peak error

It is assumed that the results regarding the *IFE* will be similar to the findings in [26]. In this paper they varied in all possible dynamic system parameters. In the human part they varied in human natural frequency (f_h), human mass (m_h) and human damping (ζ_h). In the structural part they also varied

in structural natural frequency (f_s), structural mass (m_s) and structural damping (ζ_s). The paper concludes that all system parameters have some influence on the *IPE* but some contribute more than others.

To find out how these system parameters influence the *IPE* a great deal can be learned from the findings in [26], these findings are depicted in figure 24 in section 2.3.1. It can be obtained that in general, when m_h increases, the *IPE* increases. This is according to contact mechanics, because when m_h increases, it transfers more kinetic energy to the structural DoF during impact and therefore remains with less energy. However, *IPE* does not show significant sensitivity to ζ_h . *IPE* is more sensitive to f_h when $5 \text{ Hz} < f_h < 20 \text{ Hz}$ and in general increases as ζ_h increases. Up to 8% and 18% overestimation of peak impact force is expected within this f_h range for the selected building floor and raised floor systems, respectively. In the next set of simulations, the mass of the building floor and the raised floor SDOF models varied between $1,000 \text{ kg} < m_s < 8,000 \text{ kg}$ (Figure 24(c)) and $100 \text{ kg} < m_s < 1000 \text{ kg}$ (Figure 24(d)), respectively. ζ_h was taken equal to 10% in these simulations. Both figures show the considerable sensitivity of the *IPE* (up to 12% and 37% error for building and raised floor systems, resp.) to the ratio of the mass of the floor structure to the human model mass. The lower this ratio is (higher human mass and lower structure mass) the more prominent the contribution of the floor dynamics in the impact force experienced by the falling human is. In the last set of simulations, the natural frequency of the floor structure varied between $5 \text{ Hz} < f_s < 40 \text{ Hz}$ (Figures 24(e) and 24(f)). Similar to the effects of ζ_h (Figures 24(a) and 24(b)), *IPE* is more sensitive to f_s when $5 \text{ Hz} < f_h < 20 \text{ Hz}$ and generally increases as f_s decreases. In general, the effects of floor dynamics are more prominent when the structure is lightweight and has lower frequency. The effects of structural natural frequency are more visible when the falling human is characterized with a low frequency and high mass model.

In this research the focus is on jumping humans. This results in a low human natural frequency in comparison with free falling humans. In [26] they assumed a head-first collision between human and structure. An average contact time (Δt) of such a collision is about 0.01 seconds. If the collision force curve is assumed to be half a sinusoidal cycle then $f_h = \frac{1}{2 \cdot 0.01} = 50 \text{ Hz}$. In a jump the impact force is absorbed by the legs which can bend a great deal and gives more time to the human body to decelerate. This results in a typical jumping frequency of approximately 2 Hz ($\Delta t = 0.25$ seconds). In figure 24, subfigures b, d and f can be best compared to the researched structure as they are the lightest and have the highest natural frequency. In all 3 subfigures it can be obtained that the *IPE* decreases for a decreasing f_h . The only situation in which the *IPE* increases is in subfigure b where they assume ζ_h to be 30%, but since it is assumed that ζ_h is equal to 0% in this research, it is expected the *IPE* in this model will be lower than 10%.

4.2 Hypothesis on the impact factor

From the RHDHV rapport [3] it can be concluded that the impact factor is dependent on the course of the dynamical force in time caused by a jump and the fundamental frequency of the structure. In the researched case this is the first natural frequency in vertical direction.

The impact factor is equal to 1.0 for rigid structures. Whenever its stiffness decreases, the impact factor first increases and for very flexible structures it decreases again. For very flexible structures the impact factor can get lower than 1.0, just as can be obtained in normalized seismic response spectra. For most floor systems on which jumping forces occur, the impact factor lies between 1.05 and 1.9.

In figure 34 of section 2.4.1 it can be obtained how the natural frequency of the structure influences the impact factor as the structure is excited by a sinusoidal load of 2 Hz. The left 2 graphs represent a structure with $f_s = 10 \text{ Hz}$ and the right two graphs represent a structure with $f_s = 5 \text{ Hz}$. It can be obtained how the impact factor increases for the 5 Hz structure. In this research the load curve is considered to also be a sinusoidal load with a 2 Hz frequency. Knowing the natural frequency of this structure will be around 30 Hz, it is expected that the impact factor in this case will be even lower than in the left two graphs of figure 34.

It is assumed that the coordination factor will cause the cumulative excitation curve of all jumping persons on the structure to have a longer period. The coordination factor will cause time intervals between each person, this can only result in a longer excitation period. Figure 36 shows the results of the linear SDOF analysis in [3] for the undamaged structure ($f_s = 10 \text{ Hz}$) when excited by a combination

of a pulse and a sinusoidal load and a square-shaped pulse load.

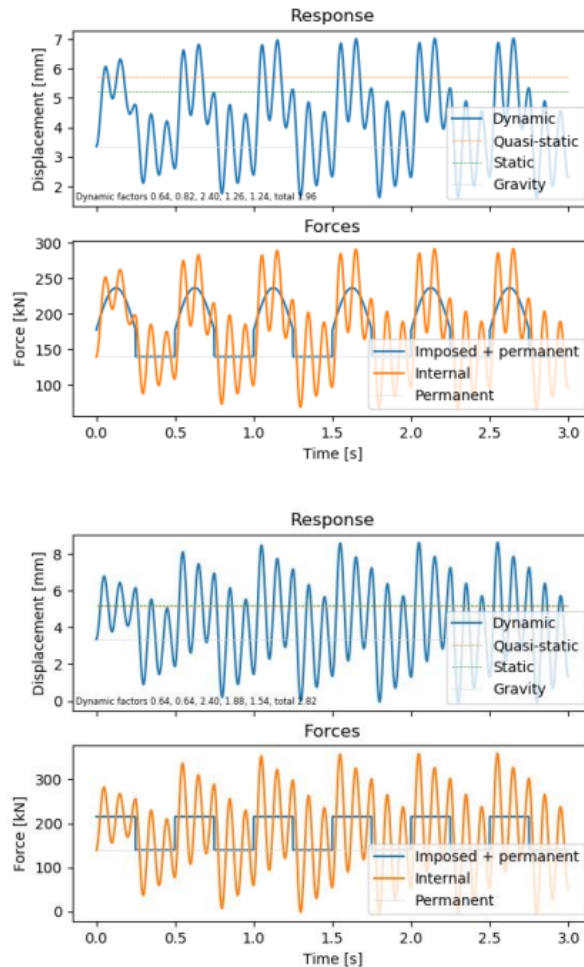


Figure 36: Results linear SDOF analysis, combination of square-shaped pulse load and sinusoidal load (upper two graphs) and square-shaped pulse load (lower two graphs) [3]

From figure 36 it can be concluded that for a structure with a natural frequency of 10 Hz, a faster increasing load causes a higher impact factor. Because the coordination factor will cause the total load to increase slower, it is expected that this results in a lower impact factor.

5 Model

5.1 Choice in model software

The first important choice to make is which software to use regarding this problem. This problem is dynamic in nature, so software is needed which is capable to deal with dynamic problems. Next to that, software is needed which is able to read structural data such as stresses and deformations.

Adams is software in which multibody dynamic simulations can be modelled. Mechanical engineers often use it to determine governing load cases in machines. Adams can be used to simulate a wide variety of problems and might be suitable to provide proper answers to the research questions. But after analysing output data and seeing how these bodies are modelled, it is assumed that Adams falls a bit too short when considering structural details. Moreover, nobody in the thesis committee has much experience regarding Adams which makes it harder to learn to work with the software.

The author believes **Abaqus** is great software to use regarding the problem. It is widely used to

simulate structural dynamic problems, can deliver highly detailed results, and is used by some of the thesis committee members. For these reasons it is decided to use Abaqus as modeling software.

5.2 Modelling plan

It is intended to model a jumping crowd on an event deck structure as realistic as possible. The interest lies in the two factors mentioned in the main research question. To answer all the sub questions the following plan is set up.

First a rigid structure will be modelled. This rigid structure represents a load plate placed on a rigid surface. This way it is possible to replicate the conditions used in conventional studies on human excitations in which human-structure interactions are not considered. On top of this rigid structure a spring is modelled which represents the interaction between the structure and a mass. The mass represents the mass of a human. The energy in the system will come from an initial velocity assigned to the mass.

This rigid situation will be used to replicate the conditions of a jumping person without taking HSI into account. After the rigid system is calibrated the right stiffnesses will be assigned to the structural elements which makes the structure more flexible. This causes HSI to be taken into account. After that it is possible to add more people (mass-spring systems) to the system to simulate a crowd. This will simulate a crowd of people jumping exactly at the same moment in time. But according to the literature study, people never really land exactly at the same moment in time. So to make the simulation even more realistic, time lags will be modelled in between jumps. And finally, a situation will be modelled in which the crowd jumps two times in a row. This way it is possible to find out how structural vibrations affect the system. Details about the model and what assumptions were made is explained in the following subsections.

5.3 Modeling the human part of the system

As is explained in the modelling plan, a jump excitation based on the data from existing literature will first be simulated. It is known from studies like [12] and the implementation of ISO 10137:2007 that the excitation resulting from a jumping person has a sinusoidal shape, this is emphasized again in figures 37a and b.

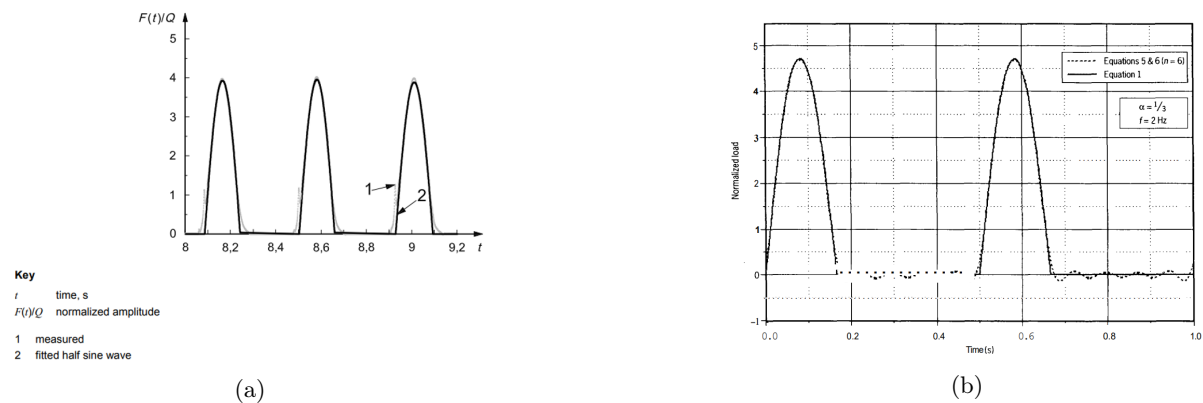


Figure 37

From basic structural dynamics it is known that a mass-spring system with an initial velocity and zero initial displacement results in a sinusoidal load on a rigid surface. So a mass-spring system will be used to model the excitation by a jumping human. Some literature suggests using a mass-spring-damper system to simulate human-structure interaction. But in most cases this is because they focus on how HSI affects the dynamical properties of the system. In this research on the other hand, the focus is on the peak excitation reduction and the impact factor. Adding a dashpot to the human part of the system will result in a force curve with an instant force (like a sinusoidal curve starting at $t = 1/4\pi$),

so this does not match the excitation shape which is tend to be replicated. Next to this reason it is expected that even without adding a dashpot, the changing dynamical properties will still be taken into account as [15] found good results using its model 2. This model only took the addition of human mass into account. Another important reason for not adding a dashpot is that a crowd is modelled which is jumping in a repeated manner, so the energy the crowd has lost during the contact time with the structure is compensated with their own muscular energy.

5.3.1 A non-linear spring

So the interaction between human and structure is modelled by means of a spring. But in the situation of a human jumping on a surface, the human will never be able to apply an upward force to the structure. If a linear spring is used to model the interaction, it would create an upward force whenever the spring is in tension. So to simulate a force curve like in figures 37a and b, a non-linear spring is applied. Whenever the spring is in compression, it will have its determined stiffness. And whenever the spring is in tension, the spring will have a stiffness of 0 N/m .

5.3.2 Determination of human system parameters

The human system parameters which need to be determined are the human mass (m_h), the spring stiffness (k_h) and the initial velocity (V_0). The human mass will be **85 kg** as this is the average weight of a Dutch male. The initial velocity which is assigned to the human mass must represent the velocity a real person has just before hitting the surface. This initial velocity is calculated by the well-known formula of $V_0 = \sqrt{2gh}$. So V_0 will be dependent on the height which is assumed the person to "fall" free from. This is obviously what happens in real life. The higher a person jumps, the higher his initial velocity will be before hitting the floor. The higher its velocity, the higher its dynamic amplification factor ($\frac{F(t)}{Q}$). This means V_0 will be determined by choosing the magnitude of $\frac{F(t)}{Q}$. In this model a jump of average height will be simulated. Knowing the dynamic amplification factor of a jumping person lies between 2.3 and 4.7, it is decided to let $\frac{F(t)}{Q}$ be equal to 3.

On the determination of k_h is not much literature available. Most studies in which human jumps are modelled the spring stiffness is determined by assuming a reasonable value and then use system identification to be more precise. In this model k_h will be determined in the same manner. k_h affects the contact time between human and structure. According to [12] a dynamic amplification factor of 3 means the contact ratio will be approximately 1/2. It is assumed that the crowd jumps to a 120 bpm (beats per minute) beat. This is equivalent to a jumping frequency (f_j) of 2 Hz. Together with a contact ratio of 1/2, this results in a contact time of 0.25 seconds.

Table 5: Jumping properties rigid situation

Dynamic amplification factor ($\frac{F(t)}{G}$)	Jumping frequency (f_j)	contact ratio (α)
3 [-]	2 [Hz]	0.5 [-]

Figure 38 shows the results of 1 person jumping on a rigid structure. The force amplitude is 2502 N, the contact time is 0.25 seconds and the shape is sinusoidal.

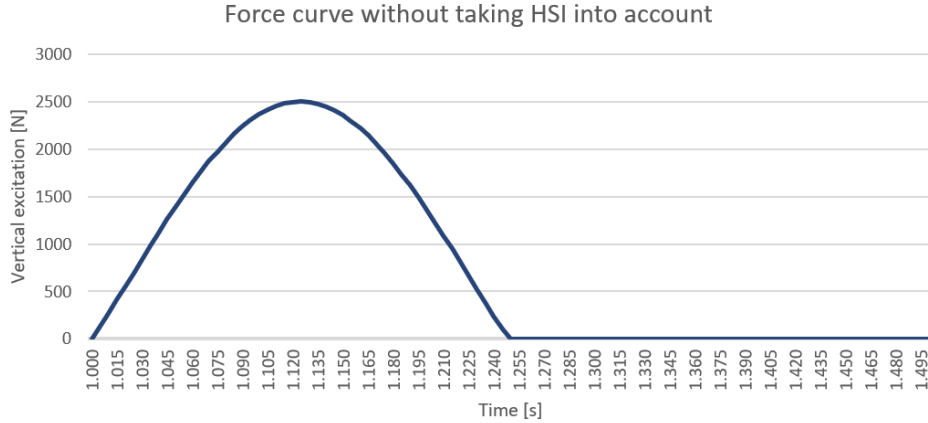


Figure 38

This excitation curve is the result of the system parameters in table 5.

Table 6: System parameters regarding human jump

Human mass (m_h)	Initial velocity (V_0)	Spring stiffness (k_h)
85 [kg]	1.515 [m/s]	17500 [N/m]

To determine the peak force of a single person the static load of a person will be multiplied with the dynamic amplification factor:

$$G[kg] \cdot g[\frac{m}{s^2}] \cdot \frac{F(t)}{Q} = F_{max}[N]$$

$$85 \cdot 9.81 \cdot 3 = 2502N$$

5.4 Modeling the structural part of the system

In this research the focus is on event deck structures. An example of such a structure is shown in figure 39.



Figure 39: Platform structure at a festival

It is beneficial that the findings of this research can be generally applied in the industry, so it is preferred that the model not too specific. This way conclusions can also be drawn about event deck structures with other dimensions. To learn more about the general dimensions of elements used for these types of structures, research has been done on existing options. Layher is a prominent company

regarding event deck structures. On their website layher.nl their catalogue on stages can be found. The first important feature of an event deck structure is its repeating characteristic. So to model an event deck it is not necessary to model everything, only a section of a deck will do. Figure 40 shows a more detailed structure used by Layher. Its dimensions are variable and are discussed in section 5.4.1.



Figure 40: The considered event deck

This is a structure consisting of 4 sections. Only 1 section will be modelled because of the symmetry in the structure. All floor panels are hinged, so stresses in neighboring floor panels do not affect other floor panels. All significant elements of the structure in figure 40, their properties and available dimensions are mentioned in the next section. This is according the Layher catalogue on stages.

5.4.1 Structural elements, properties and dimensions

- The floor panels

Figure 41a shows a widely used floor panel to build event deck structures. The short sides of the panel are connected to a transom, the long sides are not connected to any structural parts. A floor panel is made out of a wooden plate which lays on top of an aluminum frame, this aluminum frame runs along the edges of the plate. Its dimensions can be obtained in figure 41b. Figure 41c shows a cross section of 2 floor panels mounted on an event transom. From this figure it can be obtained how the elements are resting on each other.

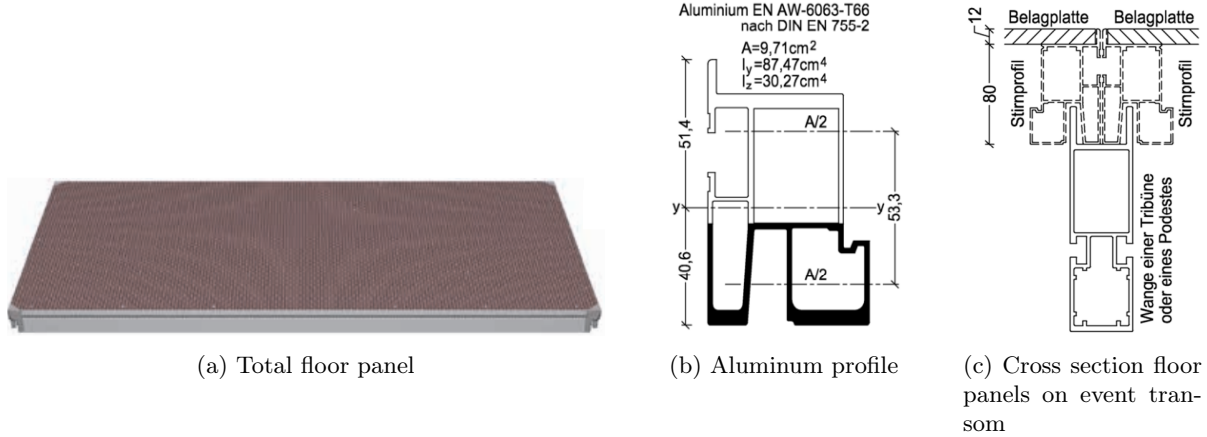


Figure 41

For the aluminum profile, A6063 is used. This type of aluminum has a Young's modulus (E) of 68.3 GPa, a density (ρ) of 2950 kg/m^2 and a Poisson ratio (ν) of 0.36. Its moment of inertia for both direction and its surface is shown in figure 41b. The wooden plate is made of Finnish Birch Plywood and is 12 mm thick. The Young's modulus for this plywood panel is $E_{m,mean,\parallel} = 900 kN/cm^2$ and $E_{m,mean,\perp} = 500 kN/cm^2$, its density is 700 kg/m^2 with a Poisson ratio of 0.3. Floor panels can vary in length and width. Table 7 shows all dimensions and weights per panel used by Layher. These dimensions cover almost all options which are regularly used in the industry. The reason why floor panels do not get much larger is for the fact that they need to be light in order to install the structure by hand. In this model a floor panel of 1.00 x 2.00 m is applied because this type is used very often.

Table 7: Floor panel properties

Dimensions L x W [m]	Weight approx. [kg]
0.86 x 1.04	16.9
0.86 x 2.07	30.2
0.86 x 2.57	36.7
1.00 x 1.00	18.3
1.00 x 2.00	32.5
1.04 x 1.04	19.3
1.04 x 2.07	34.3

- The event transoms

The floor panels rest on an event transom as is depicted in figure 42. The length of a transom varies between 0.86 meter and 2.57 meter. The length depends on the width and amount of floor panels it must carry. This model will contain out of 2 floor panels which means an event transom of 2 meters in length will be used. For the transoms A6063 is also used.



Figure 42: An event transom

- The columns

The columns of an event deck mainly consist out of 2 structural elements, a stalk and a foot spindle. These 2 elements are depicted in figure 43. A stalk is a pipe with rosettes attached to it. These rosettes can be used to attach other elements on to the stalk like an event transom or scaffolding pipes. The height of stalks varies from 0.5 to 3 meter. It is expected that the tallest stalks cause the heaviest displacements so stalks of 3 meters are used in the model. To mount the stalk to the ground a foot spindle is used. This spindle slides into the stalk, so this connection is only based on a slide-in mechanism

and is not able to resist tensile forces. The handle on the foot spindle can be used to align the structure. Both elements are made of S235JRH steel.

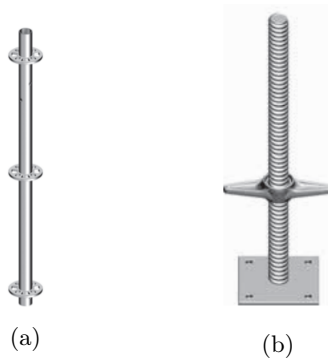


Figure 43: (a) A stalk, (b) A foot spindle

- The horizontal and diagonal scaffolding pipes

The last important structural elements in an event deck structure are the horizontal and diagonal scaffolding pipes. These pipes provide stability to the structure. Most pipes are 48.3 mm in diameter and have a thickness of 3.2 mm. Just like the columns they are made of S235JRH steel. These dimensions will be used in the model.

5.4.2 Model assumptions

To design the structure in Abaqus the following assumptions are made:

- The connections

In the event industry stalks, scaffolding pipes and transoms are connected using a wedge-pin joint. At each end of the scaffolding pipes and transoms are wedge-pins attached, like the ones that can be obtained in figure 44. This wedge-pin can slide in the rosettes, after given the pin a hit with a hammer, the connection is made. In [34] they studied the differences between a FE model with a detailed mesh and an equivalent analytical model. Figure 44a shows what kind of wedge-pin joint they modelled. The difference in wedge-pin connections between the one in [34] and in the structure in this research is that [34] uses an U-socket and in this research rosettes are used but the joints are very similar in quality. Figure 44b shows the FE model of the joint.

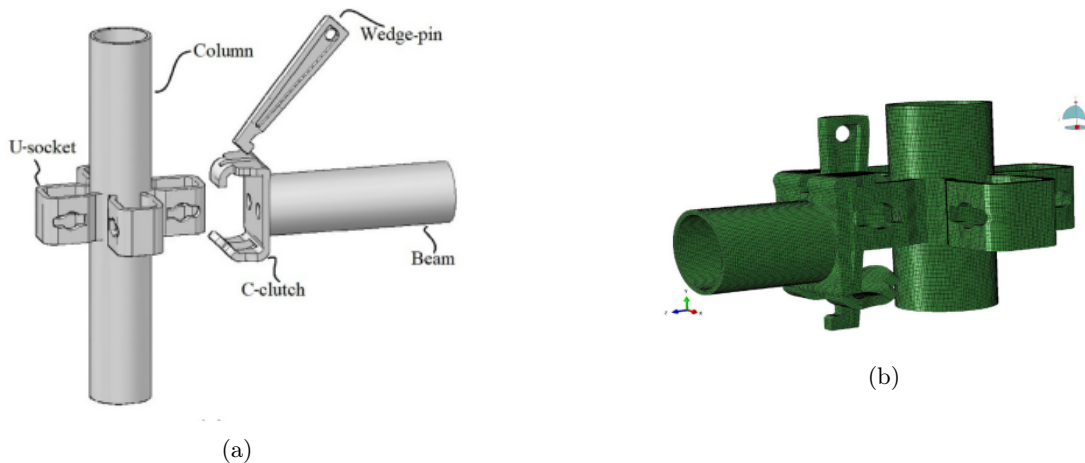


Figure 44

In figure 45 it can be obtained how the 2 models are build and figure 46 shows the differences in outcomes. From these results it can be concluded that the difference between the analytical model and the FE model are not significant.

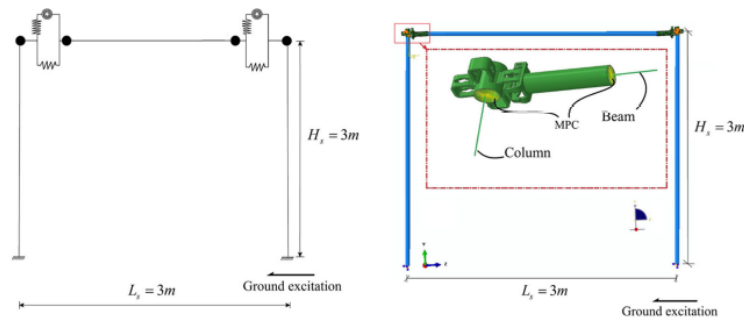


Figure 45: Schematization analytical and FE model in [34]

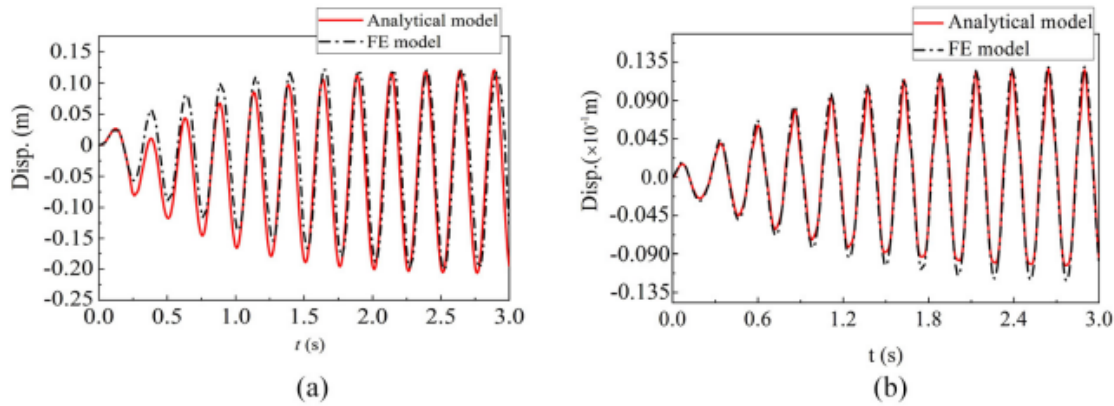


Figure 46: Results analytical and FE model in [34] with (a) showing the horizontal displacement and (b) showing the vertical displacement

After reading the conclusions in [34] it is known that it is not necessary to model the connections with the same level of detail as they did in their FE model.

In the event deck designs of Tentech they assume a $M-\phi$ diagram as depicted in figure 47 to model the rigidness of the connection. The same diagram will be implemented in this model for the connections between the stalks, the scaffolding pipes, and the transoms.

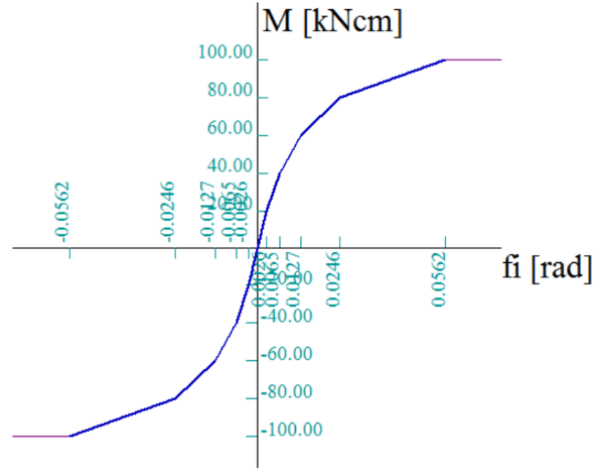


Figure 47: $M - \phi$ diagram used by Tentech

It is assumed that the columns of the structure are pinned to ground because the foot spindles are not anchored in the soil. Vertical soil displacements resulting from differing ground pressures are also neglected. The food spindle and the stalk will be designed as one column. Because of the slide-in connection between the stalk and the foot spindle some instant horizontal displacements are expected but they will not affect the factors researched in this paper. Lastly, the floor panels can rotate freely around the transom.

- Profiles

The stalk+foot spindle and the scaffolding pipes are modelled as a pipe profile with a diameter of 48.3mm and a thickness of 3.2mm. The event transom and the aluminum frame of the floor panels have a detailed cross-section. That is why equivalent box-shaped profiles with a similar moment of inertia are used. For the aluminum frame of the floor panel a 80x40x5mm (height x width x thickness) box-shaped profile is used. The moment of inertia of this profile is equal to 84.9 cm^4 in y-direction. The event transom profile which is used in the model is a 180x50x5mm (height x width x thickness) box-shaped profile. It is assumed the box-shape is a good estimation compared to the real profile. The moment of inertia is equal to 792 cm^4 .

5.5 FEM model

Figure 48 shows a total image of the model. It shows how the structure is oriented in terms of x-, y- and z-direction at the bottom of the first column. The figure shows how the horizontal and diagonal scaffolding pipes are oriented. The floor panels span from left to right in this figure. The black t-shaped lines on top of the floor panels are there for modelling purposes only and do not have a structural influence. The thick black line running from left to right on top of the floor panels show how the panels are separated. There is no connection between the 2 floor panels, so they deflect separately. In figure 48 it can be obtained how one cylinder is hanging above each floor panel, these cylinders represent lumped masses to simulate a person. So in this model two jumping humans are simulated. The blue dashed lines connecting the cylinders to the floor panel represent the springs to simulate the interaction. Figure 49a shows how the beam profiles are rendered. This picture is taken from another angle to get a better view. It can be obtained how all the scaffolding pipes and the columns are pipe-profiles, the transoms are rectangular with the right orientation and it shows the aluminum frame of the floor panels. In reality the profiles are stacked upon each other, this detail is neglected in the model.

Figure 49b shows how the model is meshed. B31 elements were used for the beams, S4R elements for the floor panels and C3D8R elements to model the cylinders. Because the Abaqus/CAE 2020 student edition is used, the model is limited to a thousand nodes. To reduce the amount of used nodes, the largest possible mesh is used to model the cylinders. The cylinders only provide mass and are not meant to deform so there is no need to model detailed cylinders. During the modelling stage of this research it was found that the floor panels have the most influence on the two considered factors. So it is important that the floor panels are meshed in the right way. From the results of the simulations it is found that the mesh does not have to be smaller than 125x125mm because the required level of detail is then reached. Regarding the simulation time it is decided to not make the mesh dimensions smaller. For the beam elements a length of 0.2 meter is used. After running simulations to check the mesh sensitivity it was obtained that the results did not change after further downsizing the elements.

No convergence problems were faced during the simulations. All materials were modelled linear elastically so there is no need to consider any physical non-linearity's. This is not necessary because no plastic stress levels are reached in the structure under the dynamic loads. The deflections in the model are not extreme there is no need to consider geometrical linearity's either. For this reason a wide range of time intervals between each step is possible. But because the excitation period is only 0.25 seconds, a 0.001 second step size is chosen.

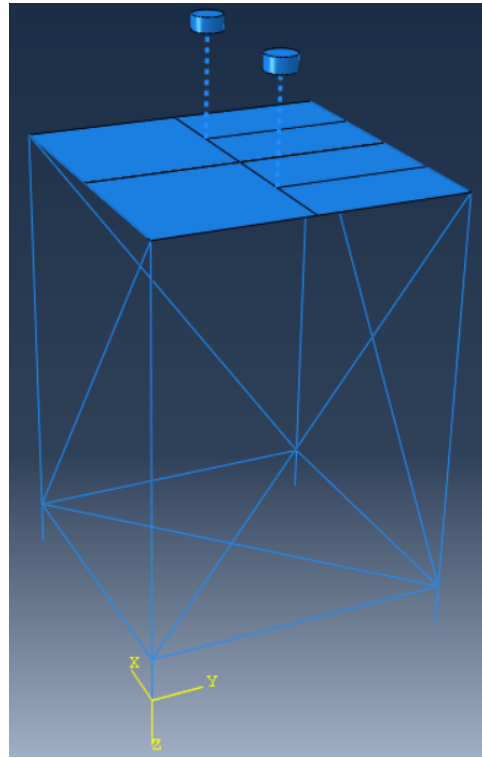
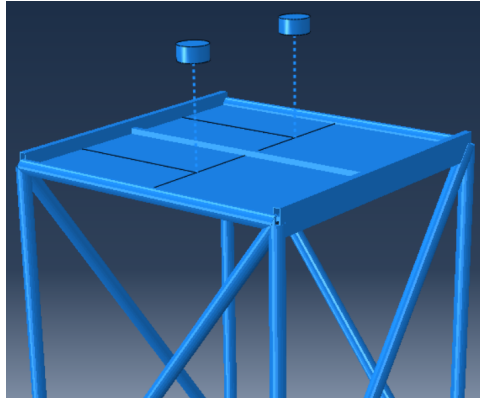
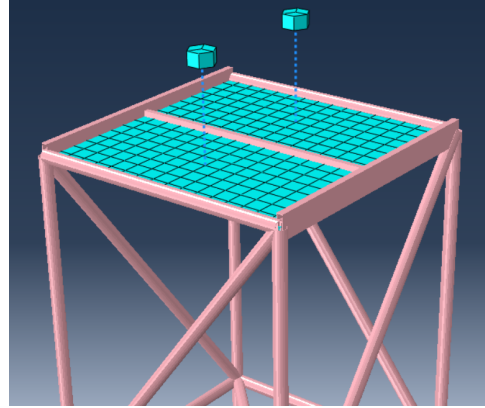


Figure 48: An overview of the total model



(a) Model with rendered beams



(b) The model mesh

Figure 49

5.6 Modelling randomly timed group jumps

As is explained in section 2.2.3, a perfectly synchronized group jump is not possible. This is why a randomly timed group jump is modelled. This means that every jumping individual collides with the structure at a different moment in time, this automatically creates time lags between each individual. The first moment of contact is determined using data from [17]. How they conducted this data is briefly explained in section 2.2.3, more details about how they conducted this data can be found in [17].

To determine the time lags between each participant, the PDF shown in figure 15b in section 2.2.3 is used. The PDF follows a normal distribution with an average value of 0 and a standard deviation of 0.05 seconds. Using a standard deviation of 0.05 is equivalent to applying a coordination factor of 0.8 according to [17]. The PDF in figure 15b shows data of a jumping crowd on a 1.8 Hz frequency. In this research a crowd jumping at 2 Hz is considered, but the differences in PDF for the time lags are negligible, this is concluded by [17]. To set the first moments of contact for each participant, Excel is used. The sheet in figure 50 shows 16 randomly generated numbers in column A. These numbers are generated based on a normal distribution with an average of 0 and a standard deviation of 0.05. A jumper position is assigned to each number in column B. The first jumper needs to get in contact with the structure at $t=0$, so all negative numbers need to become positive. This is done by adding the highest negative number to all random numbers. This number is determined in column C. Column D contains all moments of first contact. The order of jumpers is added in column E. The method can be checked by finding the first jumper. This is the person in row 13, its position is 3,4 and his first moment of contact is at $t=0$.

	A	B	C	D	E
1	Random moments start jump	Position jumper	First jump time	setting the first jump to t=0	Order of jumpers
2		0.025 1,1	-0.072	0.097	9
3		-0.001 1,2		0.071	8
4		-0.017 1,3		0.055	7
5		0.098 1,4		0.170	16
6		-0.025 2,1		0.046	4
7		0.071 2,2		0.143	15
8		0.052 2,3		0.123	13
9		0.032 2,4		0.104	10
10		-0.029 3,1		0.042	3
11		0.049 3,2		0.121	12
12		-0.041 3,3		0.031	2
13		-0.072 3,4		0.000	1
14		0.035 4,1		0.107	11
15		-0.022 4,2		0.050	5
16		-0.018 4,3		0.054	6
17		0.055 4,4		0.127	14

Figure 50: Example of determination of the first moments of contact

In Abaqus it is possible to activate forces in different moments in time. But initial velocities will all be activated at $t=0$. So it is not possible to change the velocity of an individual during the simulation. To create a time lag between individuals, different vertical positions are assigned s to each person. This is shown in figure 51.

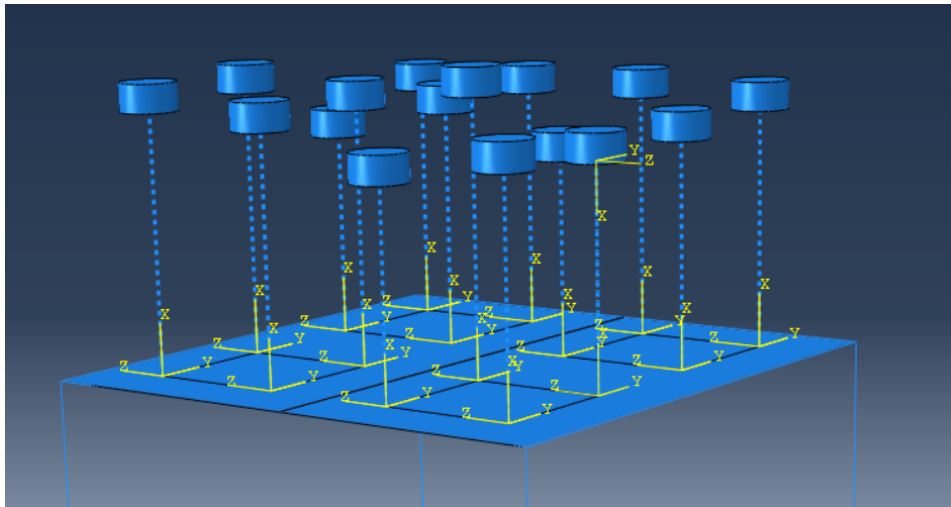


Figure 51: Height difference of individuals

At $t=0$, all individuals will have the same initial velocity. The first human to hit the structure, which is determined using the sheet in figure 50, is placed closest to the structure at a height of 0.7 meters above the floor panels. This height is just a reference height and is for modelling purposes only, so it does not affect the simulation itself. If a different reference height is applied, the model will give the same results. It is now necessary to determine how much higher each individual must be than the first colliding human. The initial velocity (V_0) and the time interval (Δt) between each person is known. So the other jumpers are shifted $V_0 \cdot \Delta t = \Delta h$ upwards.

During the time lag, the jumper must retain its initial velocity. So during this part of the fall, no forces will be applied to the human mass. Spring forces are avoided by starting the compression stiffness at $U_c = \Delta h$. Figure 52 shows how a non-linear spring is designed with its compression stiffness starting at $U_c = -0.269\text{m}$. U in figure 52 represents its own longitudinal displacement. After reaching U_c it can be obtained how the spring has a stiffness of 17500 N/m .

Data		
	F or M	U or UR
1	-17500	-1.269
2	0	-0.269
3	0	1

Figure 52: Non-linear spring with $U_c = -0.269m$

Other than the spring force, gravitational force will be applied to the human mass. For the human mass to retain its initial velocity, gravity will not be applied until the human mass reaches its initial height (0.7m above the structure). This is solved by applying gravity to each participant after the time determined in column D of figure 50. The forces on the human weight are also described using equations of motion and are added in the appendix.

5.7 Soundness of the model - *IPE*

Because the model is based on some assumptions it is important to check the soundness of the model. At first, the focus is on the reduction of peak contact force between human and structure (*IPE*). Because of the lack in published papers about *IPE* factors, the results of [26] will be used to check the soundness of the system. This paper is written by prominent researchers on this subject. Researchers like Aleksandar Pavic already conducted multiple papers about human-structure interaction. This provides certainty in the soundness of their models and their results.

The model used in [26] is different than the model which is proposed in this research, but it is possible to modify the system parameters in such a way that this model is comparable to theirs. The first difference between this model is the model type itself. In this research a 3D Abaqus Finite Element model is used, in [26] they make use of 2 SDOF models which are connected by an agent-based model (ABM). The ABM regulates the interactions between the two models. A schematic of this model is depicted in figure 23. To compare the two models, it is necessary to know how to convert a continuous model to a discrete model. Converting a 2D beam to a discrete SDOF system is a well-known topic in structural dynamics. Figure 53 shows a table of equivalent substitute SDOF parameters for single span beams with various support and load conditions. The model which is described in section 5.4.3 will be used to generate results regarding the research questions. But this model is not ideal to convert to a SDOF system. So to check the soundness of this model it is modified in such a way that it is comparable to a simply-supported beam with a point load at mid-span. Figure 54 shows the simplified model.

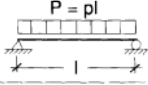
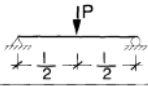
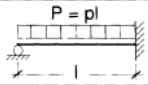
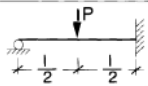
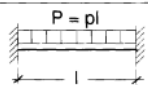
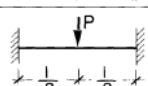
Loading and support conditions Reference point at $l/2$	Load factor ϕ_L	Mass factor ϕ_M		Effective beam stiffness k	Stiffness factor ϑ
		Lumped mass	Distributed mass		
	0.637	—	0.5	$\frac{384 EI}{5 \cdot l^3}$	48.7
	1.0	1.0	0.5	$\frac{48 EI}{l^3}$	48.7
	0.595	—	0.479	$\frac{185 EI}{l^3}$	113.9
	1.0	1.0	0.479	$\frac{107 EI}{l^3}$	113.9
	0.523	—	0.396	$\frac{384 EI}{l^3}$	198.5
	1.0	1.0	0.396	$\frac{192 EI}{l^3}$	198.5

Figure 53: [30]

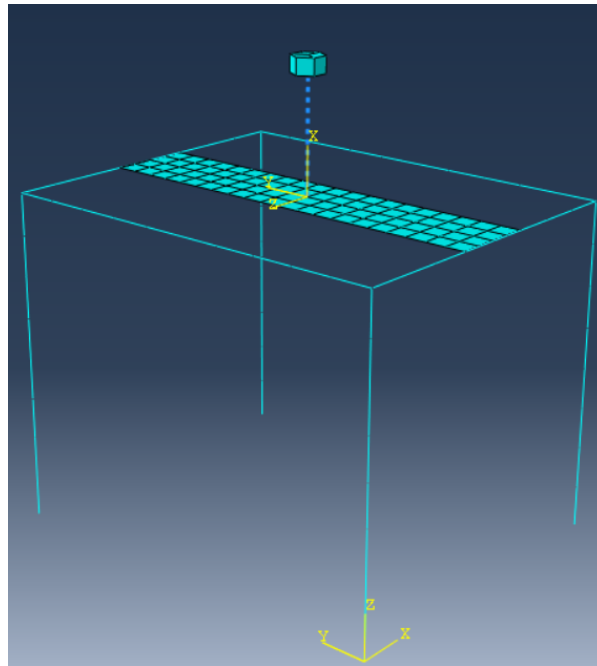
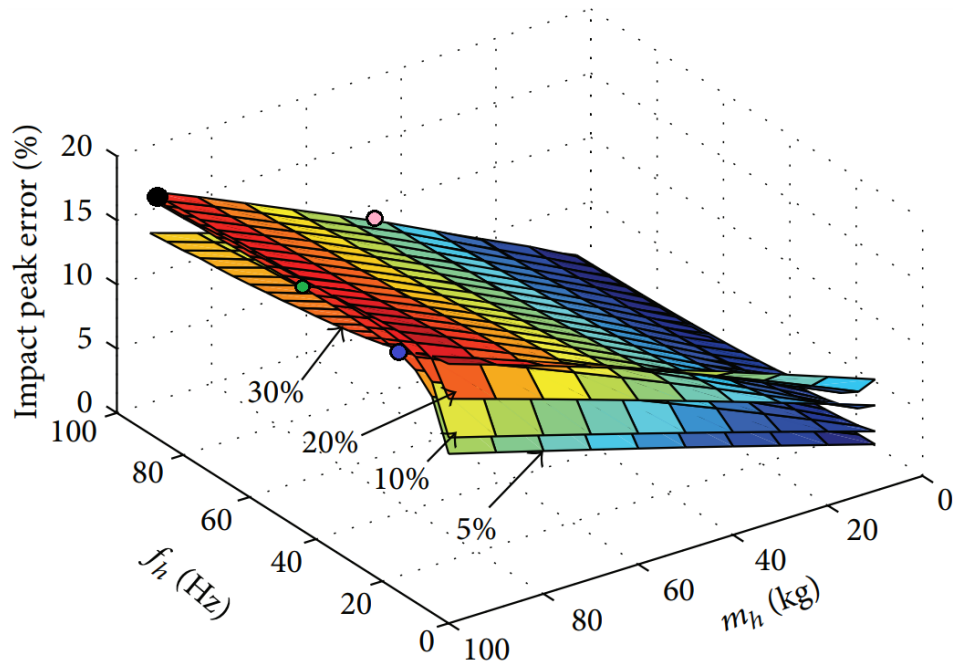


Figure 54: Simplified model to check its soundness

The frame in the simplified model is made rigid by applying a Young's modulus which is $10E6$ times higher than the original. The floor panel is simply supported by the frame. In the figure it can be obtained that the floor panel is less wide as the original. The floor panel is given a width of 0.5 meter to approach the mechanical properties of a 2D beam. The aluminum frame to stiffen the floor panel is removed to create a uniform cross-section over its width. The density (ρ) and the Young's modulus (E) of the floor panel are adjusted in such a way that it can be converted to have similar SDOF properties as

used in [26]. The floor panel will have hypothetical mechanical properties and is assumed to be isotropic. By placing one person at mid-span of the floor panel, the second situation as depicted in figure 53 is created, a simply supported beam subjected by a point load at mid-span. So to convert the model to a SDOF system, a load factor (Φ_L) of 1.0 and a mass factor (Φ) of 0.5 is used. This implies that the excitation must be multiplied by 1.0 and the total mass by 0.5 to get the values needed for a comparable SDOF system.

Damping is not included in the model. The reasoning for this decision is explained earlier. To make the best comparison between this model and the model used in [26], the results are compared in which they applied to lowest damping ratio's. In figure 55 the results of their parametric study can be obtained, varying in human damping (ζ_h), human natural frequency (f_h) and human mass (m_h).



(b) $\zeta_h = 5\%$, 10% , 20% , and 30% ; $m_s = 500$ kg; $f_s = 20$ Hz; $\zeta_s = 1\%$

Figure 55: Results parametric study by [26]

The results of [26] with the following system parameters are compared:

- $m_h = 100$ kg
- $f_h = 100$ Hz
- $\zeta_h = 5\%$
- $m_s = 500$ kg
- $f_s = 20$ Hz
- $\zeta_s = 1\%$

These system parameters represent the black dot in the upper left side of figure 55. With these parameters [26] found the *IPE* to be approximately 16-17%. From the figure it can be also concluded that the human damping ratio barely influences the *IPE* at the coordinate of the black dot. So no large differences are expected in the results for the researched case in which $\zeta_h = 0$. Also the structural damping in the models of [26] is only 1%. The *IPE* is measured by analysing a single peak force in

a short time span (about 0.01 second), which implies that the structural damping will not have much effect on the results.

Now the Abaqus model must be designed in such a way that it is comparable with the model used in [26]. The discrete structural mass (\tilde{m}_s) in figure 55 is equal to 500 kg, it is assumed that the participating mass of the model is 50% ($\Phi_m = 0.5$). So the total mass of the floor panel must weigh 1000 kg. With its dimensions being 2.5x0.5x0.025 m (LxBxH) this results in its density (ρ) being 32000 kg/m^3 . The floor panel must have a fundamental natural frequency (f_n) of 20 Hz. It is known that for a mass-spring system:

$$f_n = \frac{1}{2\pi} \cdot \sqrt{\frac{\tilde{k}}{\tilde{m}_s}} \quad (9)$$

So \tilde{k} is equal to:

$$\tilde{k} = f_n^2 \cdot 4\pi^2 \cdot \tilde{m}_s = 7895684 N/m$$

From figure 53 it is known that the effective beam stiffness is:

$$\tilde{k} = \frac{48EI}{l^3} \quad (10)$$

I is equal to:

$$I = \frac{1}{12} \cdot b \cdot h^3 = \frac{1}{12} \cdot 0.5 \cdot 0.025^3 = 6.51 \cdot 10^{-7} m^4 \quad (11)$$

And $l = 2.5m$. After rewriting equation 10 it is known that E must be:

$$E = \tilde{k} \cdot \frac{l^3}{48I} = 7895684 \cdot \frac{2.5^3}{48(6.51 \cdot 10^{-7})} = 3.9478 \cdot 10^{12} N/m^2$$

So by using a hypothetical material with $\rho = 32000 kg/m^2$ and $E = 3.9478 \cdot 10^{12} N/m^2$ a model with similar system parameters is created. In figure 56 the results of an interactive and a non-interactive model are compared. From the peak values the IPE is distracted.

$$IPE = \left[\frac{(168741 - 140507)}{168741} \right] \cdot 100 = 16.7\%$$

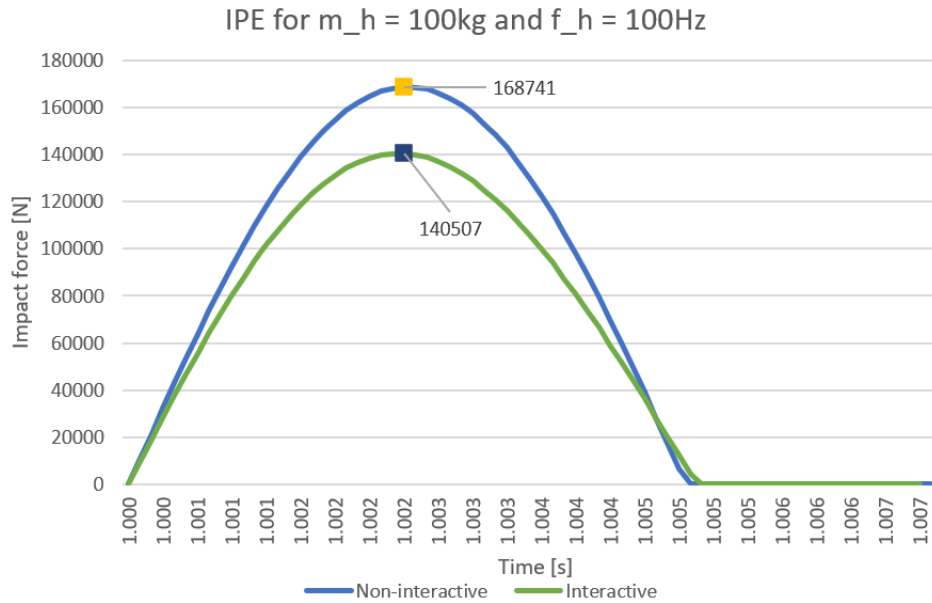


Figure 56

It is obtained that the outcome of this model is very similar to that of [26], this confirms the soundness of the model. Multiple coordinates will be considered to check the soundness of the model. For the second coordinate the following system parameters are chosen:

- $m_h = 50 \text{ kg}$
- $f_h = 100 \text{ Hz}$
- $\zeta_h = 5 \%$
- $m_s = 500 \text{ kg}$
- $f_s = 20 \text{ Hz}$
- $\zeta_s = 1\%$

These system parameters represent the pink dot in figure 55. The interactive and non-interactive output is shown in figure 57. From the peak values the *IPE* is determined again.

$$IPE = \left[\frac{(81166 - 74496)}{81166} \right] \cdot 100 = 8.2\%$$

For the second coordinate very similar results are obtained again.

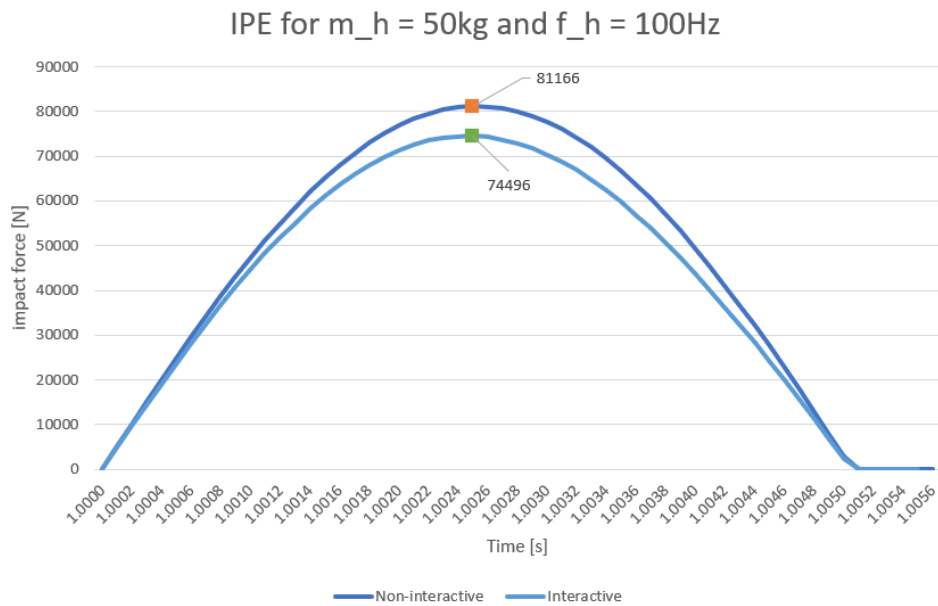


Figure 57

The next coordinate which is checked is represented by the green dot in figure 55. The third coordinate represents the following system parameters:

- $m_h = 100 \text{ kg}$
- $f_h = 50 \text{ Hz}$
- $\zeta_h = 5 \%$
- $m_s = 500 \text{ kg}$
- $f_s = 20 \text{ Hz}$
- $\zeta_s = 1\%$

In figure 55 one can obtain how the *IPE* decreases for a decreasing human natural frequency (f_h) in case of a low human damping ratio (ζ_h). In this case, a lower human damping ratio means a lower *IPE*. In the model of figure 54 the human damping ratio is 0%, so it is expected that a decreased *IPE* is found when checking the soundness of the model. The interactive and non-interactive output regarding the system parameters of the third coordinate can be obtained in figure 58.

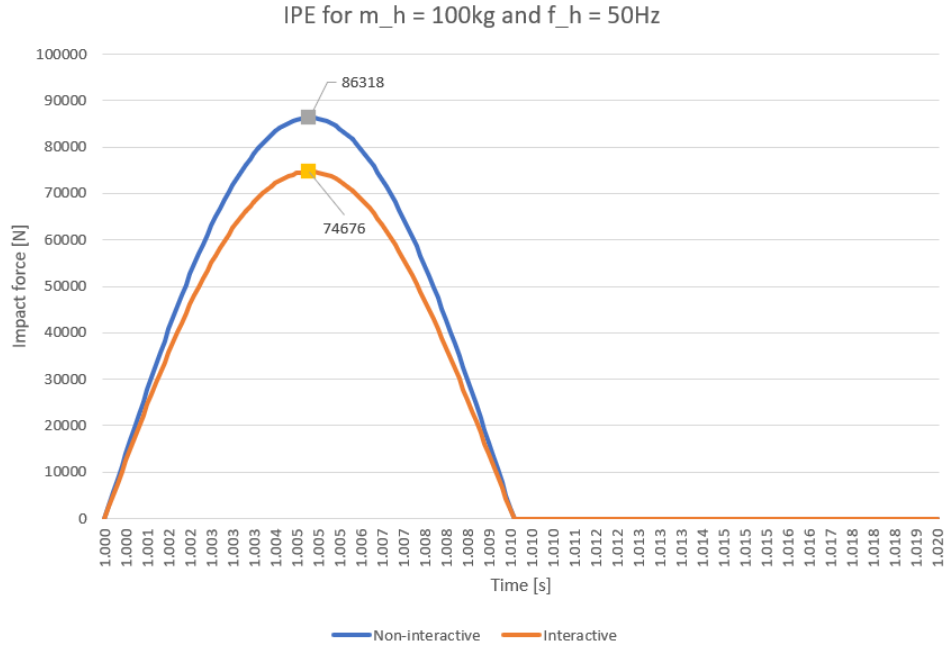


Figure 58

$$IPE = \left[\frac{(86318 - 74676)}{86318} \right] \cdot 100 = 13.5\%$$

A decreased *IPE* of 13.5% is found for the third coordinate. This is a lower value compared to the first coordinate. From figure 55 it can be concluded that there should be no difference between the *IPE* of the black and the green dot. But because of the decreasing trend in *IPE* for models with a low human damping ratio, the result of 13.5% is still assumed to be valid because in this situation there is no human damping at all.

To finish checking the soundness of the model regarding the *IPE* values, a fourth coordinate is considered. The fourth coordinate is depicted by the blue dot in figure 55 and represents the following system parameters:

- $m_h = 100$ kg
- $f_h = 20$ Hz
- $\zeta_h = 5$ %
- $m_s = 500$ kg
- $f_s = 20$ Hz
- $\zeta_s = 1$ %

Just as with the third coordinate, a decreased *IPE* is expected for the fourth coordinate because now the human natural frequency is even lower. Figure 59 shows the difference in contact force for non-interactive and interactive models regarding the system parameters of the fourth coordinate.

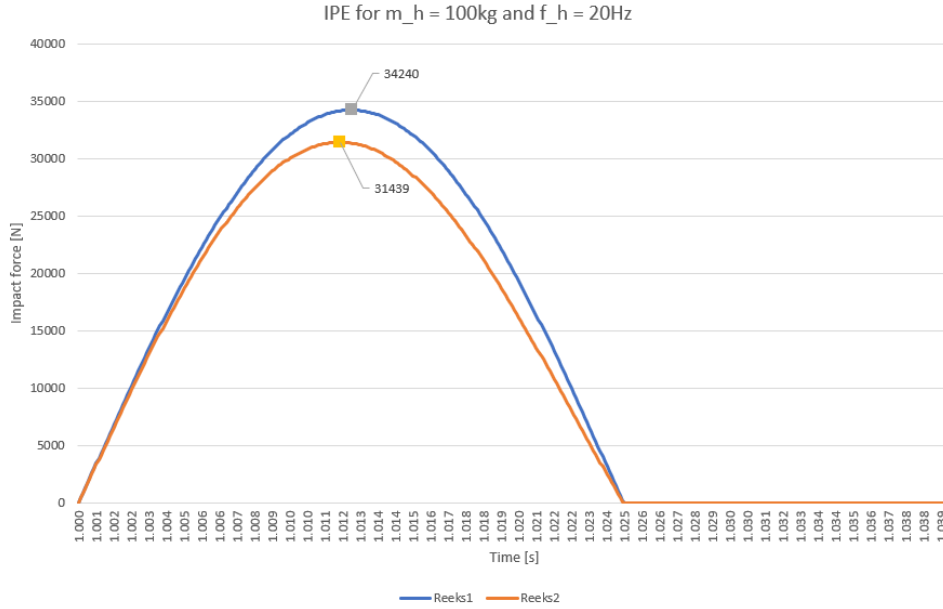


Figure 59

$$IPE = \left[\frac{(34240 - 31439)}{34240} \right] \cdot 100 = 8.2\%$$

The *IPE* resulting from the model of figure 54 is lower than was found in figure 55. But it can be obtained that the *IPE* is more sensitive to f_h when $5 \text{ Hz} < f_h < 20 \text{ Hz}$ and in general decreases as ζ_h decreases. This explains the lower *IPE*.

5.8 Soundness of the model - *IF*

This research focuses on the impact force peak error and the impact factor. So the soundness of the model must also be checked regarding the impact factor. To do that, the results from [3] are used to compare. In [3] the *IF* is determined by using a force-only SDOF model. So to compare their results, the model suggested in figure 54 is used again. To check the soundness, two models from [3] with different system parameters are considered. The output of these models is shown in figure 60. The left figure shows a system with $f_s = 10 \text{ Hz}$ and the right figure shows a system with $f_s = 5 \text{ Hz}$. Both are excited by a jumping force with a 2 Hz frequency. The blue line represents the imposed + permanent force and the orange line represents the internal force.

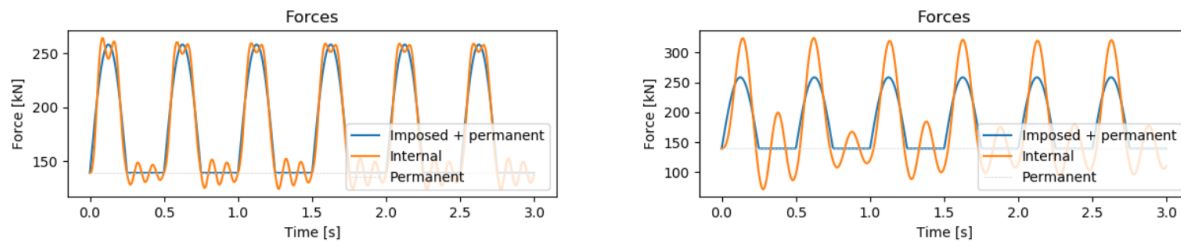


Figure 60: SDOF model excited by a jumping force with a 2 Hz frequency, for the left figure $f_s = 10 \text{ Hz}$ and for the right figure $f_s = 5 \text{ Hz}$

To determine the *IF* of these two models, the internal peak force is divided by the imposed peak force. Only the dynamic forces are considered in the determination of the impact factor, so the permanent forces will not be taken into account. From the left graph in figure 60 it can be obtained that the

maximum internal force is equal to 270 kN, the maximum imposed force is equal to 260 kN, and the permanent force is equal to 150 kN. So the impact factor for this system is:

$$IF = \frac{(270 - 150)}{(260 - 150)} = 1.09$$

From the right graph in figure 60 it can be obtained that the maximum internal force is equal to 330 kN, the maximum imposed force is equal to 250 kN, and the permanent force is equal to 150 kN. So the impact factor for this system is:

$$IF = \frac{(330 - 150)}{(250 - 150)} = 1.80$$

The suggested model in figure 54 is converted to have a natural frequency equal to 10 Hz to make a good comparison. The structure is excited by a similar jumping force in terms of shape and frequency. The results can be obtained in figure 61.

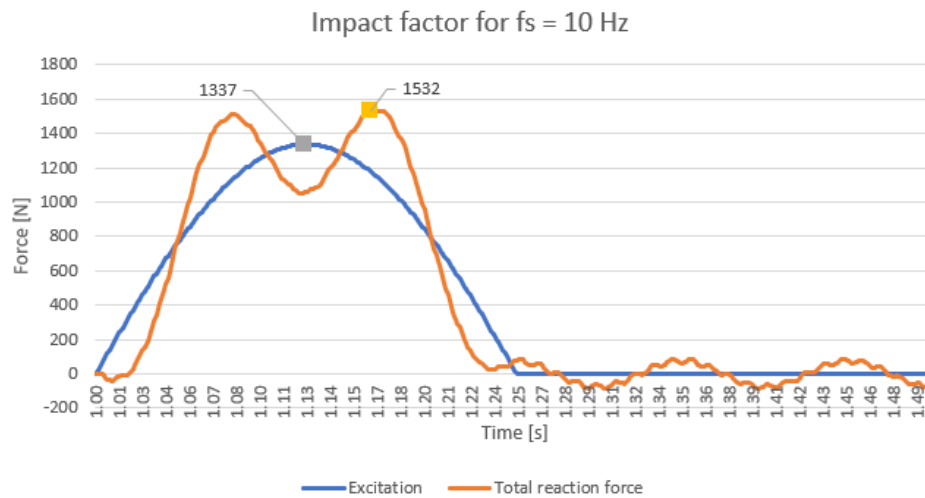


Figure 61

The maximum dynamic excitation and the total reaction force of the structure are displayed in figure 61. From these values, the IF can be calculated.

$$IF = \frac{1532}{1337} = 1.14$$

There is a 0.05 difference between the impact factors. This can be caused by the fact that the suggested model is a 3D Abaqus model and no SDOF model. This will always result into minor differences. And the excitation in the suggested model is coming from a mass-spring system with an initial velocity while the system in [3] is excited by a force over time. This can be a reason for the different results as well. Nevertheless, a difference of 0.05 is considered to be within boundaries.

Figure 62 shows the results of the model in figure 54 which is converted to have a natural frequency of 5 Hz. An impact factor of 1.81 is found. Comparing this value with the IF found for the right graph of figure 60 which had an IF of 1.80, it can be concluded that the results are similar. Also, the shape of the total reaction force is similar for both situations. This confirms the soundness of the model.

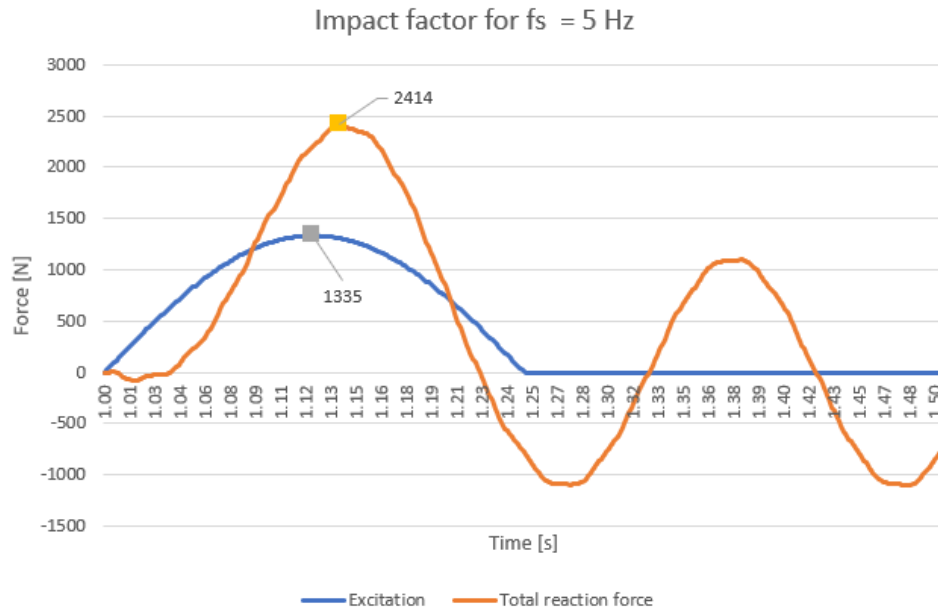


Figure 62

$$IF = \frac{2414}{1335} = 1.81$$

6 Results

6.1 The impact force peak error

6.1.1 Simultaneous group jump

From [26] it is known how different system parameters influence the *IFE*. In section 4 the hypotheses is stated and by using the results from the model it is possible to check if they are correct.

First it is researched to what extend the impact force peak error influences the imposed force on an event deck structure which is excited by a jumping crowd. This is done by modeling a crowd of 4 people per square meter on the design which is discussed in section 5. Figure 63 shows how each individual is positioned on the deck. Because of the symmetry in the structure and the positioning of each individual, only the data of the people on position H_11, H_12, H_21 and H_22 is needed.

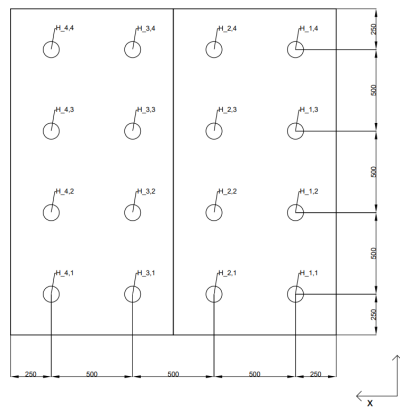


Figure 63: Positioning crowd, units in mm

Each individual is named as H_xy with x and y ranging from 1 to 4. Figure 64 shows the impact forces between human and structure for H_11, H_21, H_12 and H_22. The results in figure 64 are in line with the hypotheses. It is obtained that for every individual, the impact force is reduced. Next to that, it is obtained how the excitation periods (Δt) have become longer (more than 0.25 seconds). And for the individuals on position H_12 and H_22 it can even be obtained how the structural vibrations influence the impact force during the moment of contact. By using formula (7) it is possible to calculate the *IFE*. All peak impact forces are labelled in figure 63 and the peak of the non-interactive (rigid) and the most reduced peak (H_22) is taken to determine the *IFE*.

$$IFE = \left[\frac{(2502 - 2367)}{2502} \right] \cdot 100 = 5.4\%$$



Figure 64

When comparing this result with the findings in [26], it is found that they are quite similar. The event deck structure has a fundamental natural frequency in the excitation direction of 33 Hz (shown in figure 65). Figure 24f shows how fast the *IPE* decreases for low human natural frequencies. In [26] they varied in f_h starting at 5 Hz up until 100 Hz with a 5 Hz interval, so this case where $f_h = 2$ Hz falls just out of range. Knowing it is a lightweight structure and the human damping ratio is 0%, it can be concluded that the results are comparable.

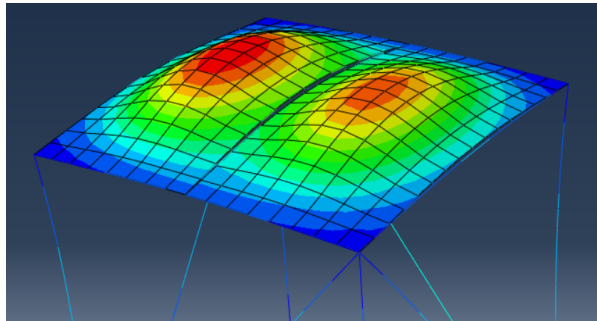


Figure 65: Fundamental natural frequency in vertical direction, $f_s = 33$ Hz.

Because the interaction between human and structure is modelled by means of a spring, it can be checked how the structural vibrations influence the impact force. Figure 66a shows the structural displacements at all relevant positions and 66b the displacements of each relevant individuals.

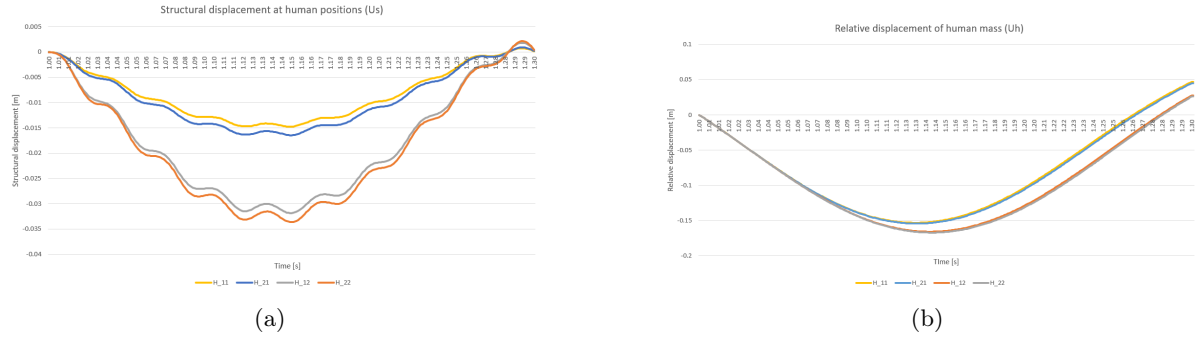


Figure 66

6.1.2 Randomly timed group jump

Figures 67 and 68 show 2 simulations, both based on a coordination factor of 0.8. How the time lags are modelled is explained in section 5.6. It can be seen how each jumper gets in contact with the structure at different moments in time. Therefore, the excitation is spread out over time and the total peak excitation is lower, just as would happen in reality. The legends in both figures depict each participant in the same manner as they are positioned on the structure.

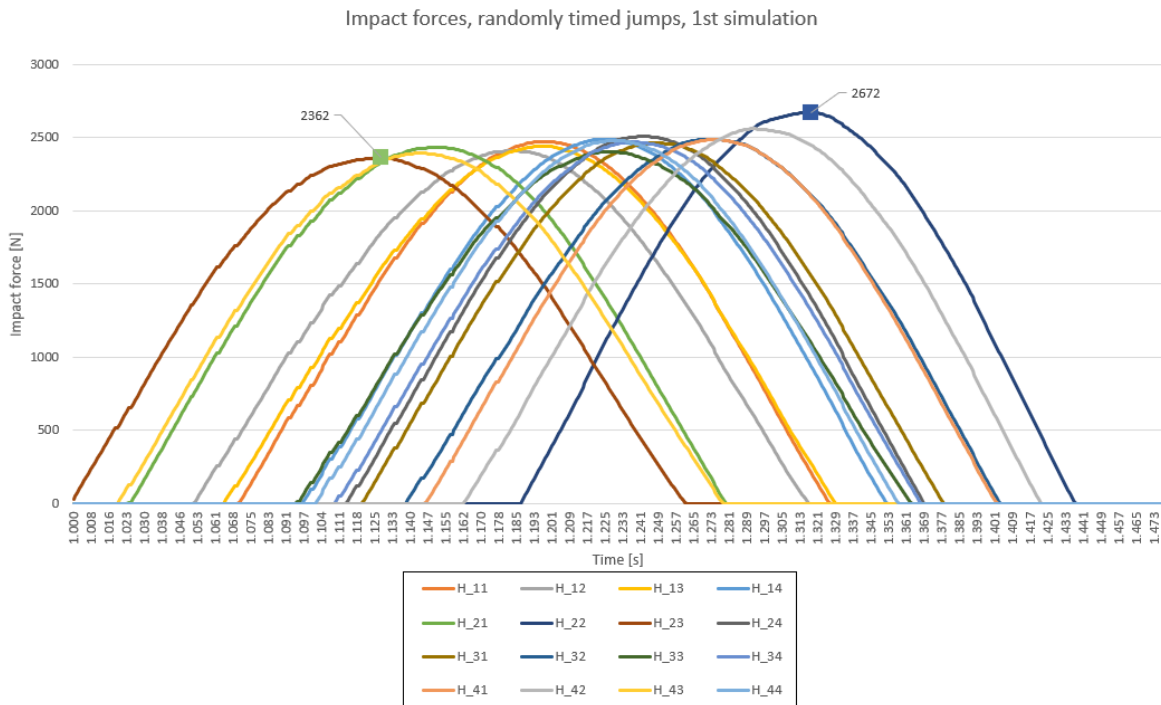


Figure 67: 1st random jump simulation

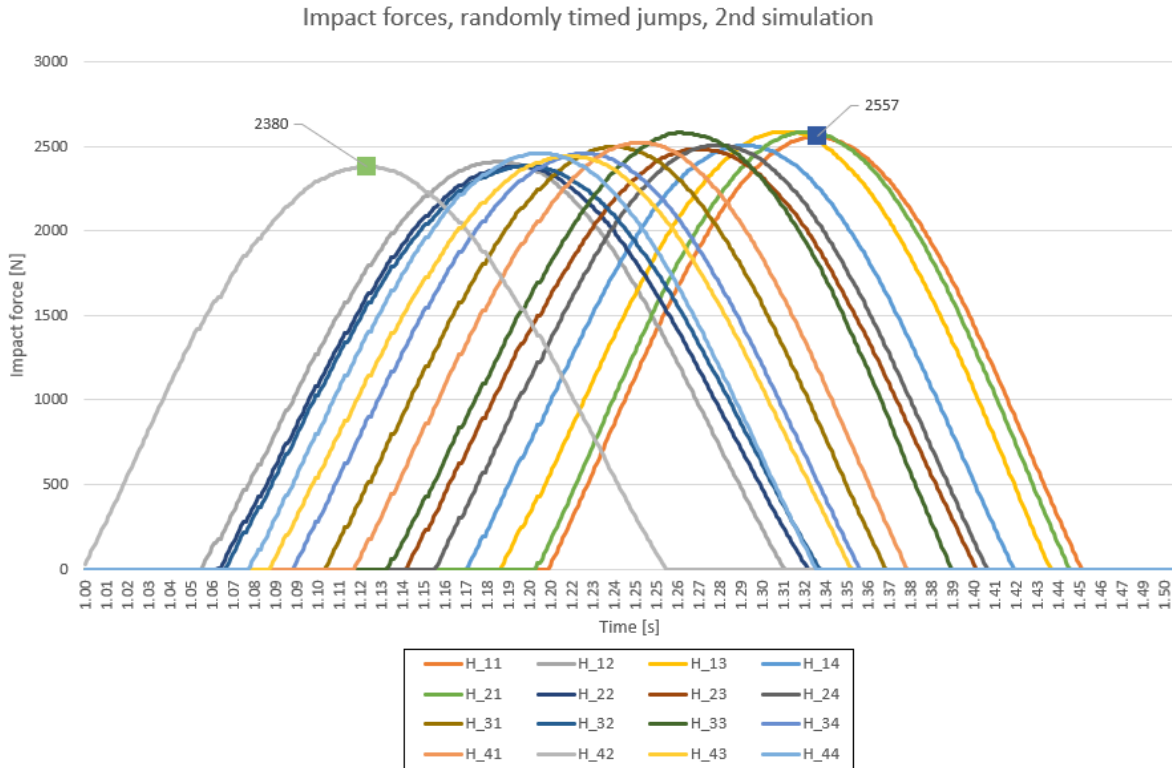


Figure 68: 2nd random jump simulation

After analysing figures 67 and 68, several observations can be made. The first interesting thing which can be observed is the trendline in peak excitation. The lowest peaks are reached by the first people who touch the structure and the highest by the latest jumpers. There are two explanations for this phenomenon. The first explanation regards the deflection of the structure. At the moment the last person touches the structure, the floor panel is deflected already. This results into a slightly longer airtime for the jumper. Longer airtime results into a higher impact velocity which causes a higher impact force peak. Even structural deflections of 10 to 20 millimeters can cause higher contact forces. The last jumper in the first simulation touches the structure at $t = 1.187s$, at this moment in time the floor panel is deflected 16mm, see figure 69.

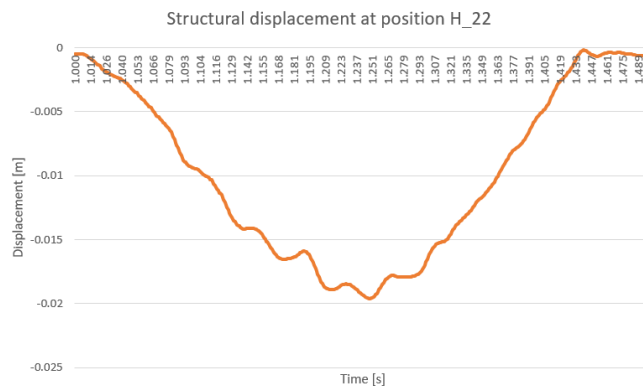


Figure 69

We assumed an initial velocity of 1.515 m/s . Using the well known formula:

$$V_0 = \sqrt{2gh}$$

With $g = 9.81m/s^2 \rightarrow h = 0.117m$. If 16mm is added to the initial falling height, this results in $V_0 = 1.615 m/s^2$. The increased V_0 causes in a rigid situation a peak impact force which is 108N higher than the original situation.

But as can be obtained in figure 67, the difference between the lowest and highest peak impact force is equal to $2672 - 2362 = 310N$. This leads to the second phenomenon to discuss, the effect of structural vibration. It is assumed that the structural vibrations of the floor panels cause the rest of the increase in the impact peak force. Figure 70 shows the vertical motions of the first and last timed jumper in red and blue respectively. The motion of the floor panel at midpoint is indicated by the yellow line.

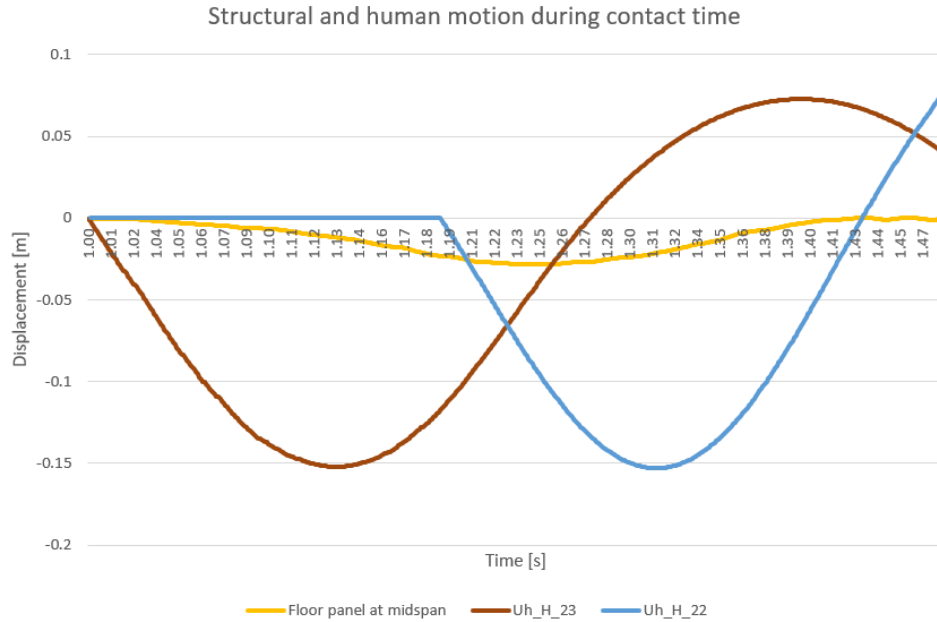


Figure 70

The graph in figure 70 contains 3 lines, the motion of the floor panel at midpoint and the motion of the person on H_23 and H_22. The reason for the differing impact force peaks is because of the structural motion of the floor panel. The first people to get in contact with the panel will experience a structure which moves downwards. This results in a "softer" landing. The swaying motion of a structure is what causes an *IPE* in the first place. For people who land on the floor panel at a later moment in time, such as participant H_22, will experience a structure which bounces back in upward motion. This causes the exact opposite effect of what participant H_23 experiences. This upward motion causes an impact force peak which is even higher compared to landing on a rigid structure. In the first simulation this causes an *IPE* of:

$$\left[\frac{(2502 - 2672)}{2502} \right] \cdot 100 = -6.8\%$$

The maximum *IPE* in the first simulation is reached by person H_23 and results in an *IPE* of:

$$\left[\frac{(2502 - 2362)}{2502} \right] \cdot 100 = 5.6\%$$

The second simulation shows similar results as the first one and results in a maximum *IPE* of:

$$\left[\frac{(2502 - 2382)}{2502} \right] \cdot 100 = 4.9\%$$

And a minimum *IPE* of:

$$\left[\frac{(2502 - 2557)}{2502} \right] \cdot 100 = -2.2\%$$

6.1.3 Double randomly timed group jump

Figure 71 shows the results of 2 randomly timed jumps in one simulation. This case is modelled to check whether structural vibrations caused by the first jump have any influence on the second jump. It can be observed that even without structural damping, the influence of structural vibrations on impact forces are negligible. This is emphasized by figure 72 in which the displacement of the floor panel at midpoint is shown. The structural vibrations which are obtained in between the two large waves are so small compared to each other that the influence of the structural vibrations can be neglected.

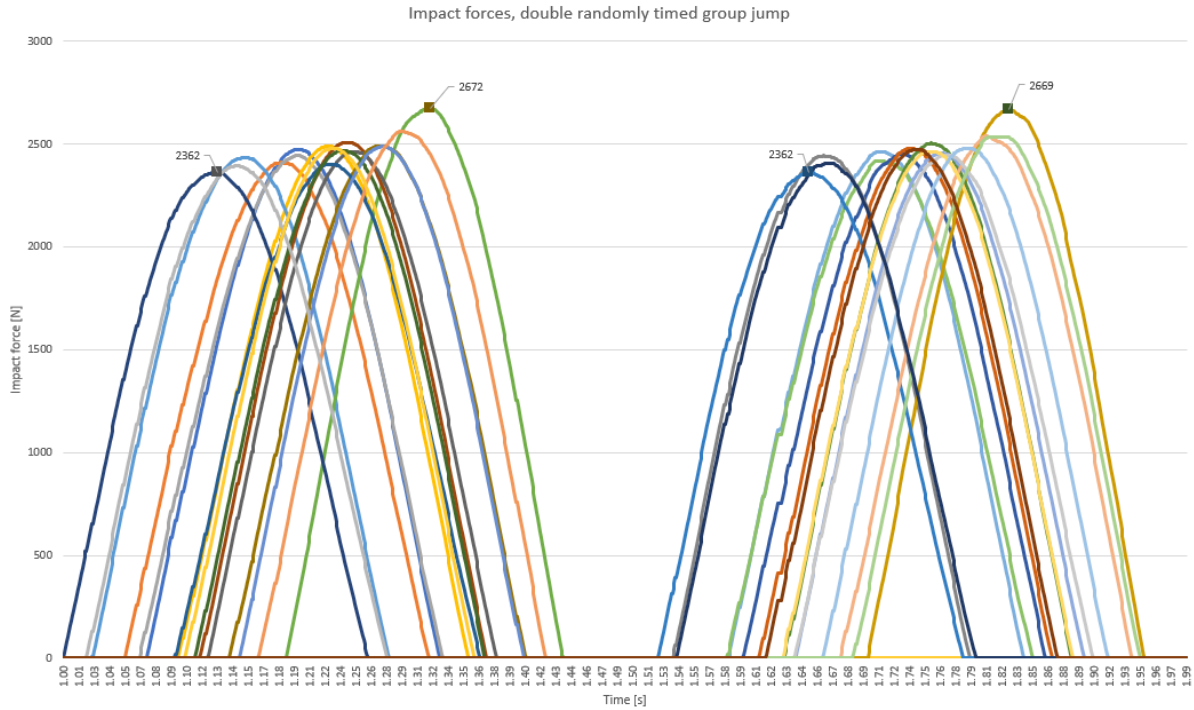


Figure 71: Double randomly timed group jump

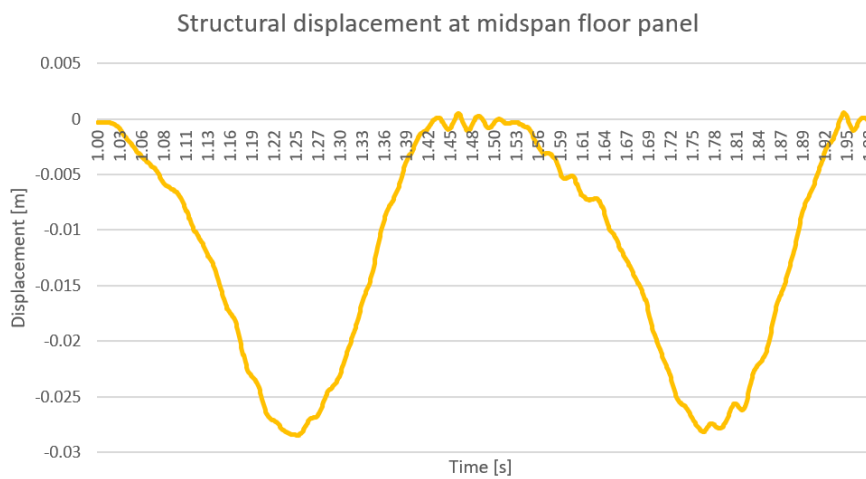


Figure 72: Structural displacement double randomly timed group jump

6.2 The impact factors (IF)

The impact factor is determined by the first vertical natural frequency of the structure and the shape of the excitation. The spectra of impact factors can be compared with a seismic response spectrum like they use in earthquake engineering. The force propagation in the model is determined by the natural frequency and the initial velocity of the human part of the system. The force of a jumping person has a sinusoidal shape, this is why excitations propagating in other ways are not considered.

In figure 73 it can be obtained how the total reaction force propagates compared to the total excitation in a rigid structure. All reaction forces at the base of the columns are added up to get the total reaction force. The excitation line and the line representing the total reaction force overlap each other perfectly. Because there are no structural vibrations, the IF is equal to 1.0.

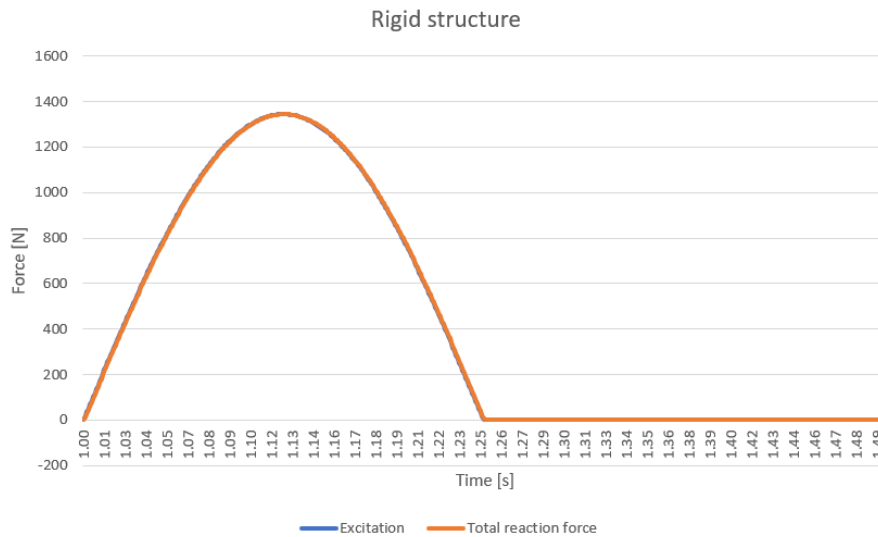


Figure 73: Excitation and reaction force propagation over time

6.2.1 Simultaneous group jump

To find out what impact factors can be expected in event deck structures, the ratio between total reaction force and total excitation force is determined. Figure 74 shows the forces in the model resulting from a simultaneous jumping crowd of 16 people. It can be obtained how the structural vibrations influence the reaction force over time. By dividing the maximum reaction force by the total excitation force, the IF is determined. The fundamental natural frequency in vertical direction is 33 Hz.

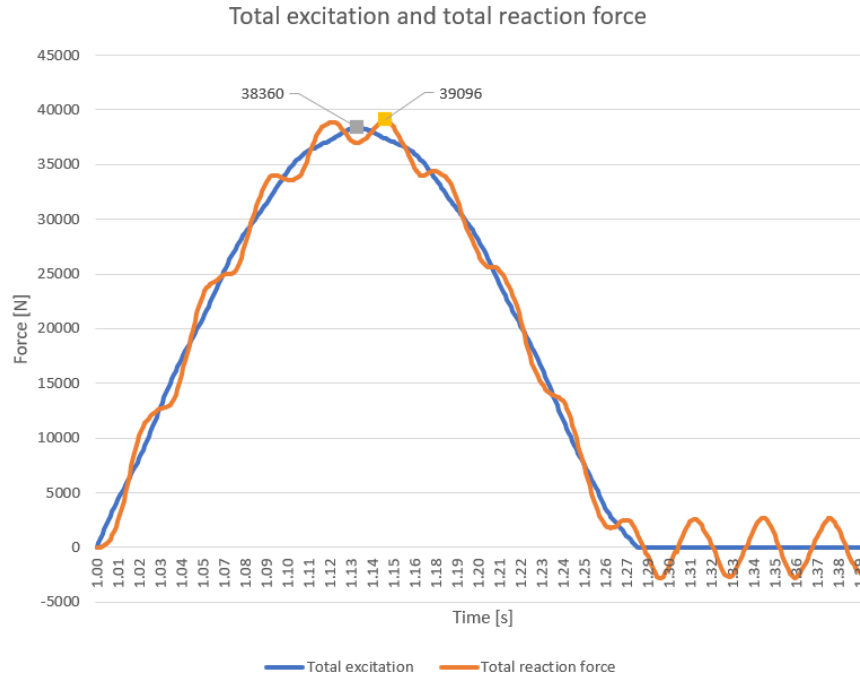


Figure 74: Simultaneous group jump of 16 people on a structure with $f_s = 33$ Hz

$$IF = \frac{39096}{38360} = 1.02 = 2\%$$

So the internal stresses amplify with 2% in this situation.

In section 5.8 the soundness of the model is checked regarding the impact factor. It is obtained how the IF amplified for a structure with a lower natural frequency. The event structure used in figure 74 makes use of floor panels with dimensions 1 x 2m (width x length). To address the widest range of event deck structures, the IF for event deck structures with the longest floor panels (0.87 x 2.57m) is determined as well. First the fundamental frequency for this type of floor panel is determined using Abaqus. Because the scaffolding frame is very stiff and the floor panels are simply supported, only the floor panel is modelled. This first mode is depicted in figure 75.

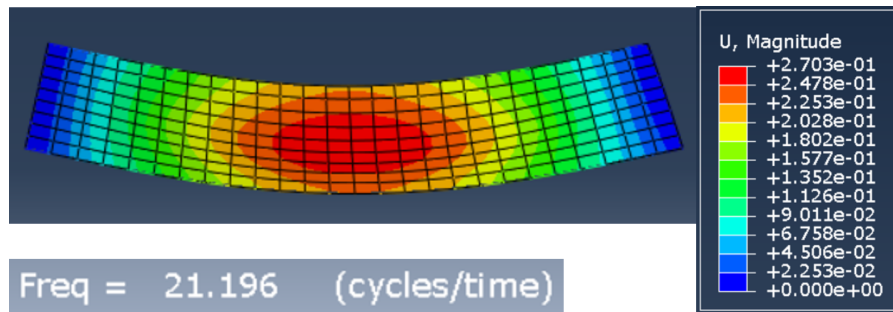


Figure 75: First mode of floor panel (0.86 x 2.57), $f_s = 21.2$ Hz

To determine the IF of an event deck structure with 0.86 x 2.57m floor panels, the same model is used which is used to check the soundness of the model. The system parameters are changed to simulate a structure with a fundamental frequency of 21.2 Hz. The results can be obtained in figure 76.

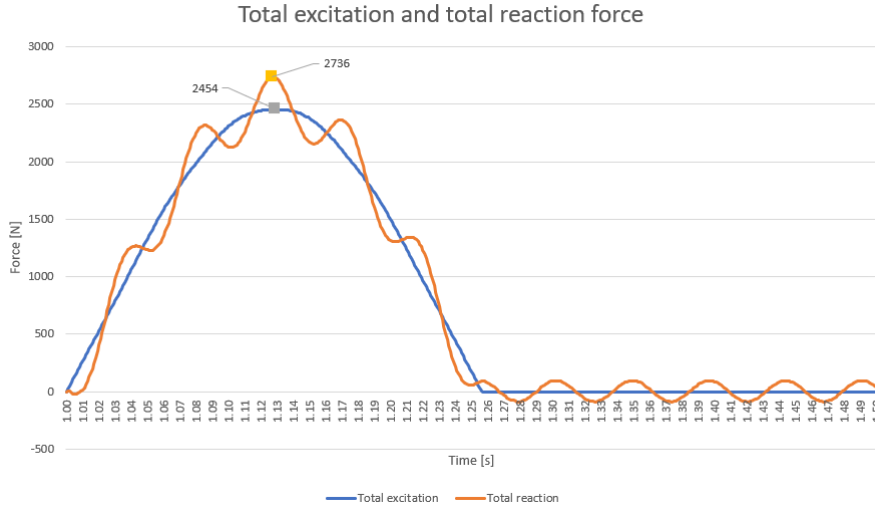


Figure 76: 1 person jumping on the model suggested in figure 54 with $f_s = 21$ Hz

As expected, the impact factor is larger. The impact factor now reached as value of:

$$IF = \frac{2736}{2454} = 1.11 = 11\%$$

So the internal stresses amplified 11% in this situation.

After varying in the natural frequency of the structure, the influence of the excitation frequency on the IF will now be considered. A person can jump in different frequencies, but it has its limits. According to [12], the frequency of a jumping person (f_j) can vary from 1.5 to 2.8 Hz. In [3] it can be obtained that the IF is getting larger for high frequency structures which were excited by suddenly changing forces, like square-shaped pulse forces. In this research the focus is on sinusoidal load shapes, but to create a faster changing force curve, a person jumping on the highest possible frequency of 2.8 Hz is considered. The results are shown in figure 77.

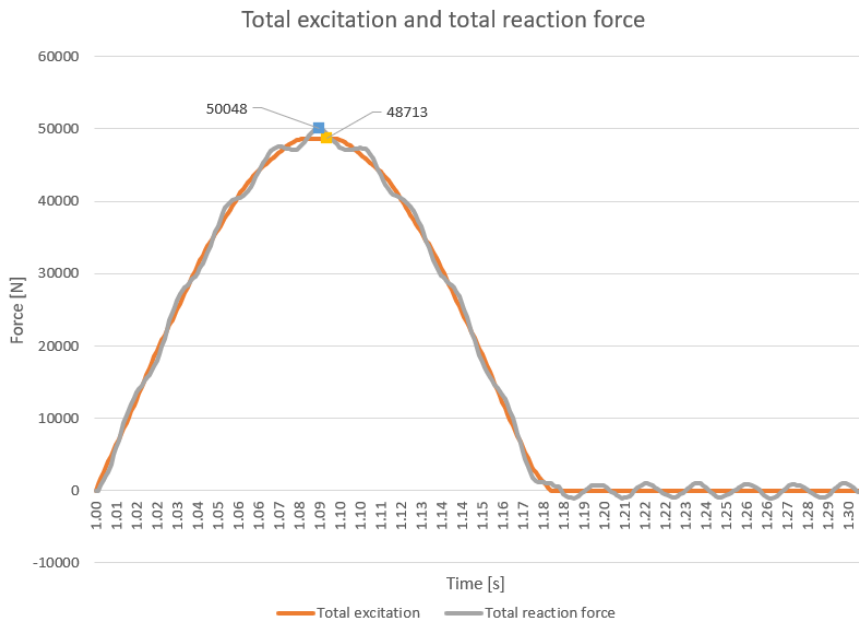


Figure 77: Simultaneous group jump of 16 people with $f_j = 2.8$ Hz and $f_s = 33$ Hz

$$IF = \frac{50048}{48713} = 1.03 = 3\%$$

It can be seen that the change in jumping frequency barely influences the IF . This is because the jumping frequency and the natural frequency of the structure lay too far apart from each other. A change in jumping frequency starts to make a difference when the natural frequency of the structure comes close to it. Then a change in jumping frequency will have a similar effect on the impact factor as changing the structural natural frequency. To sum up the results, a spectrum for the impact factors with differing structural periods (T_s) is made.

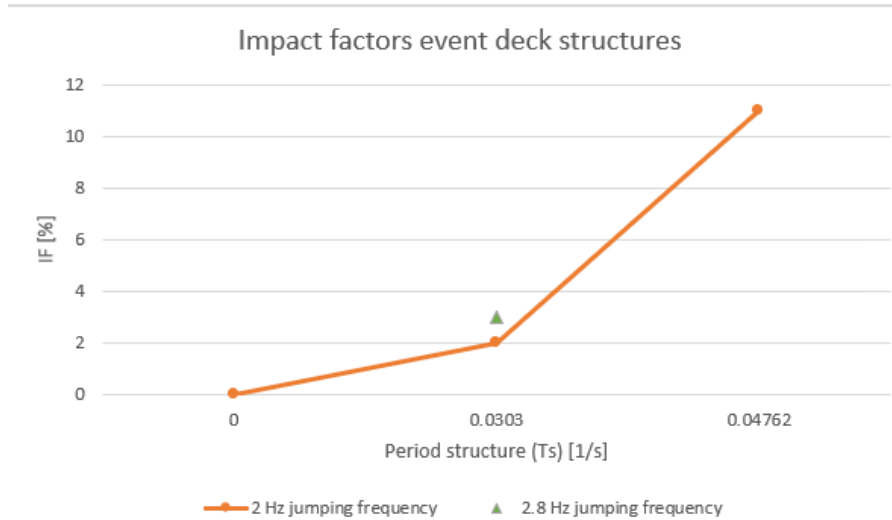


Figure 78: Spectrum impact factors, simultaneous group jump

To put the results in perspective, all results regarding the impact factor are added in figure 79. This spectrum contains the impact factors which are obtained for event deck structures (with T_s ranging from 0 to 0.048 [1/s]), the impact factors which were obtained from checking the soundness of the model ($T_s = 0.1$ and $T_s = 0.2$ [1/s]) and the impact factors for structures with $T_s = 0.5$ and $T_s = 1$ [1/s] ($f_s = 2$ Hz and $f_s = 1$ Hz respectively) are added. The last two values were added to show how the spectrum peaks at resonance frequency and then drops for structures with lower natural frequencies.

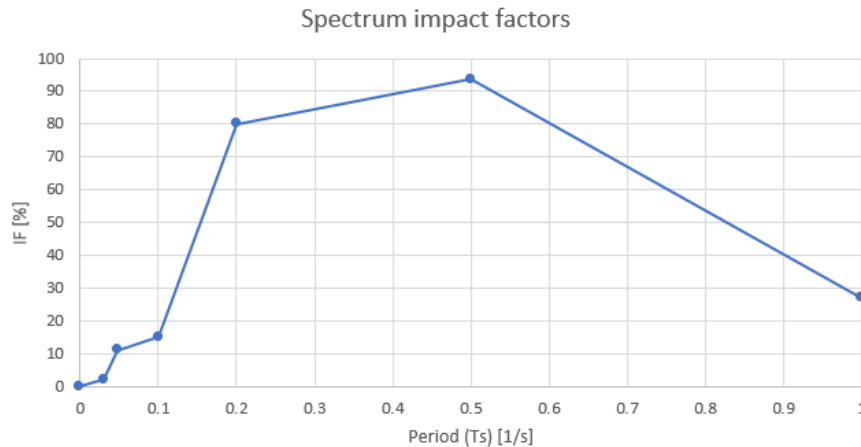


Figure 79: Total spectrum for impact factors regarding a sinusoidal load shape with a 2 Hz frequency

6.2.2 Randomly timed group jump

Figure 79 shows the total excitation force and the total reaction force for a randomly timed group jump. It can be obtained how the total excitation force now increases a lot slower. This is caused by the time lags between the jumpers. The more subtle increasing force curve causes the structural vibrations to be more suppressed compared to a simultaneous group jump. This results in a lower IF . The time lags between the jumpers also results in a lower force frequency. The total excitation drops to zero again at $t=1.438$ seconds. So the force frequency is equal to $\frac{1}{2 \cdot 0.438} = 1.14$ Hz.

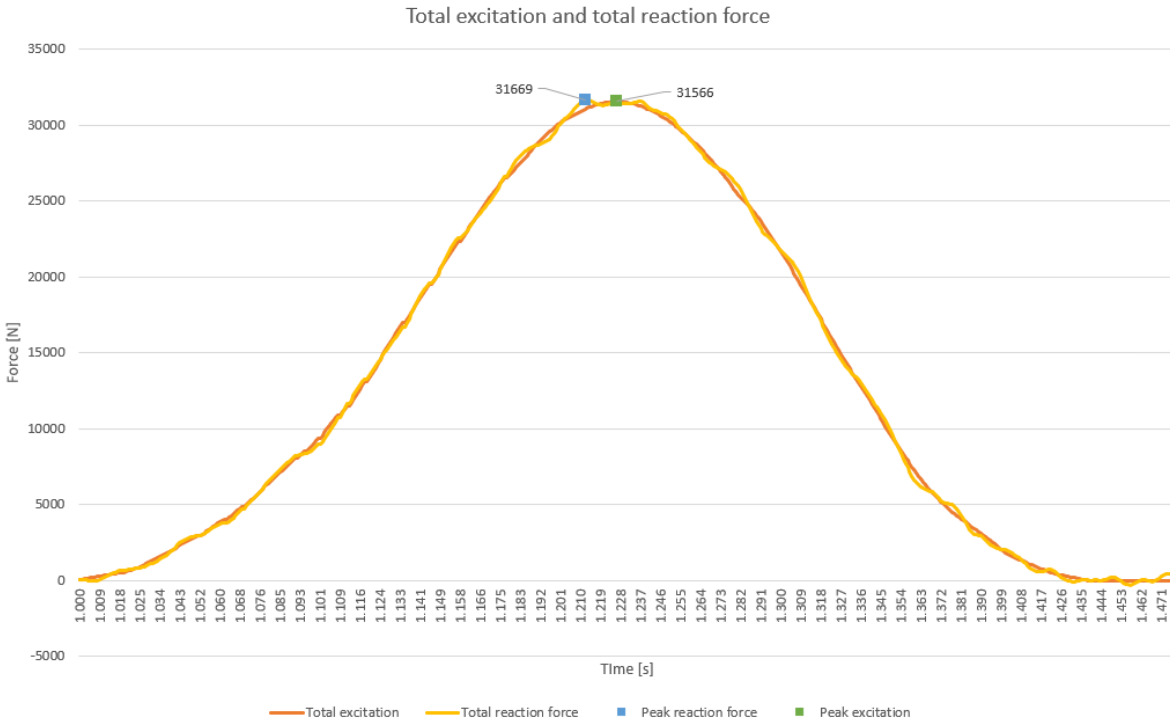


Figure 80: First simulation randomly timed group jump

$$IF = \frac{31669}{31566} = 1.003 = 0.3\%$$

Similar results are found in the second simulation. For this situation the IF is equal to:

$$IF = \frac{30904}{30423} = 1.016 = 1.6\%$$

A small increase of the impact factor is obtained for the second simulation. In figure 68 a large time lag can be obtained between the first and the second jumper. After the second jumper makes contact with the structure, the rest of the jumpers follow with a relatively small time lag. Because the second simulation approaches a simultaneous jump better than the first simulation, this results in a higher IF . The second reason for the increased IF is the timing of the peak in the total reaction force. In the second simulation, the peak value of the total reaction force is better aligned with the peak excitation force than in the first simulation. This also results in a slightly higher IF .

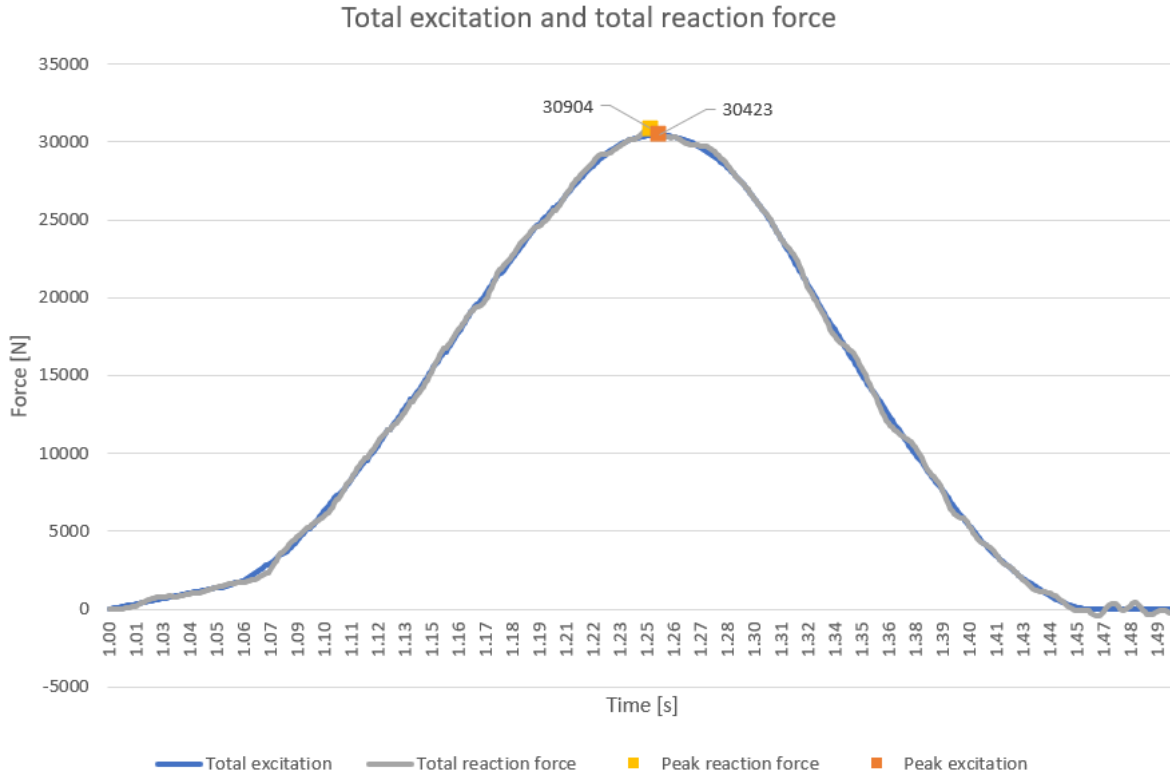


Figure 81: Second simulation randomly timed group jump

6.2.3 Double randomly timed group jump

Figure 82 shows the total excitation force, the total reaction force and both its peak values. A double randomly timed group jump is simulated to check whether already existing structural vibrations influence the impact factor. But just as can be obtained in section 6.1.3, the structural vibrations are too small to influence the peak values of the total reaction force.

In this simulation, similar results can be obtained as in section 6.3.2. The impact factor regarding the first jump is equal to:

$$IF = \frac{31669}{31566} = 1.003 = 0.3\%$$

And the for the second jump:

$$IF = \frac{31767}{31482} = 1.009 = 0.9\%$$

In figure 71 it can be observed that there is a relatively large time lag between the third and the fourth jumper regarding the second jump. All thirteen other jumpers who come in contact with the structure after the third jumper have relatively small time lags in between them. So they create a better approach to a simultaneous jump as well. Next to that, the peak values of the total excitation and the total reaction force are again better aligned in the second jump.

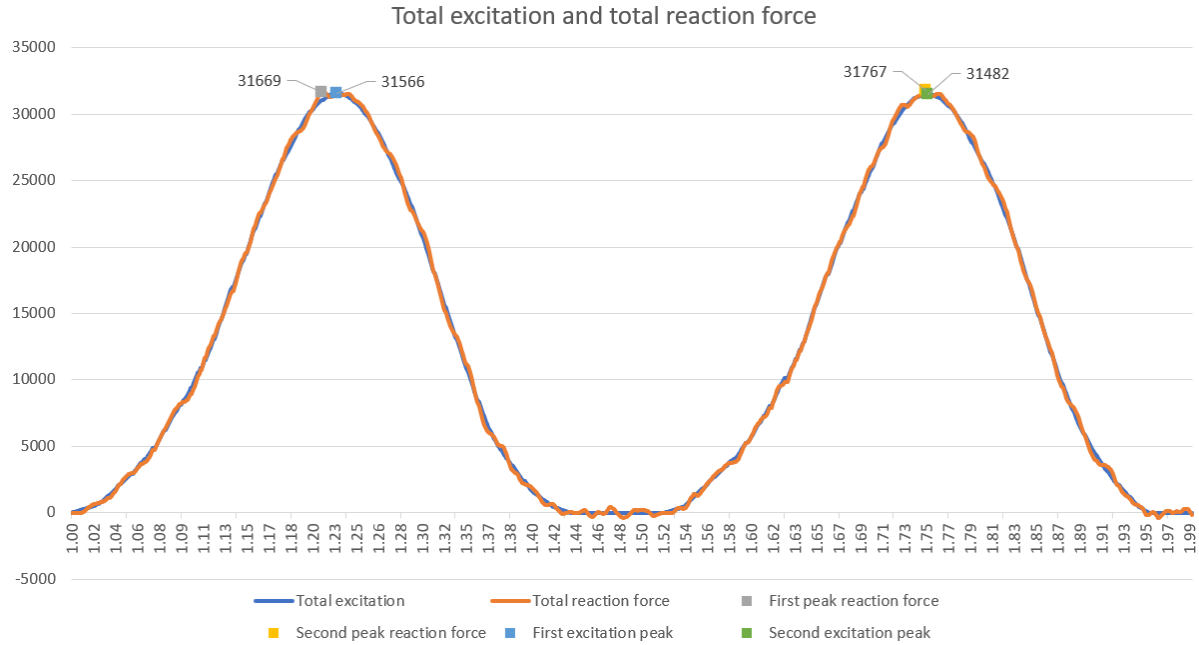


Figure 82: Double randomly timed group jump

7 Discussion

During this research, several assumptions were made. This section touches on all relevant assumptions which were made to get to the conclusions. Other researchers can pick up on these points of discussion to redefine the results which are created during this process.

- Human and structural damping factors

In section 5 it is explained why human damping and structural damping is not applied in the model. However, in most studies that touch upon human-structure interaction it is not common to model the interaction between a person and a structure by only using a spring. Most studies either choose no interactive elements, only an added human mass, or the combination of a spring and a dashpot. The assumption in this research to only use a spring to model the excitation resulted in a good estimation compared to the prescribed force curves by the existing literature. This convinces the author that the right decision was made.

- The contact ratio

The contact ratio (α) is a ratio which is not exactly determined by existing literature. According to [12] the contact ratio relates to the dynamic amplification factor by means of the following formula:

$$\frac{F_{max}}{G_s} = \frac{\pi}{2\alpha} \quad (12)$$

With:

- F_{max} = The peak dynamic load
- G_s = The static load of the jumper
- α = Contact ratio

A dynamic amplification factor of 3 is assumed, so according to [12] the contact ratio should be equal to 0.52. In this research α is equal to $\frac{1}{2}$. This difference is negligible according to the author. It is known that the contact ratio relates to the dynamic amplification factor and the jumping frequency, but it varies with a small range depending on human posture, gender and several other factors according to [25]. This justifies the assumption for the combination of a dynamic amplification factor of 3 with a contact ratio of $\frac{1}{2}$.

- A linear spring to simulate the human interaction mechanism

During a collision, the mechanism which interacts with a structure is very important. In the case of a human jumping on a structure, the interaction mechanism of the human part is defined mainly by the legs. The rotational stiffness in the knees, toes, hips and ankles cause the legs to work like a spring to slow down the deceleration of the body. The mechanism of the legs is modelled as a spring which is linear in compression. But the compressive stiffness of the legs is probably not exactly linear as is assumed. But because existing literature concludes that a sinusoidal curve fits the human jumping excitation best (without taking HSI into account), the assumption of a linear spring in compression is a good estimation.

- Structural level of detail of the Abaqus model

During the design of the model, the cross-section of some structural parts is simplified. There is always room for improvement on this subject, but because elements with similar structural parameters are used, improving the structural level of detail will probably not result into significantly better results.

8 Conclusions

The results and observations of this research are used to answer the main research question:

What is the effect of dynamic interaction on an event deck structure when it is vertically excited by a jumping crowd?

In this research, dynamic interaction regards the impact force peak error and the impact factor. The conclusions and recommendations are drawn in the same order as the sub questions.

8.1 The impact force peak error (*IPE*)

- Which parameters influence the *IPE* and how do they influence the *IPE*?

Figure 24 shows the results of the parametric study conducted in [26]. From this figure it can be observed how each system parameter influences the *IPE* for 2 floor systems.

- To what extent does the impact force peak error influence the imposed force on an event deck structure which is excited by a jumping crowd?

The general influence of each system parameter on the *IPE* is depicted in figure 24. Now the focus is on event deck structures with a natural frequency above 20 Hz which are subjected by a jumping crowd. Event deck structures are light in weight so they can be installed by hand. This results in floor panels with a natural frequency (f_s) of 20 Hz or higher. A standard jumping person is limited to a jumping frequency (f_j) of approximately 2.8 Hz, higher frequencies like 3.5 Hz can be reached but are not likely to occur, especially not at real-life events. The combination of these two system parameters, f_s and f_j , lead to low *IPE* values. The results show no *IPE* values above 6%. Because the natural frequency of floor panels will not be any lower than 20 Hz and jumping frequencies not higher than 2.8 Hz, the *IPE* will never reach significant values to consider in the design of event deck structures.

-
- Does the coordination factor of a jumping crowd affect the impact force peak error?

In figures 67 and 68 it can be observed how the impact force increases for people who land at a later moment in time on the structure. What could be concluded from this is that the coordination factor does influence the *IPE* value, but this is not really true. The coordination factor takes the fact into account that people do not land on a surface exactly at the same moment in time. This reduces the total excitation curve. Because the coordination factor is simulated by modelling time lags between each person, every person lands on the floor panel while it is in a different stage of its motion. Because the floor panel deflects over time, the impacting velocity is slightly higher for the last person to touch the panel. This results in a higher impact force. Next to this mechanism, the direction of motion of the panel is important. In figure 70 it can be seen how the floor panel is in an upward moving motion for most of the time the last person is in contact with the panel. The reduction of the impact force is caused because the structure moves along with the person, for the last person the opposite is true. An upward moving structure causes a higher impact force with a person.

It was assumed that an interactive floor structure always reduces the impact force. But now it can be concluded that the opposite can also be true. If a jumping crowd on an event deck structure is considered, it can be stated that the chances of a jumper touching the floor panel in a downward moving state or an upward moving state is equal. Given this, it can be concluded that the average *IPE* value in a randomly timed group jump is 0%. So it is not necessary to take the *IPE* into account for a jumping crowd on an event deck structure.

- Do structural vibrations influence the impact force peak error?

It is now known that the motion of a structure can influence the *IPE*. But figure 72 shows how small the amplitude of the structural vibrations of the floor panels are in between two jumps, compared to the displacement during the impact. So the structural vibrations will not significantly influence the *IPE* values.

8.2 The impact factor (*IF*)

- What parameters influence the *IF* and how do they influence the *IF*?

From the rapport by Royal HaskoningDHV on the collapse of a grandstand element at the Goffertstadion, many conclusions can be drawn. It is known that the impact factor depends on the course of the excitation over time and the first natural frequency of the structure in the direction of the excitation. It is known that the spectrum of the impact factor is similar to a response spectrum used in earthquake engineering. And that for most structures on which people jump, the impact factor lies between 1.05 and 1.9.

- To what extent does the impact factor influence the stresses in an event deck structure which is excited by a jumping crowd?

In this study the focus is on event deck structures with a natural frequency above 20 Hz which are excited by a jumping crowd. The course of the excitation of a jumping person can best be described by a half a sinusoidal cycle. So apart from the frequency and amplitude of the excitation, no variations in the shape of the excitation will be made. This an important restriction on the determination of the impact factor. For a simultaneous jumping crowd the impact factor can lead to a significant amplification of stresses in a structure. Figure 76 shows how internal forces can reach values which are more than 10% higher than equivalent static forces. This amplification is caused by structural vibrations during the excitation. Figure 79 shows the spectrum of the impact factors relating to a sinusoidal load with a 2 Hz frequency. It can be obtained how the spectrum peaks when the load is applied on a structure with the same natural frequency and decreases after that frequency is reached.

- Does the coordination factor of a jumping crowd affect the impact factor?

The increase of internal stresses which are obtained in section 6.2.1 are based on an individually jumping person and a simultaneous jumping crowd. In both cases the total excitation has a sinusoidal shape.

But when a randomly timed group jump is considered, figures 80 en 81 show how the total excitation gets spread out due to the time lags between each participant. This results in a different total excitation shape which amplifies slower than a sinusoidal shape and has a higher contact ratio. Both aspects of the total excitation shape cause the impact factor to reduce. In section 6.2.2 it can be obtained that for randomly timed group jumps the impact factor does not even amplify the excitation with 2%. It can be concluded that the stresses in a typical event deck structure with a natural frequency higher than 20 Hz will not be significantly amplified due to the impact factor when it is excited by a jumping crowd. So during the design of an event deck structure, it is not necessary to take the impact factor into account if the load case of a synchronous jumping crowd is checked.

- Do structural vibrations influence the impact factor in event decks?

In figure 82, no significant differences are obtained between the total reaction forces of the first jump and the second jump. The structural vibrations which are obtained in between the two jumps are negligible compared to the stresses obtained during the moments of contact. From this observation it can be concluded that structural vibrations do not influence the impact factor in event deck structures when they are excited by a jumping crowd.

9 Recommendations

In section 8 it is concluded that for the design of event deck structures with a natural frequency above 20 Hz which are excited by a jumping crowd, it is not necessary to take human-structure interaction into account. This means that equation (2) is accurate enough to calculate the amplitude of the crowd-induced dynamic force. Equation (2) is again formulated below:

$$N \cdot Q \cdot \frac{F(t)}{Q} \cdot C(N) = q(t)$$

In which:

- N = The amount of people per square meter
- Q = The static load of a person
- F(t) = The dynamic peak load of a jumping person
- C(N) = The coordination factor
- q = Vertical load per square meter

It is known from the literature study that the vertical load per square meter can vary a great deal. But it is possible to recommend values for this formula based on past events like the collapse of the NEC grandstand.

[3] concluded that approximately 4 people per square meter were present on the grandstand at the moment of collapse. So it can be assumed that this density can be reached by a lively crowd.

The static load of a person is determined by their weight. Dutch males and females weigh around 85 kg and 72 kg on average respectively. To determine the average weight of a crowd it could be assumed that there is a 50/50 (male/female) distribution present on the structure. In that case an average human weight of $\frac{(85+72)}{2} = 78.5kg$ could be assumed. But the type of event must be considered in this assumption as well, because for hooligan crowds the majority of the crowd is male. In [3] they assumed the average weight of a Dutch male. This is equal to a static load of 0.834 kN

To determine the dynamic amplification factor and the coordination factor, figure 83 provides a good insight of the possibilities. The vertical axis indicates the dynamic amplification factor multiplied by the coordination factor and the horizontal axis indicates time. The blue, orange and green lines correspond to a contact ratio of $\frac{2}{3}$, $\frac{1}{2}$ and $\frac{1}{3}$ respectively. The thin solid lines represent an individually jumping person, the thick solid lines represent a group jump with a high coordination factor, the dotted lines represent a group jump with an average coordination factor and the dashed lines represent a group jump

with a low coordination factor. It can be concluded from the figure that the contact ratio affects the coordination factor. Because of the smaller time span of a jump with a low contact ratio, a time lag between two jumping people results in a lower coordination factor for a jump with a low contact ratio compared to a jump with a high contact ratio.

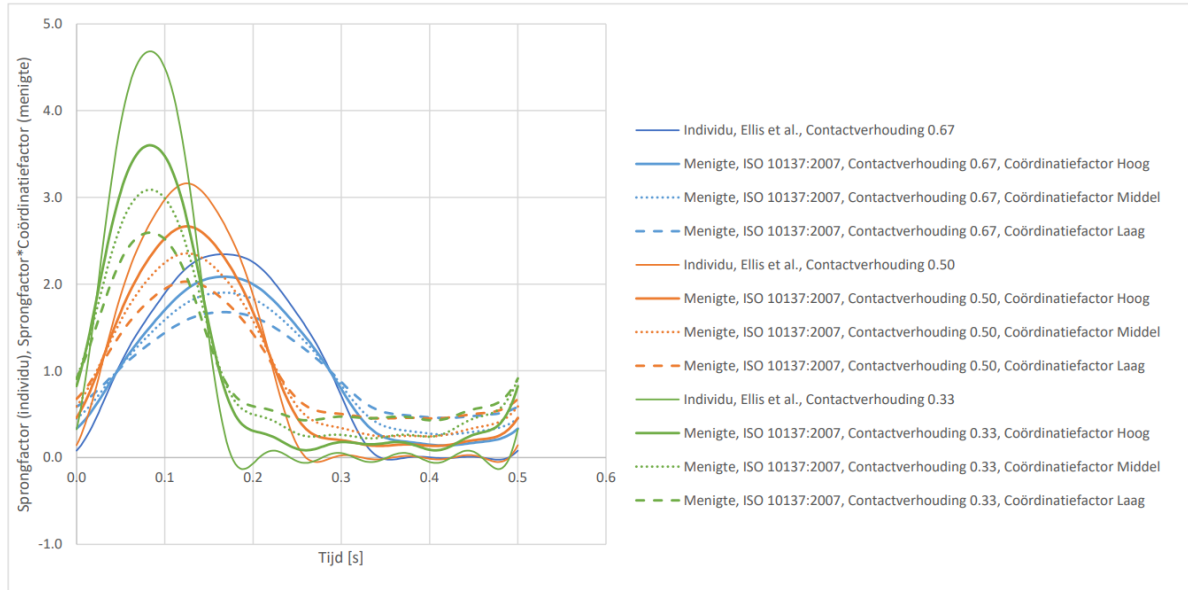


Figure 83: Dynamic amplification factor for an individual according to [12] with six Fourier terms and the product of the dynamic amplification factor with the coordination factor according to [2]

In [3] the product of the dynamic amplification factor with the coordination factor is determined to be 2.3. Considering this value and figure 83, it can be assumed that a value of 2.5 for the combination of the dynamic amplification factor and the coordination factor covers most of the possibilities. Considering these values, it can be assumed that a lively crowd can produce a vertical load per square meter of:

$$4 \cdot 0.834 \cdot 2.5 = 8.34kN/m^2$$

This is a significantly higher value than the prescribed value of $5kN/m^2$ by the Dutch design codes. So for cases where a synchronically dancing crowd is expected, it is recommended that a higher equivalent static load is applied to event deck structures during the design. A "heavy dance crowd" load case already exists in England. Also Royal HaskoningDHV concludes that most football stadiums in The Netherlands are not designed to bare the loads generated by a very lively crowd.

References

- [1] Crowd density considerations. Cabinet Office, EPC, Serco.
- [2] ISO 10137. Bases for design of structures - serviceability of buildings and walkways against vibration. 2007.
- [3] Koper A and Kortenaar M. Onderzoek naar de technische oorzaken van het bezwijken van het tribune-element van het goffertstadion te nijmegen. 2022.
- [4] A. Comer, A. Blakeborough, and M. S. Williams. Crowd coordination in jumping tests on a model grandstand. In *7th European Conference on Structural Dynamics, EURO-DYN 2008*, 2008. Cited By :4.
- [5] C. Z. Cory, M. D. Jones, D. S. James, S. Leadbeatter, and L. D. M. Nokes. The potential and limitations of utilising head impact injury models to assess the likelihood of significant head injury in infants after a fall. *Forensic science international*, 123(2-3):89–106, 2001. Cited By :41.
- [6] Rosman Cyril. Nederlanders steeds langer én steeds zwaarder. 2019.
- [7] de Winter P.E. Achtergronden van de belastingen volgens concept nen 6702. 1989.
- [8] I. M. Díaz, C. A. Gallegos, J. Ramírez Senent, and C. M. C. Renedo. Interaction phenomena to be accounted for human-induced vibration control of lightweight structures. *Frontiers in Built Environment*, 7, 2021. Cited By :2.
- [9] Paloheimo E and Ollila M. Researches in the live load of persons. 1973.
- [10] B. R. Ellis and T. Ji. Human-structure interaction in vertical vibrations. *Proceedings of the Institution of Civil Engineers: Structures and Buildings*, 122(1):1–9, 1997. Cited By :151.
- [11] T Ellis B.R.; Ji. Loads generated by jumping crowds: experimental assessment. 2002.
- [12] T Ellis B.R.; Ji. Loads generated by jumping crowds: numerical modelling. pages 35–40, 2004.
- [13] Ellis B.R. et al. *The response of grandstands to dynamical crowd loads*. ICE Proceedings Structures and Buildings, 2004.
- [14] C. Gaspar, E. Caetano, C. Moutinho, and J. G. S. Da Silva. Biodynamic modelling of human rhythmic activities. In *Procedia Engineering*, volume 199, pages 2802–2807, 2017. Cited By :1.
- [15] C. Gaspar, E. Caetano, C. Moutinho, and J. G. S. da Silva. Active human-structure interaction during jumping on floors. *Structural Control and Health Monitoring*, 27(3), 2020. Cited By :5.
- [16] L. Gustafsson and M. Sternad. Consistent micro, macro and state-based population modelling. *Mathematical biosciences*, 225(2):94–107, 2010. Cited By :23.
- [17] Chen J., Tan H., Van Nimmen K., and Van Den Broeck P. Data-driven synchronization analysis of a bouncing crowd. *Shock and Vibration*, 2019, 2019. Cited by: 1; All Open Access, Gold Open Access, Green Open Access.
- [18] N. R. Jennings, K. Sycara, and M. Wooldridge. A roadmap of agent research and development. *Autonomous Agents and Multi-Agent Systems*, 1(1):7–38, 1998. Cited By :1536.
- [19] P; Pavic A Jones, C.A.; Reynolds. Vibration serviceability of stadia structures subjected to dynamic crowd loads: A literature review. 2010.
- [20] Sentler Lars. *Live load surveys: a review with discussion*. Tekniska hogskolan i Lund, Lund, 1976.
- [21] Arnold P.O.S.; de Ridder Huib Li, Jie; Vermeeren. Designerly ways of exploring crowds. 2014.

-
- [22] G. Li, T. Ji, and J. Chen. Determination of the dynamic load factors for crowd jumping using motion capture technique. *Engineering Structures*, 174:1–9, 2018. Cited By :9.
- [23] M. W. Macy and R. Willer. *From factors to actors: Computational sociology and agent-based modeling*, volume 28 of *Annual Review of Sociology*. 2002. Cited By :870.
- [24] P. Mazzoleni and E. Zappa. Vision-based estimation of vertical dynamic loading induced by jumping and bobbing crowds on civil structures. *Mechanical Systems and Signal Processing*, 33:1–12, 2012. Cited By :30.
- [25] M. G. McDonald. Experimental characterisation of jumping and bobbing actions for individuals and small groups. *PhD thesis, University of Warwick (UK)*, 2015.
- [26] E. Shahabpoor and A. Pavic. Human-structure dynamic interaction during short-distance free falls. *Shock and Vibration*, 2016, 2016. Cited By :2.
- [27] E. Shahabpoor, A. Pavic, V. Racic, and S. Zivanovic. Effect of group walking traffic on dynamic properties of pedestrian structures. *Journal of Sound and Vibration*, 387:207–225, 2017. Cited By :51.
- [28] R. G. SNYDER. Human tolerances to extreme impacts in free-fall. *Aerospace Medicine*, 34:695–709, 1963. Cited By :42.
- [29] Keith Still. Crowd safety and crowd risk analysis, 2019. Static crowd density (general).
- [30] W. Thomson and Dahleh M.D. *Theory of Vibration with Applications (5th Edition)*. Pearson, 1997.
- [31] Racic V., Brownjoh J.M.W., and Pavic A. Dynamic loads due to synchronous rhythmic activities of groups and crowds. 2011. Cited by: 1.
- [32] K. Van Nimmen, A. Pavic, and P. Van den Broeck. A simplified method to account for vertical human-structure interaction. *Structures*, 32:2004–2019, 2021. Cited By :2.
- [33] De Brito V.L. and Pimentel R.L. Cases of collapse of demountable grandstands. *Journal of Performance of Constructed Facilities*, 23(3):151 – 159, 2009.
- [34] Q. Yang, L. Xu, Y. Hui, H. Li, and J. Qin. Modeling of wedge-pin joint for the dynamic analysis of a planar temporary demountable structure. *Advances in Structural Engineering*, 24(5):929–946, 2021.
- [35] S. Yao, J. R. Wright, A. Pavic, and P. Reynolds. Forces generated when bouncing or jumping on a flexible structure. In *Proceedings of the 2002 International Conference on Noise and Vibration Engineering, ISMA*, pages 563–572, 2002. Cited By :33.
- [36] S. Zivanović. Modelling human actions on lightweight structures: Experimental and numerical developments. In *MATEC Web of Conferences*, volume 24, 2015. Cited By :17.

A Jumping simulation

This appendix explains how the randomly timed group jump is simulated in terms of equations of motion. Figure 84 shows a simplified schematic of the system. A continuous 2D beam with a mass-spring system attached at mid-span. Figure 84 shows how the 2D model can be converted to a 2DOF system. In the simulation multiple mass-spring systems are attached to the 3D model, each mass-spring system (person) has its own initial height as can be obtained in figure 51. This initial height is coupled to U_c as is explained in section 5.6. The height differences are applied to simulate the time lags between each person. The equations of motion below represent a person how collides with the structure **after 0.1 seconds**. The left graph in figure 85 provides a better insight on how the non-linear spring works and the right graph helps with understanding the meaning of t_c (time of contact) and t_{ac} (time after contact). Please note that k_h is a non-linear spring.

For $0 \leq t < t_c$:

$$m_h \ddot{x}_h + x_h k_h - x_s k_h = 0 \quad (13)$$

$$m_s \ddot{x}_s + x_s (k_h + k_s) - x_h k_h = m_s g \quad (14)$$

With initial conditions of (13):

$$x_h(0) = \dot{x}_h(0) \cdot t_c = 1.515 \cdot 0.1 = 0.1515$$

$$\dot{x}_h(0) = 1.515$$

With initial conditions of (14):

$$x_s(0) = 0$$

$$\dot{x}_s(0) = 0$$

For $t_c \leq t < t_{ac}$:

$$m_h \ddot{x}_h + x_h k_h - x_s k_h = m_h g \quad (15)$$

$$m_s \ddot{x}_s + x_s (k_h + k_s) - x_h k_h = m_s g \quad (16)$$

With initial conditions of (15):

$$x_h(t_c) = 0$$

$$\dot{x}_h(t_c) = 1.515$$

With initial conditions of (16):

$$x_s(t_c) = \textit{Determined by solution (13) \& (14)}$$

$$\dot{x}_s(t_c) = \textit{Determined by solution (13) \& (14)}$$

For $t_{ac} < t$:

$$m_h \ddot{x}_h + x_h k_h - x_s k_h = 0 \quad (17)$$

$$m_s \ddot{x}_s + x_s (k_h + k_s) - x_h k_h = m_s g \quad (18)$$

With initial conditions of (17):

$$x_h(t_{ac}) = \textit{Determined by solution (15) \& (16)}$$

$$\dot{x}_h(t_{ac}) = \textit{Determined by solution (15) \& (16)}$$

With initial conditions of (18):

$$x_s(t_{ac}) = \textit{Determined by solution (15) \& (16)}$$

$$\dot{x}_s(t_{ac}) = \textit{Determined by solution (15) \& (16)}$$

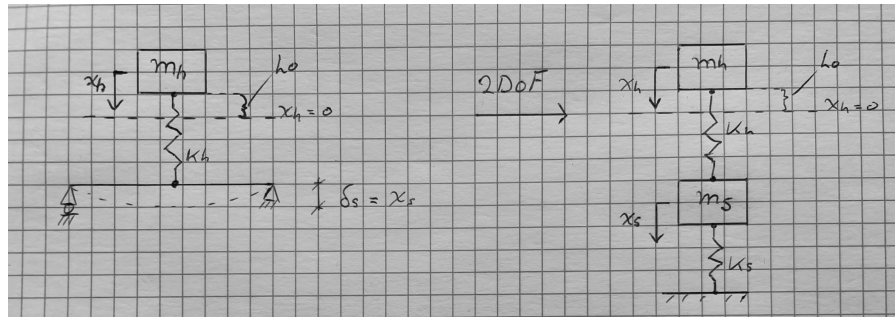


Figure 84: Schematic of the continuous 2D beam model converted to a 2DOF system

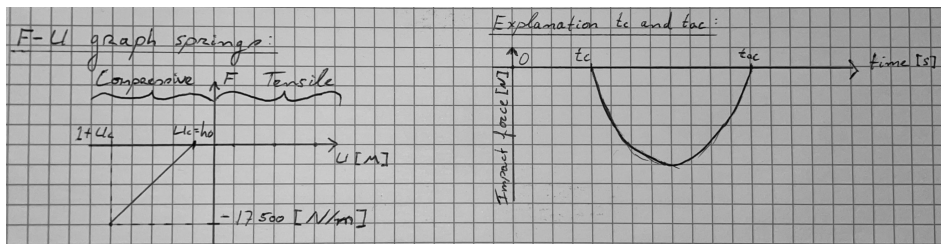


Figure 85: F-U graph of the non-linear spring (left) and the explanation of t_c and t_{ac} (right)